TELAC REPORT 93-17

A FORMULATION OF NONLINEAR LIMIT CYCLE OSCILLATION PROBLEMS IN AIRCRAFT FLUTTER

Final Technical Report for Period: 15 September 1992 - 14 July 1993
AFOSR Contract No. F49620-92-J-0513

Warren C. Chen and John Dugundji
Research Assistant Professor

Technology Laboratory for Advanced Composites
Department of Aeronautics and Astronautics
Massachusetts Institute of Technology
77 Massachusetts Avenue
Cambridge, Massachusetts 02139

September, 1993

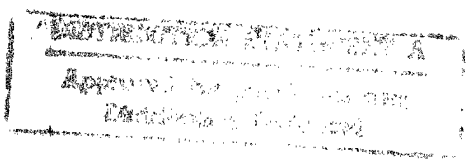

SECURITY CLASSIFICATION OF THIS PAGE

AFOSR-TR-96 97

0030

REPORT DOCUMENTATION PAC

proved
.0704-0188

1a. REPORT SECURITY CLASSIFICATION UNCLASSIFIED	1b. RE
2a. SECURITY CLASSIFICATION AUTHORITY	3. DISTRIBUTION/AVAILABILITY OF REPORT unlimited
2b. DECLASSIFICATION/DOWNGRADING SCHEDULE	
4. PERFORMING ORGANIZATION REPORT NUMBER(S) TELAC Report 93-17	5. MONITORING ORGANIZATION REPORT NUMBER(S)
6a. NAME OF PERFORMING ORGANIZATION Technology Laboratory for Advanced Composites, MIT 6b. OFFICE SYMBOL (If applicable)	7a. NAME OF MONITORING ORGANIZATION Same as 8a
6c. ADDRESS (City, State, and ZIP Code) M.I.T., Room 33-307 77 Massachusetts Avenue Cambridge, MA 02139	7b. ADDRESS (City, State, and ZIP Code) Same as 8c
8a. NAME OF FUNDING/SPONSORING ORGANIZATION AFOSR 8b. OFFICE SYMBOL (If applicable) NA	9. PROCUREMENT INSTRUMENT IDENTIFICATION NUMBER F49620-92-J-0513
8c. ADDRESS (City, State, and ZIP Code) Bolling Air Force Base Washington, DC 20332-6448	10. SOURCE OF FUNDING NUMBERS PROGRAM ELEMENT NO. / PROJECT NO. / TASK NO. / WORK UNIT ACCESSION NO.

11. TITLE (Include Security Classification)
A Formulation of Nonlinear Limit Cycle Oscillation Problems in Aircraft Flutter.

12. PERSONAL AUTHOR(S)
Warren C. Chen & John Dugundji

13a. TYPE OF REPORT	13b. TIME COVERED	14. DATE OF REPORT (Year, Month, Day)	15. PAGE COUNT
Final Technical	FROM 9/15/92 TO 7/14/93	1993 Sept 30	150

16. SUPPLEMENTARY NOTATION

17. COSATI CODES			18. SUBJECT TERMS (Continue on reverse if necessary and identify by block number)
FIELD	GROUP	SUB-GROUP	Nonlinear flutter, Stall flutter, Composites, Aeroelasticity

19. ABSTRACT (Continue on reverse if necessary and identify by block number)

A simple nonlinear aeroelastic flutter analysis method was developed. The aerodynamic forces were modeled by using the ONERA aerodynamic formulation. The ONERA aerodynamic model, a semi-empirical, unsteady, nonlinear model, was reformulated into a harmonic balance form. Fitting of the ONERA aerodynamic formulation was required to incorporate the model into the analysis. The model was fitted to experimental aerodynamic stall flutter characteristics of NACA 0012 airfoil obtained by McAlister, Pucci, McCroskey and Carr. A linear flutter analysis was performed using the U-g method as a basis for comparison with the stall flutter formulation. Nonlinear flutter calculations were done by applying the harmonic balance method to the flutter equations and solving by the Newton-Raphson technique. The results yielded nonlinear limit cycle oscillations which exhibited the expected trends. As the root angle of attack increased, the flutter speed decreased, while the flutter frequency increased toward the torsional natural frequency. The analytic results compared favorably with previous experimental works by Dunn. The current nonlinear analysis procedure seems an effective technique for analyzing stall flutter phenomena.

19970117 227

20. DISTRIBUTION/AVAILABILITY OF ABSTRACT ☐ UNCLASSIFIED/UNLIMITED ☐ SAME AS RPT. ☐ DTIC USERS	21. ABSTRACT SECURITY CLASSIFICATION
22a. NAME OF RESPONSIBLE INDIVIDUAL	22b. TELEPHONE (Include Area Code) / 22c. OFFICE SYMBOL

DD Form 1473, JUN 86 *Previous editions are obsolete.* SECURITY CLASSIFICATION OF THIS PAGE

A FORMULATION OF NONLINEAR LIMIT CYCLE OSCILLATION PROBLEMS IN AIRCRAFT FLUTTER

by

Warren C. Chen

Submitted To The Department Of
Aeronautics And Astronautics
on May 21, 1993
In Partial Fulfillment Of The Requirements For The Degree Of
MASTER OF SCIENCE IN AERONAUTICS AND ASTRONAUTICS

ABSTRACT

A simple nonlinear aeroelastic flutter analysis method was developed. The aerodynamic forces were modeled by using the ONERA aerodynamic formulation. The ONERA aerodynamic model, a semi-empirical, unsteady, nonlinear model, was reformulated into a harmonic balance form. Fitting of the ONERA aerodynamic formulation was required to incorporate the model into the analysis. The model was fitted to experimental aerodynamic stall flutter characteristics of NACA 0012 airfoil obtained by McAlister, Pucci, McCroskey and Carr. A linear flutter analysis was performed using the U-g method as a basis for comparison with the stall flutter formulation. Nonlinear flutter calculations were done by applying the harmonic balance method to the flutter equations and solving by the Newton-Raphson technique. The results yielded nonlinear limit cycle oscillations which exhibited the expected trends. As the root angle of attack increased, the flutter speed decreased, while the flutter frequency increased toward the torsional natural frequency. The analytic results compared favorably with previous experimental works by Dunn. The current nonlinear analysis procedure seems an effective technique for analyzing stall flutter phenomena.

Thesis supervisor: John Dugundji
Professor of Aeronautics and Astronautics

ACKNOWLEDGMENTS

I would like to dedicate this thesis to my loving parents, Ru-Ling and Chung-Jung Chen. Without their unwavering support and constant nurturing for the past 25 years, today would just be a dream. I will never forget their unselfish and supportive attitude for the rest of my life.

I would like to thank Professor John Dugundji for his wisdom and patience. The precious advises from Prof. Dugundji have made this thesis work much manageable. I especially appreciate his patience with my tendency to produce somewhat persistent program bugs.

I would also like to acknowledge Dave and Tina Chen for their constant caring, and to Megan, whose unwavering emotional support made difficult times much less painful to get through. Thanks.

FOREWORD

This report describes work done at the Technology Laboratory for Advanced Composites (TELAC) at the Massachusetts Institute of Technology for the Air Force Office of Scientific Research under Contract No. F49620-92-J-0513. Dr. Spencer Wu was the contract monitor.

The work reported herein, was performed during the period, 15 September 1992 through 14 July 1993, and represents an M.S. thesis by Warren C. Chen entitled, "A Formulation of Nonlinear Limit Cycle Oscillation Problems in Aircraft Flutter", June, 1993, which was completed during this period. This work was done under the supervision of John Dugundji, the Principal Investigator, and the supporting laboratory staff.

TABLE OF CONTENTS

LIST OF ILLUSTRATIONS

LIST OF TABLES

LIST OF SYMBOLS

a_{oz}	linear slope of the general aerodynamic force coefficient
a_{oL}, a_{oM}	slopes of linear lift and moment coefficient curves
b	semi-chord length
b_1	nonlinear slope of the deviation from linear force curve
c	chord length
C(k)	Theodorsen function
C_Z	total contribution to the general aerodynamic force coefficient (Z = L, lift ; Z = M, moment)
C_{Z1}	linear contribution to the general aerodynamic force coefficient.
C_{Z2}	nonlinear contribution to the general aerodynamic force coefficient
$C_{Z\gamma}$	linear, circulatory contribution to the general aerodynamic force coefficient
C_{Zo},C_{ZS1},C_{ZC1}, C_{ZS2},C_{ZC2}	mean, first and second harmonic sine and cosine components of the general aerodynamic force coefficient
C_{Z1o},C_{Z1S},C_{Z1C}	mean, sine and cosine components of the linear contribution to the general aerodynamic force coefficient
C_{Z2o},C_{Z2S1},C_{Z2C1}, C_{Z2S2},C_{Z2C2}	mean, first and second harmonic sine and cosine components of the nonlinear contribution to the general aerodynamic force coefficient

$C_{Z\gamma o}, C_{Z\gamma S}, C_{Z\gamma C}$	mean, sine and cosine components of the linear, circulatory contribution to the general aerodynamic force coefficient
e	distance from the elastic axis to the mid-chord
F	residual vector in Newton-Raphson scheme
F(k)	real part of the Theodorsen function
g	structural damping in linear U-g flutter method
G(k)	imaginary part of the Theodorsen function
h	1/4 chord tip defection
h_o, h_s, h_c	mean, sine, and cosine components of the 1/4 chord deflection
I_α	mass moment of inertia/unit length
k	reduced frequency
k_α	torsional reduced frequency
K_h	bending stiffness /unit length
K_α	torsional stiffness/unit length
[K]	stiffness matrix
K_{ij}	entries in the stiffness matrix
L	lift
L^D	lift due to disturbance
M	total mass/unit length
Mα	moment
[M]	mass matrix
M_{ij}	components of the mass matrix

M^D	moment due to disturbance
n	number of mode shapes
q_i	i-th model amplitude
q_{io}, q_{is}, q_{ic}	mean, sine, and cosine components of the i-th modal amplitude
q	dynamic pressure
Q_i	i-th modal force
Q_{io}, Q_{is}, Q_{ic}	mean, sine, and cosine components of the i-th modal force
r_1, r_2, r_3	coefficients of ONERA nonlinear aerodynamic differential equation
$r_{10}, r_{12}, r_{20}, r_{22}, r_{30}, r_{32}$	parabolic coefficients of ONERA nonlinear aerodynamic equation
S	wing surface area
s_{Z1}, s_{Z2}, s_{Z3}	coefficients of linear ONERA aerodynamic model
S_α	static moment of inertia/unit length
t	real time
U	free stream velocity
x	state vector in Newton-Raphson scheme
Z	complex eigenvalue of linear U-g flutter equation
α	angle of attack
$\alpha_o, \alpha_s, \alpha_c$	mean, sine, and cosine components of the angle of attack
α_1	stall angle
α_v	vibration amplitude of the angle of attack α

ΔC_z	deviation of the nonlinear aerodynamic force curve from the linear approximation
ΔC_{Zo}, ΔC_{ZS1}, ΔC_{ZC2}	first and second harmonic oscillatory amplitudes of the deviation of the nonlinear aerodynamic force curve from the linear approximation
ε_j	parameter of j-th beam bending mode shapes
Ω	ratio of bending to torsional frequency $= \omega_h/\omega_\alpha$
θ	pitch angle
$\theta_o, \theta_s, \theta_c$	mean, sine, and cosine components of the pitch angle
θ_R	root angle of attack
λ_1, λ_2	coefficients in linear aerodynamic force model
μ	density ratio, $= M / \pi\rho b^2$
ρ	free stream density
τ	non-dimensional time, $= tU/b$
ϕ_h	beam bending mode shape
ϕ_α	beam torsion mode shape
ω	real frequency
ω_h	bending frequency
ω_α	torsion frequency

CHAPTER 1

INTRODUCTION

Stall flutter deals with the self-excited oscillations of a wing in a separated or stalled flow. The classical flutter theory is traditionally based on small amplitude, smooth, linear potential flow and is well understood theoretically [see Refs. 1 to 3] The nonlinear behavior of the large amplitude stall flutter motions, however, involves flow separation and highly nonlinear aerodynamic phenomena. This makes it difficult to analyze analytically, and one must generally resort to either computational methods or experimental semi-empirical methods to characterize such behavior and predict its occurrence.

Problems of stall flutter arise in connection with wings at high angle of attack. If the wing is near the stall region, a nonlinear stall flutter limit cycle oscillation may occur. This nonlinear flutter phenomenon may take place at a lower velocity than linear theory would suggest. Since some current aircraft are capable of maneuvering at high angle of attack, it is of interest to explore this nonlinear stall flutter behavior.

Modeling of the dynamic stall phenomenon has been a primary concern in the study of aeroelasticity. Numerous research in this subject were done for over two decades. There were two main approaches, theoretical and semi-empirical, which bases on experimental data.

Discrete potential vortex method [Refs. 4 to 6], a theoretical approach, ignores the viscous terms in the fundamental equations and assumes potential flow without the boundary layer. The zonal methods [Refs. 7 to 9], also a common theoretical approach, under certain assumptions, models the viscous, non-viscous, and transition regions of the flow separately. These theoretical models are extremely computational intensive and are limited by the approximations of their formulation.

The semi-empirical methods attempt to use static data with corrections to model the dynamic stall event. The method only models the gross aspects of the phenomenon. This is advantageous because the static data already takes into account some of the aerodynamic parameters such as, the effects of Reynold's number and airfoil shapes. There were numerous researches on the semi-empirical analysis [Refs. 10 to 21]. The semi-empirical method is generally not computationally intensive, and is suitable for routine aeroelastic analysis. Extensive work on creating databases of static data was done by McAlister, Carr, & McCroskey [Ref. 22] for the NACA 0012 airfoil. These work was further extended by McAlister, Pucci, McCroskey, & Carr [Refs. 23 and 24] to include a wider range in the variable parameters.

The specific objectives of the current investigation are to explore analytically the roles of nonlinear aerodynamics in high angle-of-attack stall flutter of aircraft wings, while attempting to develop a simple nonlinear method of analysis that is not computationally intensive by modifying linear theory.

This research project is a part of series of studies at the Technology Laboratory for Advance Composites (TELAC) at M.I.T. in a continuing effort to investigate the aeroelastic flutter behavior of aeroelastically tailored composite

aircraft wings. The results of current investigation were compared with previous experimental work done at TELAC by Dunn [Ref. 14].

In this report, Chapter 2 contains the description of basic flutter phenomenon and reviews the linear solution methods common to aeroelastic analysis. In addition, description of the preliminary work in the current investigation using linear theory solution in preparation to approach the stall flutter problem are also included.

Chapter 3 describes the nonlinear theory which the current investigation is based on. Analytically, this chapter seeks to expand on and improve the efforts of the previous investigations. This chapter describes the simplification of modeling nonlinearity, particularly the aerodynamic formulations, over the previous investigations.

Chapter 4 details the results of the theoretical investigations, comparing results against previous works, while Chapter 5 gives concluding remarks on the significant contributions of the current investigation and recommendations for future work.

CHAPTER 2

REVIEW OF LINEAR THEORY

2.1 Flutter

Aeroelasticity deals with the interaction between aerodynamic, elastic and inertial forces. The aerodynamic forces are external forces which arise from free stream velocity. The elastic forces are internal to the airframe. Associated with the elastic forces are inertial forces which is related to the weight distribution.

Flutter is self-excited vibrations of structures caused by the inability of the structure to dissipate the energy received from the air stream. Due to the elasticity of the structure and the external force, the structure gives rise to torsional and bending motion. As the structure deflects, a new geometry is presented to the free air stream, thus the entire cycle of bending and deflection is repeated. This oscillating motion, according to linear theory, will increase exponentially if the structure cannot dissipate the external energy.

This interaction of elastic, aerodynamic and inertial forces on structure is usually analyzed by taking a typical section of the wing and modeling the torsional and bending stiffness by springs (see Figure 1). At a specific velocity, the system becomes unstable.

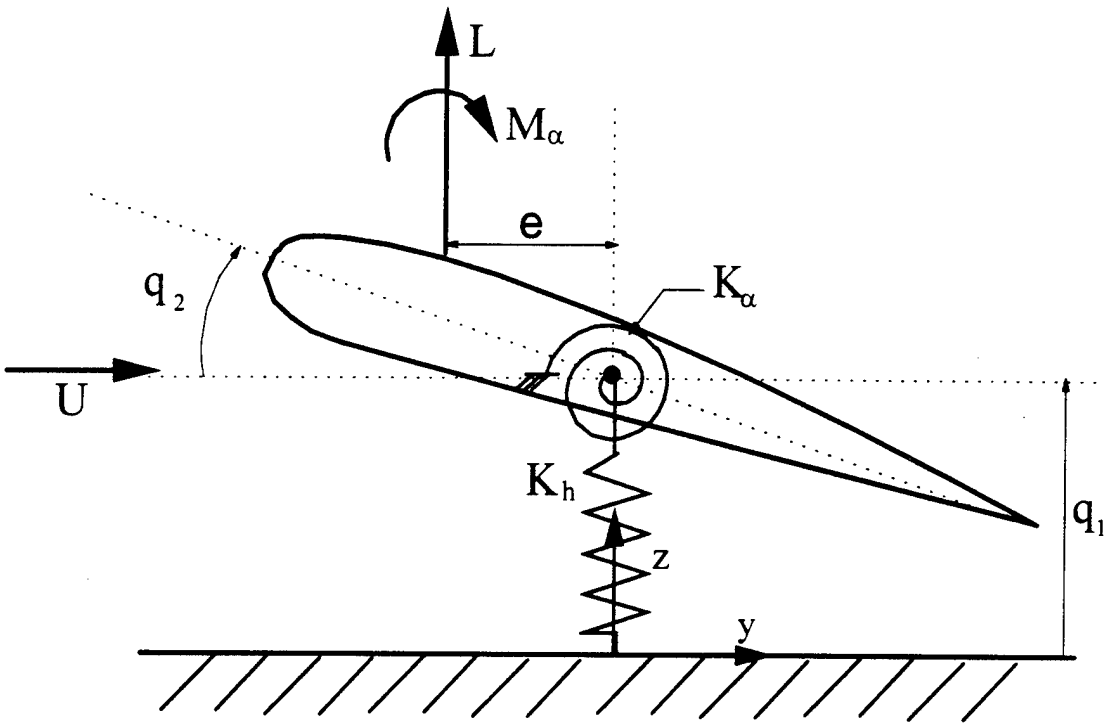

Figure 1. Typical section in flutter analysis

The two equations of motion that describe the behavior of this typical section with elastic axis at the mid-chord are derived from Hamilton's principal and are shown below

$$M\,\ddot{q}_1 - S_\alpha\,\ddot{q}_2 + K_h\,q_1 = L \tag{2.1}$$

$$-S_\alpha\,\ddot{q}_1 + I_\alpha\,\ddot{q}_2 + K_\alpha\,q_2 = eL + M_\alpha \tag{2.2}$$

where

M	mass/unit length
S_α	Static moment/unit length (+ for C.G. aft of spring)
K_h	Bending stiffness/unit length
K_α	Torsional stiffness/unit length
I_α	mass moment of inertia/unit length
q_1,q_2	generalized coordinates for bending and twisting respectively
L	Lift/unit length
M_α	Moment/unit length

2.2 Linear Flutter Analysis -- Quasi-steady

From the aerodynamic theory, lift and moment can be formulated in the approximate quasi-steady manner as

$$L = \tfrac{1}{2}\,\rho\,U^2\,c\,C_{L\alpha}\,\alpha \tag{2.3}$$

$$M_\alpha = \tfrac{1}{2}\,\rho\,U^2\,c^2\,C_{M\alpha}\,\dot{q}_2 \tag{2.4}$$

where ρ is the air density and U is the velocity. The angle of attack, α , can be separated into

$$\alpha = q_2 - \frac{\dot{q}_1}{U} \quad \text{or} \quad \alpha = \theta - \frac{\dot{h}}{U} \tag{2.5}$$

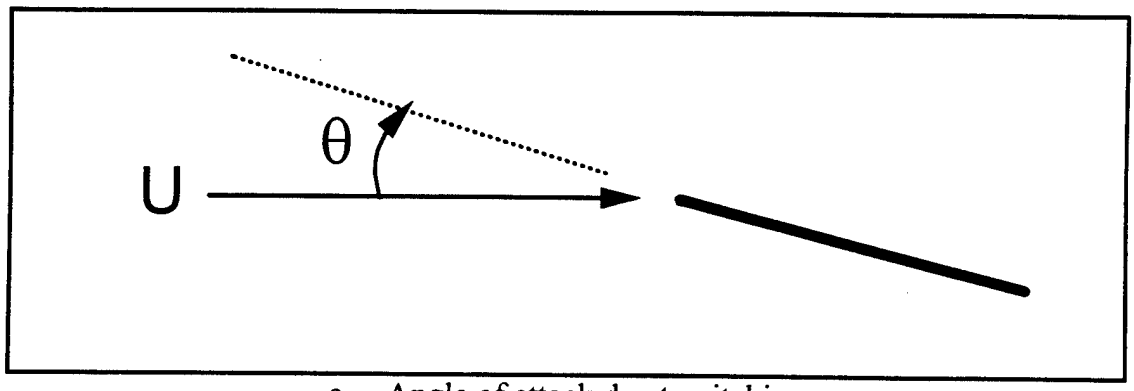

a. Angle of attack due to pitching

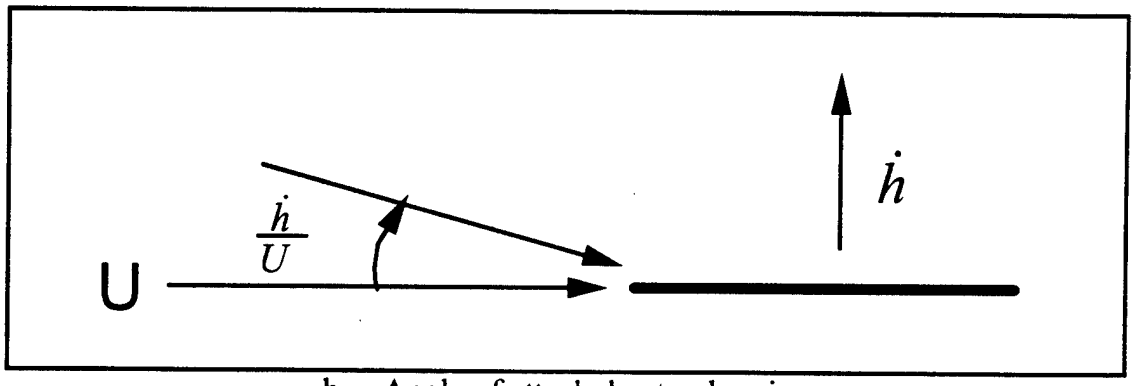

b. Angle of attack due to plunging

Figure 2. Elements of angle of attack

where θ is angle of attack due to pitching and $\dot{h}$/U is angle of attack due to vertical translation of the aircraft (see Fig. 2). Eqs. (2.1) and (2.2) then become,

$$L = q c\, C_{L\alpha}\, (q_2 - \frac{\dot{q}_1}{U}) - L^D(t) \tag{2.6}$$

$$e\, L + M_\alpha = e\, q c\, C_{L\alpha}\, (q_2 - \frac{\dot{q}_1}{U}) + q c^2\, C_{M\alpha}\, \dot{q}_2 + M^D(t) \tag{2.7}$$

where q is the dynamic pressure, $\rho U^2/2$, e is the distance between elastic axis and the mid chord, and L^D and M^D terms describing aerodynamic forces due to disturbances. Placing Eqs. (2.6) and (2.7) into (2.1) gives

$$M\, \ddot{q} + \left(\frac{q\, S\, C_{L\alpha}}{U} \right) \dot{q}_1 + K_h\, \dot{q}_1 - S_\alpha\, \ddot{q}_2 - \left(q\, S\, C_{L\alpha} \right) q_2 = L^D \tag{2.8}$$

$$\begin{aligned} -S_\alpha\, \ddot{q}_1 + \left(\frac{q\, S\, e\, C_{L\alpha}}{U} \right) \dot{q}_1 + I_\alpha\, \ddot{q}_2 - q\, S\, e\, C_{M\alpha}\, \dot{q}_2 \\ + \left(K_\alpha - q\, S\, e\, C_{L\alpha} \right) q_2 = M^D \end{aligned} \tag{2.9}$$

One can gain much insight by examining the system without damping. Setting disturbance loads and damping terms to zero, Eqs. (2.8) and (2.9) can be written in a matrix form as,

$$\begin{bmatrix} M & -S_\alpha \\ -S_\alpha & I_\alpha \end{bmatrix} \begin{Bmatrix} \ddot{q}_1 \\ \ddot{q}_2 \end{Bmatrix} + \begin{bmatrix} K_h & -q\, S\, C_{L\alpha} \\ 0 & K_\alpha - q\, S\, e\, C_{L\alpha} \end{bmatrix} \begin{Bmatrix} q_1 \\ q_2 \end{Bmatrix} = 0 \tag{2.10}$$

where the first square matrix is the symmetric mass matrix $[m_{ij}]$ and the second square matrix is an unsymmetric stiffness matrix $[k_{ij}]$. The stiffness matrix varies

depending on the dynamic pressure. It is this unsymmetric stiffness matrix which causes system instability.

Assuming sinusoidal motion, $q_i = \bar{q}_i\, e^{st}$, Eq. (2.10) then becomes,

$$\begin{bmatrix} M\,s^2 + k_{11} & -S_\alpha\,s^2 + k_{12} \\ -S_\alpha\,s^2 & I_\alpha\,s^2 + k_{22} \end{bmatrix} \begin{Bmatrix} \bar{q}_1 \\ \bar{q}_2 \end{Bmatrix} = 0 \tag{2.11}$$

For stability, examine the non-trivial solution by setting the determinate to zero, gives,

$$As^4 + Bs^2 + C = 0 \tag{2.12}$$

where the coefficients are,

$$A = M\,I_\alpha - S_\alpha^2 \tag{2.13}$$

$$B = k_{11}\,I_\alpha + k_{22}\,M + k_{12}\,S_\alpha \tag{2.14}$$

$$C = k_{11}\,k_{22} \tag{2.15}$$

The roots are then written in the form of quadratic formula,

$$s^2 = \frac{-B \pm \sqrt{B^2 - 4\,A\,C}}{2\,A} \tag{2.16}$$

Stability of the system can then be determined by examining all four roots, s, as q increases. At low values of q, all four roots are imaginary numbers. At a certain velocity, the value B^2-$4AC$ becomes negative, as a result, the roots become complex. Dynamic instability occurs at the point where the real part of any root

becomes positive. In addition, at a specific velocity, two of the roots become zero. This signifies static instability.

The quasi-steady method of describing the aerodynamic forces is an extremely crude approximation, but it gives a simple physical feel for the instability. Note, that there are no damping terms included in the above quasi-steady approximation. Due to the inaccuracy, analysis of events even with quasi-steady damping may result in an incorrect solution, particularly if the C.G. coincides with the elastic axis, i.e., $S_\alpha=0$.

2.3 Linear Flutter Analysis -- Unsteady, Padé Approximants

As a basis for comparison for the full nonlinear flutter analysis, it is beneficial to examine the linear, small amplitude flutter problem with zero root angle of attack. There are several ways to solve the system of linear flutter equations. One of the conventional ways is Padé Approximations. Using Eqs. (2.1) and (2.2), the unsteady incompressible aerodynamic force can be written in the form,

$$\begin{aligned} L_{EA} &= \pi \rho b^2 \left[-\ddot{h} + U\dot{\theta} - b a \ddot{\theta} \right] \\ &\quad + 2\pi \rho U b C(k) \left[-\dot{h} + U\theta + b\left(\frac{1}{2} - a\right)\dot{\theta} \right] \end{aligned} \tag{2.17}$$

or in Laplace Domain,

$$L_{EA} = \frac{\rho U^2}{2} b\, 2\pi \left[-\bar{p}^2 \frac{h}{b} + \bar{p}\,\theta + a\,\bar{p}^2\,\theta \right] + \frac{\rho U^2}{2} b\, 4\pi\, C(\bar{p}) \left[-\bar{p}\frac{h}{b} + \theta + \left(\frac{1}{2} - a\right)\bar{p}\,\theta \right] \tag{2.18}$$

where b is the semi-chord, a is the non-dimensional parameter defined by the distance from the mid-chord to the elastic axis divided by b, C(k) is the Theodorsen function and $\bar{p}$ is pb/U. Using the single lag approximation for the Theodorsen function in the Lapace Domain,

$$C(\bar{p}) = \frac{.55\bar{p} + .15}{\bar{p} + .15} \tag{2.19}$$

and with some algebraic manipulation, Eq.(2.18) becomes,

$$L_{EA} = \frac{\rho U^2}{2} b\, 2\pi \left[-\bar{p}^2 - 1.1\bar{p} - \frac{.135\bar{p}}{\bar{p} + .15} \right] \frac{h}{b} + \frac{\rho U^2}{2} b\, 2\pi \left[-a\,\bar{p}^2 + \left[1 + 1.1\left(\frac{1}{2} - a\right) \right] \bar{p} + 2 + \frac{\left[-.9 + .135\left(\frac{1}{2} - a\right)\bar{p} \right]}{\bar{p} + .15} \right] \theta \tag{2.20}$$

further simplification yields,

$$L_{EA} = -\frac{\rho U^2}{2} b\left[B_{2A}\bar{p}^2 + B_{1A}\bar{p} + B_{0A} + \frac{B_{3A}\bar{p}}{\bar{p}+.15} \right]\frac{h}{b} - \frac{\rho U^2}{2} b\left[B_{2B}\bar{p}^2 + B_{1B}\bar{p} + B_{0B} + \frac{B_{3B}\bar{p}}{\bar{p}+.15} \right]\theta \tag{2.21}$$

where,

$$\begin{aligned} B_{2A} &= -2\pi & B_{2B} &= -2a\pi \\ B_{1A} &= -2.2\pi & B_{1B} &= 2\pi + 2.2\pi\left(\frac{1}{2} - a\right) \\ B_{0A} &= 0 & B_{0B} &= 4\pi \\ B_{3A} &= -.270\pi & B_{3B} &= -1.8\pi + .270\pi\left(\frac{1}{2} - a\right) \end{aligned} \tag{2.22}$$

The aerodynamic moment about the elastic axis (reference line), M_{EA}, can be found in a similar way,

$$M_{EA} = \frac{\rho U^2 b^2}{2}\left[B_{2C}\,\bar{p}^2 + B_{1C}\,\bar{p} + B_{0C} + B_{3C}\,\frac{\bar{p}}{\bar{p}+.15} \right]\frac{h}{b} + \frac{\rho U^2 b^2}{2}\left[B_{2D}\,\bar{p}^2 + B_{1D}\,\bar{p} + B_{0D} + B_{3D}\,\frac{\bar{p}}{\bar{p}+.15} \right]\theta \tag{2.23}$$

where,

$$B_{2C} = -2a\pi \qquad B_{2D} = -2\pi\left(\frac{1}{8} + a^2\right)$$

$$B_{1C} = -(2.2\pi)\left(\frac{1}{2}+a\right) \qquad B_{1D} = 2\pi\left(\frac{1}{2}-a\right)\left[-1+1.1\left(\frac{1}{2}+a\right)\right]$$

$$B_{0C} = 0 \qquad B_{0D} = 4\pi\left(\frac{1}{2}+a\right) \tag{2.24}$$

$$B_{3C} = -(.270\pi)\left(\frac{1}{2}+a\right) \qquad B_{3D} = 2\pi\left(\frac{1}{2}+a\right)\left[-.9+.135\left(\frac{1}{2}-a\right)\right]$$

Here, for convenience in subsequent nonlinear analysis, the reference airforces will always be taken at the quarter-chord, so that $a = -1/2$. This gives the following simplified form of the coefficients,

$$\begin{aligned} B_{2A} &= -2\pi & B_{2B} &= \pi \\ B_{1A} &= -2.2\pi & B_{1B} &= 4.2\pi \\ B_{0A} &= 0 & B_{0B} &= 4\pi \\ B_{3A} &= -.27\pi & B_{3B} &= -1.53\pi \end{aligned} \tag{2.25}$$

$$\begin{aligned} B_{2C} &= \pi & B_{2D} &= -.75\pi \\ B_{1C} &= 0 & B_{1D} &= -2\pi \\ B_{0C} &= 0 & B_{0D} &= 0 \\ B_{3C} &= 0 & B_{3D} &= 0 \end{aligned}$$

Equations (2.21) and (2.23) would then express $L_{1/4}$ and $M_{1/4}$ respectively, with h and θ being the deflections at the quarter-chord. The corresponding structural coordinates $q_1$and q_2, which define deflections at the mid-chord as shown in Fig. 1, should then be transferred to the quarter-chord using the relations,

$$\begin{aligned} h &= q_1 + \frac{b}{2}q_2 \\ \theta &= q_2 \end{aligned} \tag{2.26}$$

Inserting Eqs. (2.26) into the unsteady, incompressible lift equation (2.21) yields,

$$L_{\frac{1}{4}} = \frac{1}{2}\rho U^2 b\left[B_{2A}\bar{p}^2 + B_{1A}\bar{p} + B_{0A} + B_{3A}\frac{\bar{p}}{\bar{p}+.15}\right]\frac{q_1}{b}$$
$$+\frac{1}{2}\rho U^2 b\left[\left(B_{2B}+\frac{1}{2}B_{2A}\right)\bar{p}^2 + \left(B_{1B}+\frac{1}{2}B_{1A}\right)\bar{p} + \left(B_{0B}+\frac{1}{2}B_{0A}\right) + \left(B_{3B}+\frac{1}{2}B_{3A}\right)\frac{\bar{p}}{\bar{p}+.15}\right]q_2 \tag{2.27}$$

Inserting Eqs. (2.26) into the moment equation (2.23) similarly yields,

$$M_{\frac{1}{4}} = \frac{1}{2}\rho U^2 b^2\left[B_{2C}\bar{p}^2 + B_{1C}\bar{p} + B_{0C} + B_{3C}\frac{\bar{p}}{\bar{p}+.15}\right]\frac{q_1}{b}$$
$$+\frac{1}{2}\rho U^2 b^2\left[\left(B_{2D}+\frac{1}{2}B_{2C}\right)\bar{p}^2 + \left(B_{1D}+\frac{1}{2}B_{1C}\right)\bar{p} + \left(B_{0D}+\frac{1}{2}B_{0C}\right) + \left(B_{3D}+\frac{1}{2}B_{3C}\right)\frac{\bar{p}}{\bar{p}+.15}\right]q_2 \tag{2.28}$$

Placing these into the basic equations of motion gives the right hand side of Eq. (2.1), L, as,

$$L = \frac{1}{2}\rho U^2 b\left[\bar{B}_{2A}\bar{p}^2 + \bar{B}_{1A}\bar{p} + \bar{B}_{0A} + \bar{B}_{3A}\frac{\bar{p}}{\bar{p}+.15}\right]\frac{q_1}{b}$$
$$+\frac{1}{2}\rho U^2 b\left[\bar{B}_{2B}\,\bar{p}^2 + \bar{B}_{1B}\,\bar{p} + \bar{B}_{0B} + \bar{B}_{3B}\frac{\bar{p}}{\bar{p}+.15}\right]q_2 \tag{2.29}$$

Similarly, combining Eqs. (2.27) and (2.28) to form the right hand side of Eq. (2.2), $eL+M_\alpha$, gives,

$$\frac{b}{2} L + M_{\underline{\alpha}} = \frac{1}{2} \rho U^2 b^2 \left[\overline{B}_{2C} \overline{p}^2 + \overline{B}_{1C} \overline{p} + \overline{B}_{0C} + \overline{B}_{3C} \frac{\overline{p}}{\overline{p}+.15} \right] \frac{q_1}{b} + \frac{1}{2} \rho U^2 b^2 \left[\overline{B}_{2D} \overline{p}^2 + \overline{B}_{1D} \overline{p} + \overline{B}_{0D} + \overline{B}_{3D} \frac{\overline{p}}{\overline{p}+.15} \right] q_2 \tag{2.30}$$

where,

$$\begin{aligned} \overline{B}_{iA} &= B_{iA} \\ \overline{B}_{iB} &= B_{iB} + \frac{1}{2} B_{iA} \\ \overline{B}_{iC} &= B_{iC} + \frac{1}{2} B_{iA} \\ \overline{B}_{iD} &= B_{iD} + \frac{1}{2} B_{iC} + \frac{1}{2} B_{iB} + \frac{1}{4} B_{iA} \qquad (i = 0,1,2,3) \end{aligned} \tag{2.31}$$

Then, introducing the augmented state variables $Y_{S,}$ defined as,

$$\begin{aligned} Y_1 &= \frac{\overline{p}}{\overline{p}+.15} q_1 \\ Y_2 &= \frac{\overline{p}}{\overline{p}+.15} q_2 \end{aligned} \tag{2.32}$$

and, reverting back to time domain, yields,

$$L = \frac{1}{2} \rho U^2 \left[\overline{B}_{2A} \ddot{q}_1 + \overline{B}_{1A} \dot{q}_1 + \overline{B}_{0A} q_1 + \overline{B}_{3A} Y_1 \right] + \frac{1}{2} \rho U^2 b \left[\overline{B}_{2B} \ddot{q}_2 + \overline{B}_{1B} \dot{q}_2 + \overline{B}_{0B} q_2 + \overline{B}_{3B} Y_2 \right] \tag{2.33}$$

$$\frac{b}{2}L + M_\alpha = \frac{1}{2}\rho U^2 b\left[\overline{B}_{2C}\,\ddot{q}_1 + \overline{B}_{1C}\,\dot{q}_1 + \overline{B}_{0C}\,q_1 + \overline{B}_{3C}\,Y_1\right] + \frac{1}{2}\rho U^2 b^2\left[\overline{B}_{2D}\,\ddot{q}_2 + \overline{B}_{1D}\,\dot{q}_2 + \overline{B}_{0D}\,q_2 + \overline{B}_{3D}\,Y_2\right] \tag{2.34}$$

$$\dot{Y}_1 + \frac{U}{b}(.15)Y_1 = \dot{q}_1 \tag{2.35}$$

$$\dot{Y}_2 + \frac{U}{b}(.15)Y_2 = \dot{q}_2 \tag{2.36}$$

The equations of motion can then be formed by placing Eqs. (2.33) and (2.34) into the right hand side of Eqs. (2.1) and (2.2). Together with the augmentated state equations (2.35) and (2.36) they can be written in the matrix form as,

$$\begin{bmatrix} M^* & 0 & 0 \\ 0 & M^* & 0 \\ 0 & 0 & I \end{bmatrix}\begin{Bmatrix} \dot{q} \\ \ddot{q} \\ \dot{Y} \end{Bmatrix} + \begin{bmatrix} 0 & -M^* & 0 \\ K^* & B^* & G^* \\ 0 & -I & H^* \end{bmatrix}\begin{Bmatrix} q \\ \dot{q} \\ Y \end{Bmatrix} = 0 \tag{2.37}$$

multiplying by inverse of first matrix gives,

$$\begin{Bmatrix} \dot{q} \\ \ddot{q} \\ \dot{Y} \end{Bmatrix} = \begin{bmatrix} 0 & I & 0 \\ -M^{*-1}K^* & -M^{*-1}B^* & -M^{*-1}G^* \\ 0 & I & -H^* \end{bmatrix}\begin{Bmatrix} q \\ \dot{q} \\ Y \end{Bmatrix} \tag{2.38}$$

where,

$$M^{*} = -\begin{bmatrix} M & -S_{\alpha} \\ -S_{\alpha} & I_{\alpha} \end{bmatrix} - \frac{1}{2}\rho U^{2}\frac{b^{2}}{U^{2}}\begin{bmatrix} \overline{B}_{2A} & b\,\overline{B}_{2B} \\ b\,\overline{B}_{2C} & b^{2}\,\overline{B}_{2D} \end{bmatrix}$$

$$= \begin{bmatrix} M - \frac{1}{2}\rho b^{2}\,\overline{B}_{2A} & -S_{\alpha} - \frac{1}{2}\rho b^{3}\,\overline{B}_{2B} \\ -S_{\alpha} - \frac{1}{2}\rho b^{3}\,\overline{B}_{2C} & I_{\alpha} - \frac{1}{2}\rho b^{4}\,\overline{B}_{2D} \end{bmatrix} \qquad (2.39)$$

$$B^{*} = -\frac{1}{2}\rho U^{2}\frac{b}{U}\begin{bmatrix} \overline{B}_{1A} & b\,\overline{B}_{1B} \\ b\,\overline{B}_{1C} & b^{2}\,\overline{B}_{1D} \end{bmatrix}$$

$$= \begin{bmatrix} -\frac{1}{2}\rho U b\,\overline{B}_{1A} & -\frac{1}{2}\rho U b^{2}\,\overline{B}_{1B} \\ -\frac{1}{2}\rho U b^{2}\,\overline{B}_{1C} & -\frac{1}{2}\rho U b^{3}\,\overline{B}_{1D} \end{bmatrix} \qquad (2.40)$$

$$K^{*} = \begin{bmatrix} K_{h} & 0 \\ 0 & K_{\alpha} \end{bmatrix} - \frac{1}{2}\rho U^{2}\begin{bmatrix} \overline{B}_{0A} & b\,\overline{B}_{0B} \\ b\,\overline{B}_{0C} & b^{2}\,\overline{B}_{0D} \end{bmatrix}$$

$$= \begin{bmatrix} K_{h} - \frac{1}{2}\rho U^{2}\,\overline{B}_{0A} & -\frac{1}{2}\rho U^{2} b\,\overline{B}_{3B} \\ -\frac{1}{2}\rho U^{2} b\,\overline{B}_{0C} & K_{\alpha} - \frac{1}{2}\rho U^{2} b^{2}\,\overline{B}_{0D} \end{bmatrix} \qquad (2.41)$$

$$G^{*} = -\frac{1}{2}\rho U^{2}\begin{bmatrix} \overline{B}_{3A} & b\,\overline{B}_{3B} \\ b\,\overline{B}_{3C} & b^{2}\,\overline{B}_{3D} \end{bmatrix}$$

$$= \begin{bmatrix} -\frac{1}{2}\rho U^{2}\,\overline{B}_{3A} & -\frac{1}{2}\rho U^{2} b\,\overline{B}_{3B} \\ -\frac{1}{2}\rho U^{2} b\,\overline{B}_{3C} & -\frac{1}{2}\rho U^{2} b^{2}\,\overline{B}_{3D} \end{bmatrix} \qquad (2.42)$$

$$H^* = \frac{U}{b}\begin{bmatrix} .15 & 0 \\ 0 & .15 \end{bmatrix} \tag{2.43}$$

and I is the identity matrix. The eigenvalues of the matrix in Eq. (2.38) are solved for different values of U. In this study, there are six eigenvalues, two pairs of complex conjugates and two real roots. These roots form a root locus plot. The flutter velocity is the velocity associated with the complex root which changes from having negative real value to positive real value. In addition, the divergence velocity can be found by examining the two real roots. One of the real root will become zero at the divergence velocity. The divergence velocity can also be found from the matrix K*. The velocity which makes the determinate of K* equal to zero is the divergence velocity. The results using the values listed in Appendix A are shown in Chapter 4.

2.4 Linear Flutter Analysis -- U-g method

Another conventional ways to analyze linear flutter problem is the U-g method. As expected, this method starts with the basic equation of motion, Eqs. (2.1) and (2.2). The forcing terms of the equations are formulated by assuming complex sinusoidal motion,

$$\begin{aligned} h(t) &= h\,e^{i\omega t} \\ \theta(t) &= \theta\,e^{i\omega t} \end{aligned} \tag{2.44}$$

The aerodynamic lift for 2-dimensional, incompressible flow is then given by,

$$L = \pi \rho b^2 \left[\omega^2 h + U i\omega \theta + \omega^2 b a \theta \right] e^{i\omega t} + 2\pi \rho U b C(k) \left[-i\omega h + U\theta + i\omega b \left(\frac{1}{2} - a \right) \theta \right] e^{i\omega t} \quad (2.45)$$

where C(k) is the Theodorsen function, and a is the same as defined in Section 2.3. With some algebraic manipulations, Eq. (2.40) becomes,

$$L = \pi \rho \omega^2 b^3 \left[l_h \frac{h}{b} + l_\theta \theta \right] \quad (2.46)$$

where,

$$l_h = 1 - \frac{2iC(k)}{k} \quad (2.47)$$

$$l_\theta = a + \frac{2C(k)}{k^2} + \frac{i}{k} \left(1 + 2C(k) \left(\frac{1}{2} - a \right) \right) \quad (2.48)$$

Similarly, the aerodynamic moment can be found by assuming complex sinusoidal motion, the final formulation are written,

$$M_\alpha = \pi \rho \omega^2 b^4 \left[m_h \frac{h}{b} + m_\theta \theta \right] \quad (2.49)$$

where,

$$m_h = a - i2 \left(\frac{1}{2} + a \right) \frac{C(k)}{k} \quad (2.50)$$

$$m_\theta = \frac{1}{8} + a^2 + 2\left(\frac{1}{2} + a\right)\frac{C(k)}{k^2} + \frac{i}{k}\left(\frac{1}{2} - a\right)\left(2\left(\frac{1}{2} + a\right)C(k) - 1\right) \tag{2.51}$$

Again, as stated in Section 2.3, the reference airforces will always be taken at the quarter-chord for later nonlinear convenience, then, a = *-1/2*. The corresponding strutural coordinates q_1 and q_2, which define deflections at the mid-chord, should also be transferred to the quarter-chord using Eqs. (2.27). Eqs. (2.41) and (2.44) then becomes,

$$L = \pi \rho \omega^2 b^3 \left[l_h \frac{q_1}{b} + \left(l_\theta + \frac{1}{2} l_h \right) q_2 \right] \tag{2.52}$$

$$M = \pi\rho\omega^2 b^4 \left[\left(m_h + \frac{1}{2} l_h \right)\frac{q_1}{b} + \left(m_\theta + \frac{1}{2} m_h \right) q_2 + \left(\frac{l_\theta}{2} + \frac{l_h}{4} \right) q_2 \right] \tag{2.53}$$

Placing a = -1/2 in Eqs. (2.42), (2.43), (2.45), and (2.46), results are much simplified, they are,

$$l_h = 1 - i\frac{2C(k)}{k} \tag{2.54}$$

$$l_\theta = -\frac{1}{2} + \frac{2C(k)}{k^2} + \frac{i}{k}(1 + 2C(k)) \tag{2.55}$$

$$m_h = -\frac{1}{2} \tag{2.56}$$

$$m_\theta = \frac{3}{8} - \frac{i}{k} \tag{2.57}$$

In formulating the structural terms, instead of incorporating viscous damping terms, structural damping terms is inserted into the Eqs. (2.1) and (2.2). The resulting equations can then be written as,

$$M\,\ddot{q}_1 - S_\alpha\,\ddot{q}_2 + K_h\,(1+ig)\,q_1 - L = 0 \tag{2.58}$$

$$-S_\alpha\,\ddot{q}_1 + I_\alpha\,\ddot{q}_2 + K_\alpha\,(1+ig)\,q_2 - \left(\frac{b}{2}L + M_\alpha\right) = 0 \tag{2.59}$$

Substituting Eqs. (2.41) and (2.44), along with the appropriate sub-components and Eqs. (2.27), into Eqs. (2.53) and (2.54), yields the following form of the equation of motion, written in matrix form,

$$\begin{bmatrix} (B_{11} - K_h\,Z) & B_{12} \\ B_{21} & (B_{22} - K_\alpha\,Z) \end{bmatrix} \begin{Bmatrix} \bar{q}_1 \\ \bar{q}_2 \end{Bmatrix} = 0 \tag{2.60}$$

where

$$B_{11} = M + \pi\rho b^2 l_h \tag{2.61}$$

$$B_{12} = -S_\alpha + \pi\rho b^3\left(l_\theta + \frac{1}{2}l_h\right) \tag{2.62}$$

$$B_{21} = -S_\alpha + \pi\rho b^3\left(m_h + \frac{1}{2}l_h\right) \tag{2.63}$$

$$B_{22} = I_\alpha + \pi\rho b^4\left(m_\theta + \frac{1}{2}m_h + \frac{1}{2}l_\theta + \frac{1}{4}l_h\right) \tag{2.64}$$

and,

$$Z = \frac{1+ig}{\omega^2} \tag{2.65}$$

The solution method is to select a value of reduced frequency, and solve Eq. (2.31) for all complex eigenvalues Z_i. For each value of Z, the corresponding structural damping, frequency and velocity are given by,

$$g = \frac{\mathrm{Im}\{Z\}}{\mathrm{Re}\{Z\}} \quad ; \quad \omega = \frac{1}{\sqrt{\mathrm{Re}\{Z\}}} \quad ; \quad U = \frac{\omega\, b}{k} \tag{2.66}$$

The procedure is repeated for several values of the reduced frequency, k, until sufficient number of data points have been generated to produce a smooth U-g diagram. The flutter point is where the structural damping, g, goes to zero. The frequency and velocity corresponding to that point is the flutter frequency and flutter velocity respectively.

At first glance, the typical section analysis seems crude. However, the method characterizes the entire wing fairly accurate. To modify the typical section for an actual wing with varying spanwise deflection, one would replace q_1 and q_2 with $\phi_1(x)\, q_1$ and $\phi_2(x)\, q_2$, where $\phi_1(x)$ and $\phi_2(x)$ represent the first bending and first torsion modes respectively. Multiplying Eq. (2.53) by $\phi_1(x)$, Eq. (2.54) by $\phi_2(x)$ and integrating over the span, $\int d\tilde{x}$, gives (for uniform wing properties),

$$I_1\, M\, \ddot{q}_1 - I_2\, S_\alpha\, \ddot{q}_2 + I_1\, k_h\, (1 + ig)\, q_1 - \int \phi_1\, L\, d\tilde{x} = 0 \tag{2.67}$$

$$-I_2\, S_\alpha\, \ddot{q}_1 + I_3\, I_\alpha\, \ddot{q}_2 + I_3\, k_\alpha\, (1 + ig)\, q_2 - \int \phi_2\, M_\alpha\, d\tilde{x} = 0 \tag{2.68}$$

where I_1, I_2, and I_3 are aerodynamic integrals defined in Appendix A. Dividing Eq. (2.62) by I_1 and similarly, divide Eq. (2.63) by I_3 and organize in matrix form similar to Eq. (2.55) gives,

$$\begin{bmatrix} (B_{11} - K_h Z) & \frac{I_2}{I_1} B_{12} \\ \frac{I_2}{I_3} B_{21} & (B_{22} - K_\alpha Z) \end{bmatrix} \begin{Bmatrix} \bar{q}_1 \\ \bar{q}_2 \end{Bmatrix} = 0 \tag{2.69}$$

The determinate is then,

$$\det[\ ] = (B_{11} - K_h Z)(B_{22} - K_\alpha Z) - \frac{I_2^2}{I_3 I_1} B_{21} B_{12} \tag{2.70}$$

The accuracy is effected by the ratio $I_2^2 / I_1 I_3$. In the present study the ratio is 0.92, which gives only a small correction to the typical section results. The results of U-g analysis is shown in Chapter 4.

CHAPTER 3

NONLINEAR THEORY

3.1 Nonlinearity in Aeroelasticity

Nonlinearity in aeroelasticity can arise from either the structure or aerodynamics. Nonlinearities related to structures are either of geometric or material origin. Geometric nonlinearities depend only on geometric quantities, such as displacement or length, such as in large deflection of beams and plates, or large displacement of helicopter blades. Material nonlinearities can arise from stiffness properties of a particular structure. On the other hand, nonlinearity due to aerodynamics can arise from stalling and the attendant flow separation of an aircraft wing.

Nonlinear limit cycle oscillations can originate from either aerodynamic or structural nonlinearity or a combination of both [Ref. 30]. A simple example of a generic system with stiffening springs can illustrate the concept of limit cycle oscillation (see Fig. 3). In such a system, if assumption of linear stiffness characteristic is prescribed, then the oscillation amplitude would grow exponentially. However, if the spring behaves nonlinearly, as the oscillation penetrates the nonlinear region, the effective stiffness may increase and the oscillation can settle down to a constant amplitude, steady, limit cycle oscillation.

The present investigation will concentrate in particular on the aerodynamic nonlinearity. The including of structural nonlinearities is discussed briefly in Appendix F.

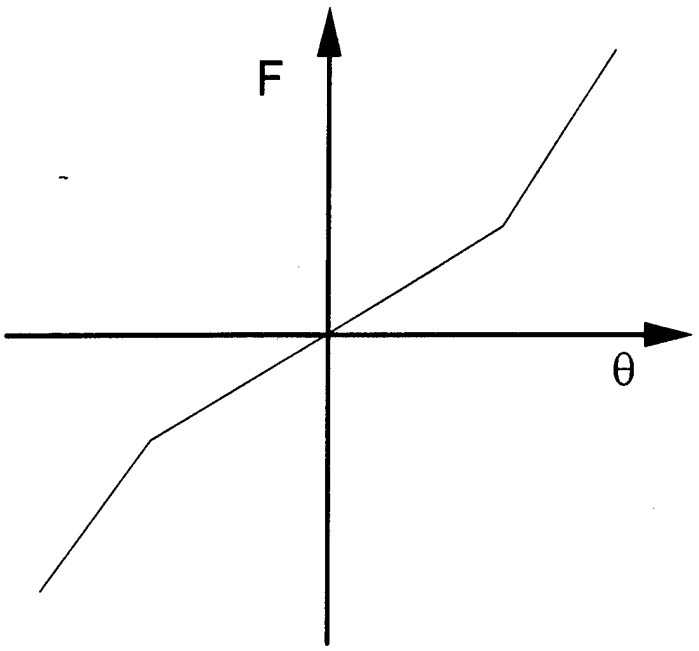

Spring force curve

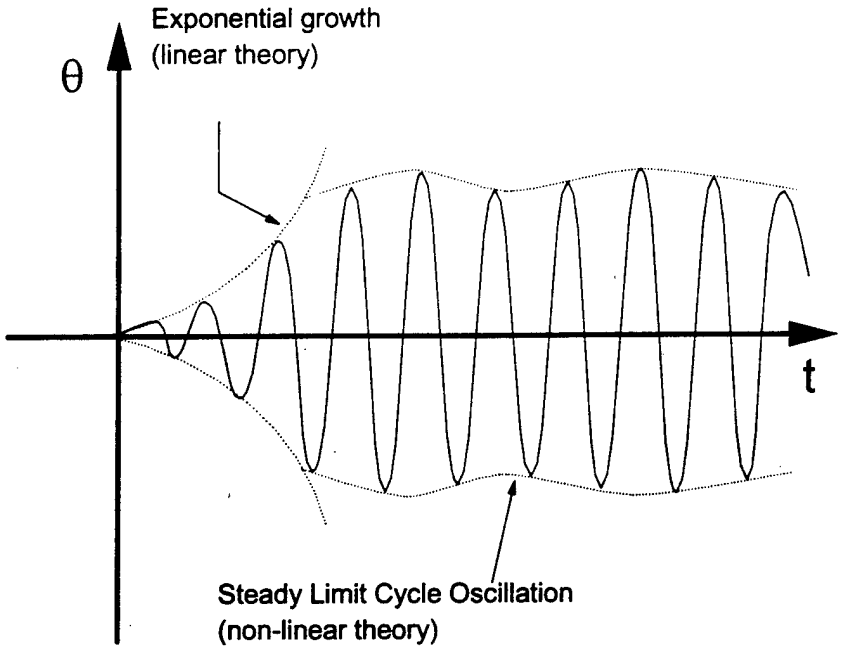

Figure 3. Example of Nonlinear Limit Cycle Oscillation

3.2 ONERA Aerodynamic Model

The aerodynamic model used for this study was initially developed at *Office National d'Etudes et de Recherché Aerospatiale* (ONERA) by Tran & Petot [Ref. 10] and by Dat & Tran [Ref. 11]. This aerodynamic model is a semi-empirical, unsteady, nonlinear model. It uses quasi-linear, small amplitude oscillation, experimental data to predict aerodynamic forces on an oscillating airfoil that experiences dynamic stall. The model incorporates the Theodorsen function for linear theory by inserting a single lag term operating on the linear part of the airfoil's static force curve. The model also includes a two lag term on the stalling portion of the airfoil's static force curve.

The ONERA model was later investigated by Peters [Ref. 12] to distinguish between the angle of attack due to pitching and angle of attack due to vertical motion of the aircraft. The final form of the ONERA model used in the present study are shown below,

$$C_z = C_{z1} + C_{z2} \tag{3.1}$$

$$C_{z1} = s_{z1}\,\dot{\alpha} + s_{z2}\,\ddot{\theta} + s_{z3}\,\dot{\theta} + C_{z_\gamma} \tag{3.2}$$

$$\dot{C}_{z_\gamma} + \lambda_1\, C_{z_\gamma} = \lambda_1\, a_{oL}\left(\alpha + \dot{\theta}\right) + \lambda_2\, a_{oL}\left(\dot{\alpha} + \ddot{\theta}\right) \tag{3.3}$$

$$\ddot{C}_{z2} + r_1\,\dot{C}_{z2} + r_2\, C_{z2} = -r_2\,\Delta C_z|_\alpha - r_3\,\Delta \dot{C}z|_\alpha \tag{3.4}$$

where the angle of attack α, is separated into pitching and plunging as illustrated in Fig. 2 and the non-dimensional time derivative is denoted by,

$$\left(\dot{}\right) \equiv \frac{\partial(\,)}{\partial\tau}\;;\; \tau \equiv \frac{Ut}{b} \tag{3.5}$$

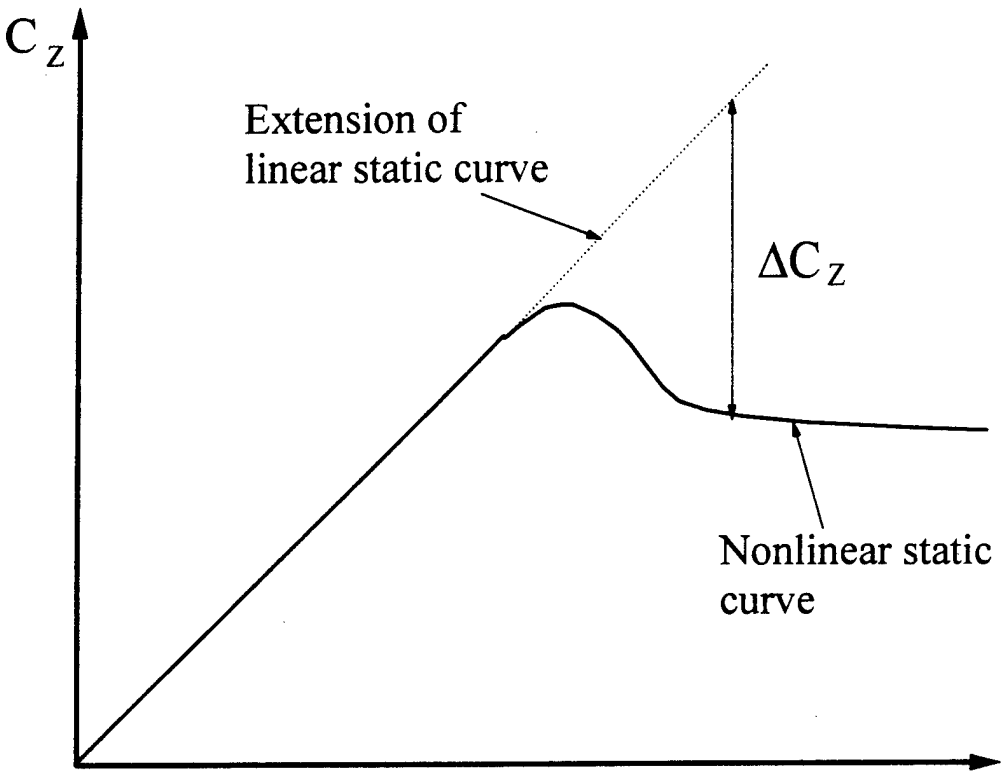

Figure 4. Description of static aerodynamic curve

The aerodynamic force curve is shown in Figure 4. The function C_Z can represent any of the relevant non-dimensional aerodynamic force coefficients: C_L, the lift coefficients, C_D, the drag coefficient or, C_M, the moment coefficient. The function C_{Z1} is the static force in linear, unstalled flow, extended to high angles of attack. The function C_{Z2} represents the nonlinear aerodynamic force contribution to the total C_Z. The ΔC_Z function is the nonlinear deviation from the extended linear force curve. In addition, ΔC_Z is also the input which determines the magnitude of the contribution of C_{Z2} to the total aerodynamic force. The coefficients, s_{Z1}, s_{Z2}, s_{Z3}, λ_1, λ_2, r_1, r_2, r_3 are determined empirically and are associated with the appropriate force coefficient. These coefficients are listed in Appendix A.

Equations (3.2) and (3.3) describes the linear portion of the model where $C_{L\gamma}$ is the linear circulatory contribution incorporating aerodynamic lag due to formation of tip vortices. The function ΔC_Z is defined positive for a decrease in the aerodynamic force beyond stall angle, as shown in Fig. 4. The general form of the static aerodynamic force curve is given by,

$$C_z(\alpha) = a_{oz}\,\alpha - \Delta C_z(\alpha) \tag{3.6}$$

where a_{oZ} is the slope of linear aerodynamic force. In general, ΔC_Z can be approximated in any manner appropriate for the particular study. In the present investigation, the objective is to develop a simple, nonlinear, analytic aeroelastic flutter analysis. The function ΔC_Z is therefore described by a single straight line fit between discrete points as shown in Figure 5.

3.3 Harmonic Balance Method

The flutter equations and related components have all been stated in differential form. It remains to reduce the system of differential equations to algebraic form so that it is more easily solved computationally. By assuming harmonic motion, the harmonic balance method is a powerful way to transform a system of nonlinear differential equations to a simpler algebraic form.

The linear and nonlinear aerodynamic force can be written with mean, sine and cosine parts as,

$$C_Z = C_{Zo} + C_{ZS1}\sin k\tau + C_{ZC1}\cos k\tau + C_{ZS2}\sin 2k\tau + C_{ZC2}\cos 2k\tau \tag{3.7}$$

$$C_{Z1} = C_{Z1o} + C_{Z1S}\sin k\tau + C_{Z1C}\cos k\tau \tag{3.8}$$

$$C_{Z2} = C_{Z2o} + C_{Z2S1}\sin k\tau + C_{Z2C1}\cos k\tau + C_{Z2S2}\sin 2k\tau + C_{Z2C2}\cos 2k\tau \tag{3.9}$$

3.3a Linear Aerodynamic Forces

As a preparation of nonlinear flutter analysis and the harmonic balance method, harmonic decomposition of the aerodynamic forces were necessary. First, harmonic motion is assumed for the pitching angle and deflection at the 1/4 chord,

$$\theta(\tau) = \theta_o + \theta_s \sin k\tau + \theta_c \cos k\tau \tag{3.10}$$

$$h(\tau) = h_o + h_s \sin k\tau + h_c \cos k\tau \tag{3.11}$$

where,

$$k = \text{reduced frequency} = \frac{\omega b}{U}$$

$$\tau = \text{non-dimensional time} = \frac{Ut}{b}$$

The first and second non-dimensional time derivative of Eqs. (3.10) and (3.11) are also needed for subsequent analysis, they are,

$$\dot{\theta} = \theta_s k \cos k\tau - \theta_c k \sin k\tau \tag{3.12}$$

$$\ddot{\theta} = -\theta_s k^2 \sin k\tau - \theta_c k^2 \cos k\tau \tag{3.13}$$

$$\dot{h} = h_s k \cos k\tau - h_c k \sin k\tau \tag{3.14}$$

$$\ddot{h} = -h_s k^2 \sin k\tau - h_c k^2 \cos k\tau \tag{3.15}$$

The angle of attack is a combination of angle of attack due to pitching and angle of attack due to plunging as stated in Eq. (2.4). Substituting Eqs. (3.10) and (3.14) into Eq. (2.4) gives,

$$\alpha = \alpha_o + \alpha_s \sin k\tau + \alpha_c \cos k\tau \tag{3.16}$$

where

$$\alpha_o = \theta_o \tag{3.17}$$

$$\alpha_s = \theta_s + \frac{h_c}{b} k \tag{3.18}$$

$$\alpha_c = \theta_c - \frac{h_s}{b} k \tag{3.19}$$

Similarly, Eq. (3.3), the circulatory part of the linear aerodynamics, can be written in the form of,

$$C_{Z\gamma} = C_{Z\gamma o} + C_{Z\gamma s} \sin k\tau + C_{Z\gamma c} \cos k\tau \tag{3.20}$$

$$\dot{C}_{Z\gamma} = k\, C_{Z\gamma s} \cos k\tau - k\, C_{Z\gamma c} \sin k\tau \tag{3.21}$$

Substituting Eqs. (3.20) and (3.21) into the left hand side of Eq. (3.3), and inserting Eqs. (3.10) and (3.11) into the right hand side of the same equation. Matching the mean, sine and cosine terms of the resulting equation, gives,

$$C_{Z\gamma o} = a_{oZ}\, \theta_o \tag{3.22}$$

$$C_{Z\gamma S} = F(k)\, L_S - G(k)\, L_C \tag{3.23}$$

$$C_{Z\gamma C} = G(k)\, L_S + F(k)\, L_C \tag{3.24}$$

where, in the present study, the F(k) and G(k) functions are the approximations to the Theodorsen function, C(k) = F(k) + iG(k), namely,

$$F(k) = \frac{k^2\lambda_2 + \lambda_1^2}{\lambda_1^2 + k^2} \tag{3.25}$$

$$G(k) = \frac{k\,\lambda_1\,(\lambda_2 - 1)}{\lambda_1^2 + k^2} \tag{3.26}$$

which result from using the single lag pole approximation of the generalized Theodorsen function, $C(p) = (\lambda_2 p + \lambda_1)/(p + \lambda_1)$, with $p = ik$, $\lambda_1 = 0.15$, $\lambda_2 = 0.55$, and where other intermediate variables are,

$$L_S = a_{oZ}\left(\theta_S - k\frac{h_C}{b} - k\,\theta_C\right) \tag{3.27}$$

$$L_C = a_{oZ}\left(\theta_C + k\frac{h_S}{b} + k\,\theta_S\right) \tag{3.28}$$

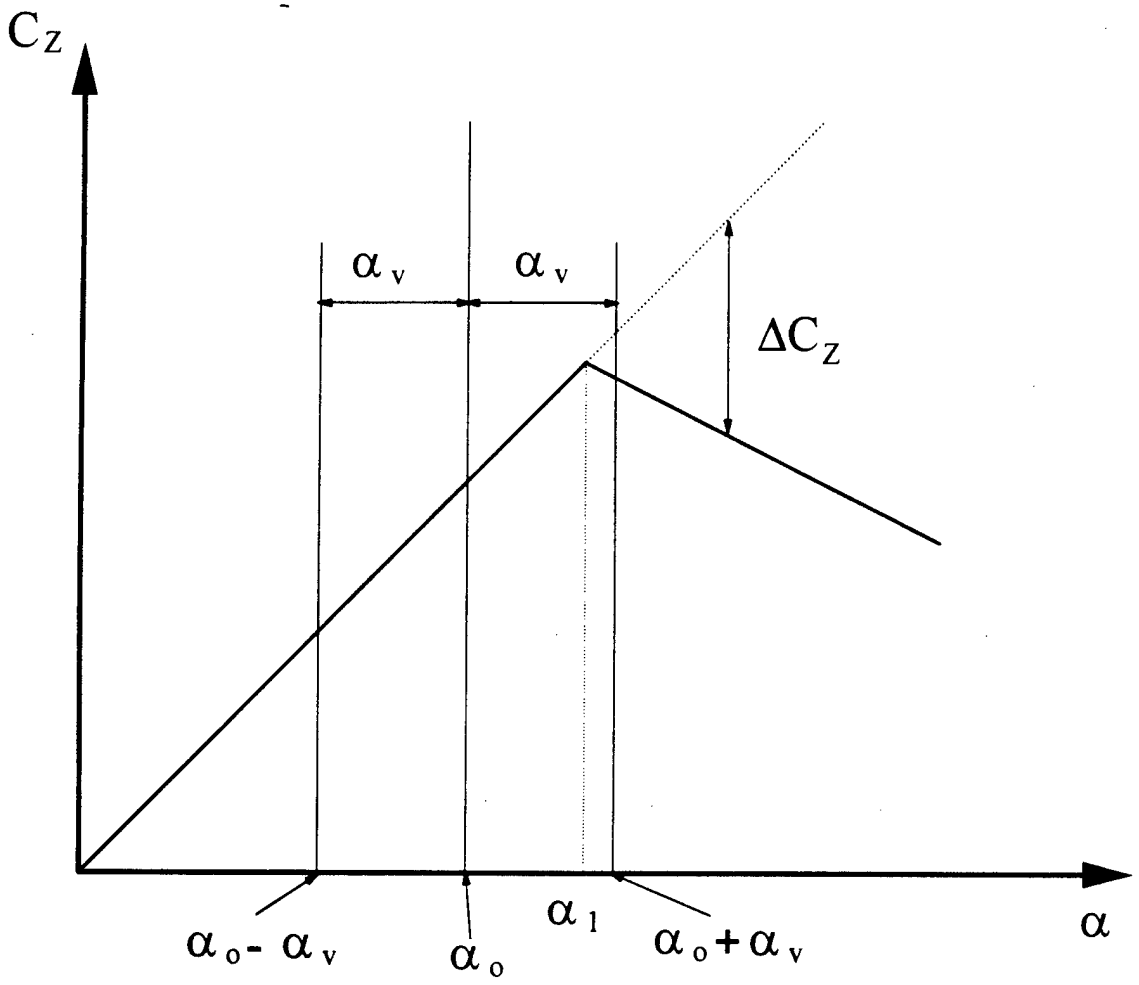

Figure 5. Example of oscillation straddling stall angle on aerodynamic force curve

Finally, combining the harmonic form of the circulatory terms, Eqs. (3.22), (3.23), and (3.24), and the harmonic form of the remaining linear terms in Eq. (3.2) gives the linear portion of the aerodynamic coefficient C_{Z1} in Eq. (3.8) as,

$$C_{Z1o} = C_{Z\gamma o} \tag{3.29}$$

$$C_{Z1S} = s_{Z1}\left(-k\,\theta_S + \frac{h_S}{b}k^2\right) - s_{Z2}\,\theta_S\,k^2 - s_{Z3}\,k\,\theta_C + C_{Z\gamma S} \tag{3.30}$$

$$C_{Z1C} = s_{Z1}\left(k\,\theta_S + \frac{h_C}{b}k^2\right) - s_{Z2}\,\theta_C\,k^2 + s_{Z3}\,k\,\theta_S + C_{Z\gamma C} \tag{3.31}$$

3.3b Nonlinear Aerodynamic Forces

For the nonlinear portion of the ONERA aerodynamic model, similar harmonic decomposition procedure was performed. As stated previously, the aerodynamic force curve is modeled by a single break point approximation. The nonlinear deviation from the extended linear force curve, ΔC_Z, is therefore parameterized by a single straight line with the form,

$$\Delta C_z = b_1(\alpha - \alpha_1) \tag{3.32}$$

where α_1 represents the stall angle. Equation (3.32) is only valid in the stalled region described in Fig. 5. The manipulations of the equations. can be further simplified if the angle of attack is put in the form where it is purely sinusoidal,

$$\alpha = \alpha_o + \alpha_\nu \sin\phi \tag{3.33}$$

where,

$$\alpha_V = \sqrt{\alpha_S^2 + \alpha_C^2} \tag{3.34}$$

$$\phi = k\tau + \xi \tag{3.35}$$

$$\xi = \sin^{-1} \frac{\alpha_c}{\alpha_v} \tag{3.36}$$

The formula for ΔC_Z can also be written in the form of sinusoidal components,

$$\Delta C_Z = \Delta C_{Zo} + \Delta C_{ZS1} \sin\phi + \Delta C_{ZC2} \cos 2\phi \tag{3.37}$$

Note that, in the above formulation, there is only sine term associated with the first harmonic. This is due to the fact that ΔC_Z is a single-valued function of α. The two functions are always in phase with each other, therefore there is no cosine term in Eq. (3.37). Similarly, there is only cosine terms associated with the second harmonic. Substituting Eq. (3.33) into Eq. (3.32), Fourier analysis then gives the relations for ΔC_{Zo}, ΔC_{ZS1}, and ΔC_{ZC2}.

$$\Delta C_{Zo} = \tfrac{1}{\pi} \int_{\phi_1}^{\frac{\pi}{2}} b_1 (\alpha_o + \alpha_V \sin\phi - \alpha_1)\, d\phi \tag{3.38}$$

$$\Delta C_{ZS1} = \tfrac{2}{\pi} \int_{\phi_1}^{\frac{\pi}{2}} b_1 (\alpha_o + \alpha_V \sin\phi - \alpha_1) \sin\phi\, d\phi \tag{3.39}$$

$$\Delta C_{ZC2} = \tfrac{2}{\pi} \int_{\phi_1}^{\frac{\pi}{2}} b_1 (\alpha_o + \alpha_V \sin\phi - \alpha_1) \cos 2\phi\, d\phi \tag{3.40}$$

After some algebraic manipulation, the equations become,

$$\Delta C_{Zo} = \frac{b_1 \alpha_V}{\pi} \left[\left(\frac{\alpha_1 - \alpha_o}{\alpha_V} \right) \left(\phi_1 - \frac{\pi}{2} \right) + \cos\phi_1 \right] \tag{3.41}$$

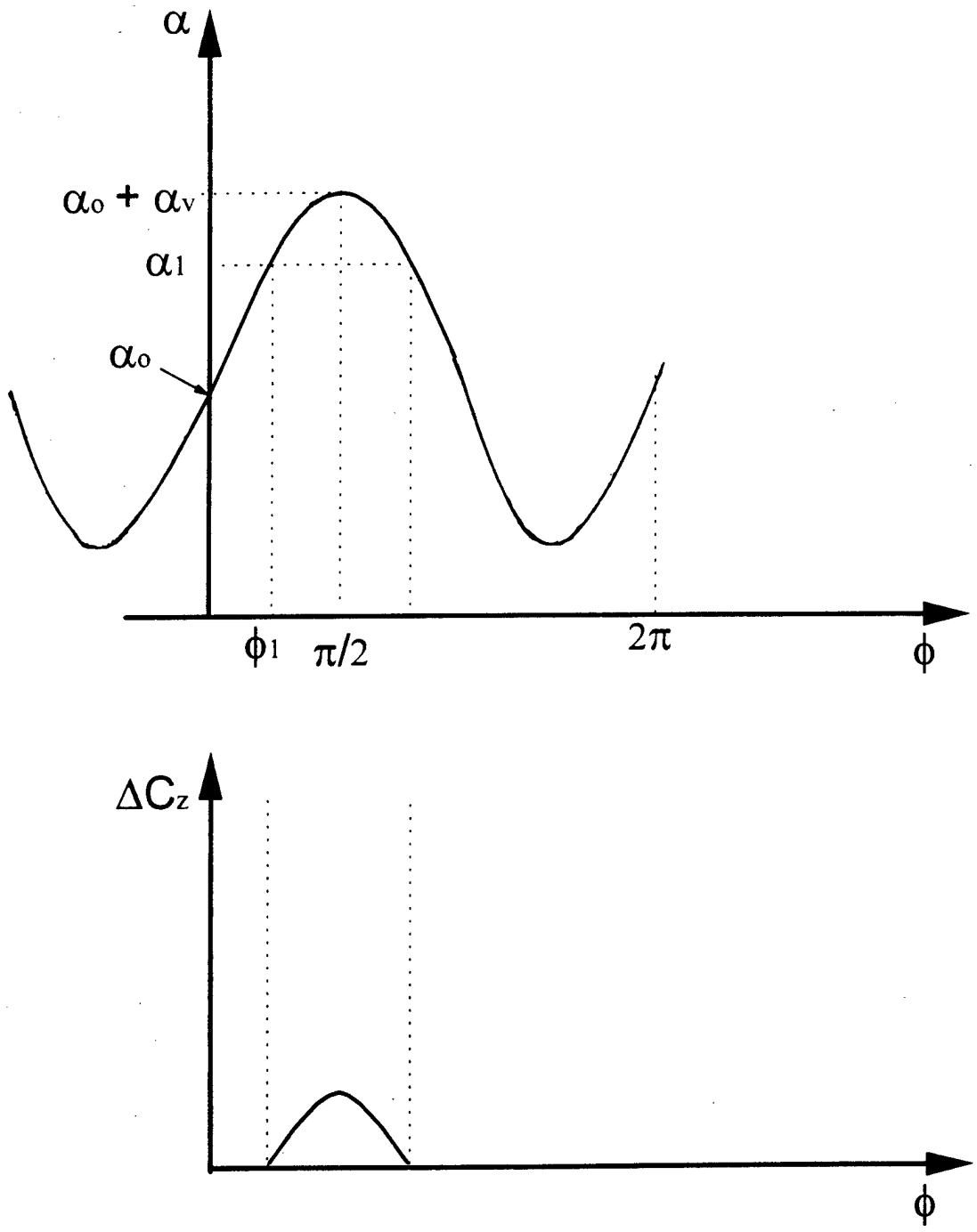

Figure 6. Oscillation straddling stall angle
in non-dimensional time domain

$$\Delta C_{ZS1} = \frac{b_1 \alpha_v}{\pi}\left[-\left(\phi_1 - \frac{\pi}{2}\right) - \frac{1}{2}\sin 2\phi_1\right] \tag{3.42}$$

$$\Delta C_{ZC2} = \frac{b_1 \alpha_v}{\pi}\left[-\frac{1}{2}\cos\phi_1 - \frac{1}{6}\sin 3\phi_1\right] \tag{3.43}$$

The parameter ϕ_1, a non-dimensional time variable associated with angle of attack, has relationships shown in Figure 6 and by the equations below,

$$\phi_1 = \sin^{-1}\delta \quad \text{if} \quad -1 < \delta < 1 \tag{3.44}$$

$$\phi_1 = \begin{cases} \frac{\pi}{2} & \text{if} \quad \delta > 1 \\ -\frac{\pi}{2} & \text{if} \quad \delta < -1 \end{cases} \tag{3.45}$$

where,

$$\delta = \frac{\alpha_1 - \alpha_o}{\alpha_v} \tag{3.46}$$

For those regions where ϕ_1 is undetermined, it takes on the values of $\pm\pi/2$, as described in Eq. (3.46). These values are arbitrarily set so that the limits of integration are correct in the Fourier analysis in Eqs. (3.38), (3.39) and (3.40). In the present analysis, the flutter oscillation amplitude may reach the negative side of the aerodynamic force curve, see Appendix D for the formulation of the symmetric force curve.

With all the components needed to formulate the nonlinear aerodynamic force in harmonic form, it is just a matter of algebra. Substituting Eq. (3.9) and its non-dimensional time derivatives into left hand side of Eq. (3.4). Similarly,

inserting Eq. (3.37) into the right hand side of the Eq. (3.4) and express this right hand side as,

$$\begin{aligned} \text{R.H.S} = {} & R_o + R_{S1} \sin\phi + R_{C1} \cos\phi \\ & + R_{S2} \sin 2\phi + R_{C2} \cos 2\phi \end{aligned} \tag{3.47}$$

where

$$R_o = -r_2 \, \Delta C_{Zo} \tag{3.48}$$

$$R_{S1} = -r_2 \, \Delta C_{ZS1} \tag{3.49}$$

$$R_{C1} = -r_3 \, k \, \Delta C_{ZS1} \tag{3.50}$$

$$R_{S2} = 2 r_3 \, k \, \Delta C_{ZC2} \tag{3.51}$$

$$R_{C2} = -r_2 \, \Delta C_{ZC2} \tag{3.52}$$

The harmonic components of nonlinear portion of aerodynamic force, C_{Z2}, are found by matching terms of both sides of Eq. (3.4) then gives,

$$\begin{aligned} C_{Z2} = {} & B_{Zo} + B_{ZS1} \sin\phi + B_{ZC1} \cos\phi \\ & + B_{ZS2} \sin 2\phi + B_{ZC2} \cos 2\phi \end{aligned} \tag{3.53}$$

where,

$$B_{Zo} = \frac{R_o}{r_2} \tag{3.54}$$

$$B_{ZS1} = \frac{K_1 R_{S1} + K_2 R_{C1}}{K_1^2 + K_2^2} \tag{3.55}$$

$$B_{ZC1} = \frac{K_1 R_{C1} - K_2 R_{S1}}{K_1^2 + K_2^2} \tag{3.56}$$

$$B_{ZS2} = \frac{K_3 R_{S2} + K_4 R_{C2}}{K_3^2 + K_4^2} \tag{3.57}$$

$$B_{ZC2} = \frac{K_3 R_{C2} - K_4 R_{S2}}{K_3^2 + K_4^2} \tag{3.58}$$

where the intermediate variables are,

$$K_1 = r_2 - k^2 \tag{3.59}$$

$$K_2 = r_1 k \tag{3.60}$$

$$K_3 = r_2 - 4k^2 \tag{3.61}$$

$$K_4 = 2 r_1 k \tag{3.62}$$

The above results are formulated with the angle of attack in the purely sinusoidal form, where all trigonometric functions are taken with respect to the non-dimensional parameter ϕ. To make subsequent analysis simpler and consistent with the linear portion of the aerodynamic force, inserting $\phi = k\tau + \xi$ from Eq. (3.35) into Eqs. (3.33) and (3.53), expanding out, gives,

$$\alpha = \alpha_o + \alpha_V \cos\xi \sin k\tau + \alpha_V \sin\xi \cos k\tau \tag{3.63}$$

$$\begin{aligned} C_{Z2} = B_{Zo} &+ B_{ZS1} \cos\xi \sin k\tau + B_{ZS1} \sin\xi \cos k\tau \\ &B_{ZC1} \cos\xi \cos k\tau - B_{ZC1} \sin\xi \sin k\tau \\ &B_{ZS2} \cos 2\xi \sin 2k\tau + B_{ZS2} \sin 2\xi \cos 2k\tau \\ &B_{ZC2} \cos 2\xi \cos 2k\tau - B_{ZC2} \sin 2\xi \sin 2k\tau \end{aligned} \tag{3.64}$$

Introducing,

$$\cos\xi = \frac{\alpha_S}{\alpha_V} \tag{3.65}$$

$$\sin \xi = \frac{\alpha_C}{\alpha_V} \tag{3.66}$$

then, Eqs. (3.63) and (3.64) become,

$$\alpha = \alpha_o + \alpha_S \sin k\tau + \alpha_C \cos k\tau \tag{3.67}$$

$$\begin{aligned} C_{Z2} = C_{Z2o} + C_{Z2S1} \sin k\tau + C_{Z2C1} \cos k\tau \\ + C_{Z2S2} \sin 2k\tau + C_{Z2C2} \cos 2k\tau \end{aligned} \tag{3.68}$$

where,

$$C_{Z2o} = B_{Zo} \tag{3.69}$$

$$C_{Z2S1} = B_{ZS1} \frac{\alpha_S}{\alpha_V} - B_{ZC1} \frac{\alpha_C}{\alpha_V} \tag{3.70}$$

$$C_{Z2C1} = B_{ZS1} \frac{\alpha_C}{\alpha_V} + B_{ZC1} \frac{\alpha_S}{\alpha_V} \tag{3.71}$$

$$C_{Z2S2} = B_{ZS2} \left(\frac{\alpha_S^2}{\alpha_V^2} - \frac{\alpha_C^2}{\alpha_V^2} \right) - B_{ZC2}\, 2 \frac{\alpha_C}{\alpha_V} \frac{\alpha_S}{\alpha_V} \tag{3.72}$$

$$C_{Z2C2} = B_{ZS2}\, 2 \frac{\alpha_C}{\alpha_V} \frac{\alpha_S}{\alpha_V} + B_{ZC2} \left(\frac{\alpha_S^2}{\alpha_V^2} - \frac{\alpha_C^2}{\alpha_V^2} \right) \tag{3.73}$$

3.3c Summary of Complete Aerodynamic Forces

The formulation of the ONERA aerodynamic forces with harmonic balance method has been completed. This section summarizes the results in preparation for the assembly of full flutter equations. The complete aerodynamic force coefficient C_Z is written as,

$$C_Z = C_{Zo} + C_{ZS1}\sin k\tau + C_{ZC1}\cos k\tau + C_{ZS2}\sin 2k\tau + C_{ZC2}\cos 2k\tau$$

where each of the harmonic components are,

$$C_{Zo} = C_{Z1o} + C_{Z2o}$$
$$C_{ZS1} = C_{Z1S} + C_{Z2S1}$$
$$C_{ZC1} = C_{Z1C} + C_{Z2C1}$$
$$C_{ZS2} = C_{Z2S2}$$
$$C_{ZC2} = C_{Z2C2}$$

linear aerodynamic coefficient, C_{Z1}, was found to be:

$$C_{Z1} = C_{Z1o} + C_{Z1S}\sin k\tau + C_{Z1C}\cos k\tau$$

where,

$$C_{Z1o} = C_{Z\gamma o}$$

$$C_{Z1S} = s_{Z1}\left(-k\,\theta_S + \frac{h_S}{b}k^2\right) - s_{Z2}\,\theta_S\,k^2 - s_{Z3}\,k\,\theta_C + C_{Z\gamma S}$$

$$C_{Z1C} = s_{Z1}\left(k\,\theta_S + \frac{h_C}{b}k^2\right) - s_{Z2}\,\theta_C\,k^2 + s_{Z3}\,k\,\theta_S + C_{Z\gamma C}$$

and the intermediate variables are,

$$C_{Z\gamma o} = a_{oZ}\ \theta_o$$
$$C_{Z\gamma S} = F(k)\ L_S - G(k)\ L_C$$
$$C_{Z\gamma C} = G(k)\ L_S + F(k)\ L_C$$

$$F(k) = \frac{k^2\lambda_2 + \lambda_1^2}{\lambda_1^2 + k^2}$$

$$G(k) = \frac{k\ \lambda_1\ (\lambda_2 - 1)}{\lambda_1^2 + k^2}$$

$$L_S = a_{oZ}\left(\theta_S - k\,\frac{h_C}{b} - k\,\theta_C\right)$$

$$L_C = a_{oZ}\left(\theta_C + k\,\frac{h_S}{b} + k\,\theta_S\right)$$

The nonlinear aerodynamic coefficient is,

$$C_{Z2} = C_{Z2o} + C_{Z2S1}\sin k\tau + C_{Z2C1}\cos k\tau + C_{Z2S2}\sin 2k\tau + C_{Z2C2}\cos 2k\tau$$

where,

$$C_{Z2o} = B_{Zo}$$

$$C_{Z2S1} = B_{ZS1}\,\frac{\alpha_S}{\alpha_V} - B_{ZC1}\,\frac{\alpha_C}{\alpha_V}$$

$$C_{Z2C1} = B_{ZS1}\,\frac{\alpha_C}{\alpha_V} + B_{ZC1}\,\frac{\alpha_S}{\alpha_V}$$

$$C_{Z2S2} = B_{ZS2}\left(\frac{\alpha_S^2}{\alpha_V^2} - \frac{\alpha_C^2}{\alpha_V^2}\right) - B_{ZC2}\, 2\,\frac{\alpha_C}{\alpha_V}\,\frac{\alpha_S}{\alpha_V}$$

$$C_{Z2C2} = B_{ZS2}\, 2\,\frac{\alpha_C}{\alpha_V}\,\frac{\alpha_S}{\alpha_V} + B_{ZC2}\left(\frac{\alpha_S^2}{\alpha_V^2} - \frac{\alpha_C^2}{\alpha_V^2}\right)$$

and,

$$B_{Zo} = \frac{R_o}{r_2}$$

$$B_{ZS1} = \frac{K_1 R_{S1} + K_2 R_{C1}}{K_1^2 + K_2^2}$$

$$B_{ZC1} = \frac{K_1 R_{C1} - K_2 R_{S1}}{K_1^2 + K_2^2}$$

$$B_{ZS2} = \frac{K_3 R_{S2} + K_4 R_{C2}}{K_3^2 + K_4^2}$$

$$B_{ZC2} = \frac{K_3 R_{C2} - K_4 R_{S2}}{K_3^2 + K_4^2}$$

$$R_o = -r_2\,\Delta C_{Zo}$$

$$R_{S1} = -r_2\,\Delta C_{ZS1}$$

$$R_{C1} = -r_3\, k\,\Delta C_{ZS1}$$

$$R_{S2} = 2\, r_3\, k\,\Delta C_{ZC2}$$

$$R_{C2} = -r_2\,\Delta C_{ZC2}$$

$$K_1 = r_2 - k^2$$

$$K_2 = r_1\, k$$

$$K_3 = r_2 - 4\, k^2$$

$$K_4 = 2\, r_1\, k$$

$$\Delta C_{Zo} = \frac{b_1 \alpha_V}{\pi}\left[\left(\frac{\alpha_1 - \alpha_o}{\alpha_V}\right)\left(\phi_1 - \frac{\pi}{2}\right) + \cos\phi_1\right]$$

$$\Delta C_{ZS1} = \frac{b_1 \alpha_V}{\pi}\left[-\left(\phi_1 - \frac{\pi}{2}\right) - \frac{1}{2}\sin(2\phi_1)\right]$$

$$\Delta C_{ZC2} = \frac{b_1 \alpha_V}{\pi}\left[-\frac{1}{2}\cos\phi_1 - \frac{1}{6}\sin 3\phi_1\right]$$

All components of the aerodynamic forces has been transformed from differential form to algebraic form using the harmonic balance method. In this form, numerical solution method can be easily implemented. Before proceeding to assemble the full 3-dimensional flutter equation several more steps remain: First, transform the general flutter equations to full 3-dimensional flutter equation. Second, transfer the aerodynamic force formulations to structural coordinate. Finally, transform the structural terms of the resulting flutter equations to algebraic form and assemble the full flutter equations.

3.4 Nonlinear Flutter Analysis

3.4a Formulation of 3-Dimensional Flutter Equations

A general Rayleigh-Ritz formulation is used to approximate plate deflection and perform modal analysis. The Rayleigh-Ritz analysis begins by assuming a deflection shape for the structure. If only out-of-plane deflection, w, and rotational displacement, α are allowed, the general deflections, written with generalized coordinates are,

$$w = \sum_{i=1}^{n} \gamma_i(x,y)\, q_i \tag{3.77}$$

$$\alpha = \bar{\theta}_R + \sum_{i=1}^{n} \frac{\partial \gamma_i}{\partial y} q_i \tag{3.78}$$

where $\gamma_i(x,y)$ represent the non-dimensional mode shapes of the i-th mode; q_i denote the generalized displacements, or modal amplitudes, of the i-th mode; n is the number of mode shapes; and θ_R is the root angle of attack.

For simplicity, it is further assumed that the mode shapes are separable in the chord-wise and span-wise directions. The mode shapes can then be written in the form,

$$\gamma_i(x,y) = \phi_{ih}(x); \qquad \text{for bending modes} \tag{3.79}$$

$$\gamma_i(x,y) = \frac{y}{c}\phi_{i\alpha}(x); \qquad \text{for torsion modes} \tag{3.80}$$

Note, in the present investigation, to simplify mathematical work and still sufficiently describe the deflection of the wing in flutter analysis, only beam out-of-plane bending modes and beam torsion modes were represented. Previous studies have used varying degree of complexity in terms of selecting mode shapes. Landsberger and Dugundji [Ref. 25] used simplified sinusoidal torsional mode shapes. and the works by Dunn [Refs. 13 and 14] incorporated mode shapes with higher degree of complexity. It was found, however, that using of mode shapes which did not meet the cantilevered root warping condition, somewhat affected the Rayleigh-Ritz prediction of modal deflection. Therefore, more complex torsional modes, which incorporated the root warping effect should be considered if highly accurate description of wing shape is required [Refs. 26 and

27]. In present analysis, root warping terms will not be incorporated into the mode shape. Furthermore, since the final stall flutter problem is expected to yield a single degree of freedom motion in either the first torsional or first bending mode, it was decided to only model the first torsion and first bending modes. The selected mode shapes are listed below. The out-of-plane bending mode is written in the form,

$$\phi_h(x) = \cosh\left(\varepsilon_1 \frac{x}{l}\right) - \cos\left(\varepsilon_1 \frac{x}{l}\right) - \alpha_1\left[\sinh\left(\varepsilon_1 \frac{x}{l}\right) - \sin\left(\varepsilon_1 \frac{x}{l}\right)\right] \tag{3.81}$$

$$\varepsilon_1 = \rho_1 \pi = 1.87510 \tag{3.82}$$

$$\alpha_1 = \frac{\sinh \varepsilon_1 - \sin \varepsilon_1}{\cosh \varepsilon_1 + \cos \varepsilon_1} = 0.72664 \tag{3.83}$$

$$\rho_1 = 0.59686 \tag{3.84}$$

The torsion mode is,

$$\phi_\alpha(x) = \sin\left(\frac{\pi x}{2l}\right) \tag{3.85}$$

Applying the Rayleigh-Ritz energy method to find the entries in the mass and stiffness matrix, where the kinetic energy, T, for the system is,

$$T = \frac{1}{2}\iint m\,\dot{w}^2\,dy\,dx$$
$$= \frac{1}{2}\sum_i\sum_j \dot{q}_i\,\dot{q}_j\,M_{ij} \tag{3.86}$$

$$M_{ij} = \iint m\,\gamma_i\,\gamma_j\,dy\,dx \tag{3.87}$$

The internal energy formulation gives,

$$U = \frac{1}{2}\int_{wing}\left[D_{11}w_{,xx}^2 + 2D_{12}w_{,xx}w_{,yy} + \cdots\right]dx\,dy$$
$$= \frac{1}{2}\sum_i\sum_j q_i\,q_j\,K_{ij} \tag{3.88}$$

Placing the kinetic and potential energy terms into Lagrange's equations, results in a set of ordinary differential equations of motion,

$$[M]\{\ddot{q}\} + [K]\{q\} = \{Q\} \tag{3.89}$$

where [M] and [K] are mass and stiffness matrices respectively. The modal force {Q} is derived from the expression of the virtual work ,

$$\delta W = \iint \delta w\,\Delta p\,dy\,dx$$
$$= \sum_i \delta q_i\,Q_i \tag{3.90}$$

$$Q_i = \iint \gamma_i\,\Delta p\,dy\,dx \tag{3.91}$$

From the above formulation, the entries of the mass matrix then are,

$$M_{11} = M\, l\, I_1 \tag{3.92}$$

$$M_{22} = M\, l \left(\frac{r_G}{c} \right)^2 I_3 \tag{3.93}$$

$$M_{12} = M_{21} = 0 \tag{3.94}$$

where $I_1 = \int \phi_h^2 \, dx$, $I_3 = \int \phi_\alpha^2 \, dx$, r_G denotes the radius of gyration, l represents the length of the wing, and c is the chord length. Again, here M is mass per unit length. The entries in the stiffness matrix [K] are,

$$K_{11} = D_{11} \frac{c}{l^3} I_6 \tag{3.95}$$

$$K_{22} = \frac{4\, D_{66}}{l\, c} I_{15} \tag{3.96}$$

where D_{11} and D_{66} denote the flexural rigidity modulus data for the composite wing. The modal forces are given by Eqs. (3.90) and (3.91),

$$Q_1 = \int_0^l \phi_h \, L_{1/2} \, dx \tag{3.97}$$

$$Q_2 = \frac{1}{c} \int_0^l \phi_\alpha \, M_{\alpha 1/2} \, dx \tag{3.98}$$

where $L_{1/2}$ and $M_{\alpha 1/2}$ are lift and moment at the mid-chord. These aerodynamic forces are related to the previous formulation, lift and moment at quarter-chord, as,

$$L_{1/2} = L_{1/4} \tag{3.99}$$

$$M_{\alpha 1/2} = M_{\alpha 1/4} + \frac{c}{4} L_{1/4} \tag{3.100}$$

Now, to make Eq. (3.89) easier for subsequent analysis, non-dimensionalization of the equations are needed. This could be accomplished by introducing $\tilde{q}_i$ and τ, where τ represents the non-dimensional time as stated in Eq. (3.5), and $\tilde{q}_i$ denotes the non-dimensionalized, generalized coordinates where,

$$\tilde{q}_i = \frac{q_i}{b} \tag{3.101}$$

and from Eq. (3.5) the normal time derivative can then be written in the form,

$$\frac{d}{dt} = \frac{U}{b}\frac{d}{d\tau} = \frac{U}{b}(\dot{\ }) \tag{3.102}$$

Substituting Eqs. (3.101) and (3.102) into Eq. (3.89). With some algebraic manipulation, Eq. (3.89) can then be written as,

$$\mu \pi I_1 \left(\ddot{\tilde{q}}_1 + \Omega^2 k_\alpha^2 \tilde{q}_1 \right) = \int_0^1 \phi_h C_{L1/2} \, d\tilde{x} \tag{3.103}$$

$$\mu \frac{\pi}{4} r_\alpha^2 I_3 \left(\ddot{\tilde{q}}_2 + k_\alpha^2 \tilde{q}_2 \right) = \int_0^1 \phi_\alpha C_{M1/2} \, d\tilde{x} \tag{3.104}$$

where, $\Omega = \omega_h / \omega_\alpha$, the ratio of the bending to torsional frequency, $k_\alpha = \omega_\alpha b/U$ is the torsional reduced frequency, and the rest of the parameters are,

$$\mu = \frac{M}{\pi \rho b^2} \tag{3.105}$$

$$r_\alpha = \frac{r_G}{b} \tag{3.106}$$

and I_1 and I_3 are aerodynamic integrals for the selected mode shape (see Appendix A).

3.4b Coordinate Transfer of Aerodynamic Forces

At present moment, all aerodynamic forces has been derived about the quarter-chord as a matter of convention. However, the structural components in this study have been formulated with the longitudinal axis placed at the mid-chord, again as a matter of convention in structural analysis. The objective of present study is to investigate the stalled flutter behavior of aircraft structures. It was therefore decided that, the aerodynamic force parameters should be transferred to conform to structure coordinates.

Transferring of the aerodynamic forces starts by converting the basic parameters, pitching angle and vertical translation. In structural coordinates, the pitching angle and vertical translation are,

$$\theta_{\frac{1}{2}} = \theta_R + \frac{1}{2}\phi_\alpha \tilde{q}_2 \tag{3.107}$$

$$h_{\frac{1}{2}} = \phi_h b \tilde{q}_1 \tag{3.108}$$

The pitching angle does not change when transferring coordinates. However, in order to express the vertical translation about the quarter-chord in structural coordinates, additional terms need to be added,

$$h_{\frac{1}{4}} = h_{\frac{1}{2}} + \frac{b}{2}\theta_{\frac{1}{2}} \tag{3.109}$$

substituting Eqs. (3.108) and (3.109) into Eq. (3.107) and denoting Eq. (3.108) in the quarter-chord subscript, then gives,

$$h_{\frac{1}{4}} = b\left(\frac{1}{2}\theta_R + \phi_h \tilde{q}_1 + \frac{1}{4}\phi_\alpha \tilde{q}_2\right) \tag{3.110}$$

$$\theta_{\frac{1}{4}} = \theta_{\frac{1}{2}} = \theta_R + \frac{1}{2}\phi_\alpha \tilde{q}_2 \tag{3.111}$$

Again, introducing harmonic motion, now in terms of the non-dimensionalized q,

$$\tilde{q}_i = \tilde{q}_{io} + \tilde{q}_{iS}\sin k\tau + \tilde{q}_{iC}\cos k\tau \tag{3.112}$$

Then, substituting Eq. (3.112) into Eqs. (3.110) and (3.111), result in the harmonic form of vertical motion and pitching angle,

$$h_{\frac{1}{4}} = h_o + h_S \sin k\tau + h_C \cos k\tau \tag{3.113}$$

where,

$$h_o = b\left(\frac{\theta_R}{2} + \phi_h \tilde{q}_{1o} + \frac{1}{4}\phi_\alpha \tilde{q}_{20}\right) \tag{3.114}$$

$$h_S = b\left(\phi_h \tilde{q}_{1S} + \frac{1}{4}\phi_\alpha \tilde{q}_{2S}\right) \tag{3.115}$$

$$h_C = b\left(\phi_h \tilde{q}_{1C} + \frac{1}{4}\phi_\alpha \tilde{q}_{2C}\right) \tag{3.116}$$

and,

$$\theta_{\frac{1}{4}} = \theta_o + \theta_S \sin k\tau + \theta_C \cos k\tau \tag{3.117}$$

where,

$$\theta_o = \theta_R + \frac{1}{2}\phi_\alpha \tilde{q}_{2o} \tag{3.118}$$

$$\theta_S = \frac{1}{2}\phi_\alpha \tilde{q}_{2S} \tag{3.119}$$

$$\theta_C = \frac{1}{2}\phi_\alpha \tilde{q}_{2C} \tag{3.120}$$

With all the building blocks at hand, transferring of the aerodynamic force coefficients can now proceed. Obtain the linear aerodynamic force coefficient, C_{Z1}, by inserting the harmonic components of vertical displacement, Eqs. (3.114), (3.115) and (3.116), along with the harmonic components of the pitching angle, Eqs. (3.118), (3.119) and (3.120), into Eqs. (3.29), (3.30) and (3.31), and their appropriate sub-components, gives,

$$C_{Z1o} = a_{oZ}\left(\theta_R + \frac{1}{2}\phi_\alpha \tilde{q}_{20}\right) \tag{3.121}$$

$$C_{Z1S} = \phi_h\left(E_{Z1}\tilde{q}_{1S} + E_{Z2}\tilde{q}_{1C}\right) + \phi_\alpha\left(E_{Z3}\tilde{q}_{2S} + E_{Z4}\tilde{q}_{2C}\right) \tag{3.122}$$

$$C_{Z1C} = \phi_h\left(-E_{Z2}\tilde{q}_{1S} + E_{Z1}\tilde{q}_{1C}\right) + \phi_\alpha\left(-E_{Z4}\tilde{q}_{2S} + E_{Z3}\tilde{q}_{2C}\right) \tag{3.123}$$

The above formulations seems complicated. However, there are only four components involved in the entire formulation, namely, E_{Z1}, E_{Z2}, E_{Z3}, and E_{Z4}. Notice the symmetries that exist between the C_{Z1S} and C_{Z1C}. Each of the sine components of C_{Z1S} is that of the cosine components in C_{Z1C}, and each of the

cosine components of C_{Z1S} is the negative value of the sine components in C_{Z1C}. These components are written as,

$$E_{Z1} = s_{Z1}\, k^2 + a_{oZ}\, G(k)\, k \tag{3.124}$$

$$E_{Z2} = a_{oZ}\, F(k)\, k \tag{3.125}$$

$$E_{Z3} = \frac{1}{4} k^2\, s_{Z1} - \frac{1}{2} s_{Z2}\, k^2 + \frac{1}{2} a_{oZ}\, F(k) - \frac{1}{4} a_{oZ}\, k\, G(k) \tag{3.126}$$

$$E_{Z4} = -\frac{1}{2} s_{Z1}\, k - \frac{1}{2} s_{Z3}\, k - \frac{1}{4} a_{oZ}\, k\, F(k) - \frac{1}{2} a_{oZ}\, G(k) \tag{3.127}$$

The nonlinear aerodynamic force coefficient, C_{Z2} can be transferred to the structural coordinate in the similar fashion. The angle of attack, α, in the structural coordinate is needed in the transferring of nonlinear force coefficient. By inserting Eqs. (3.113) and (3.117) and their non-dimensional time derivatives into Eqs. (3.17), (3.18), and (3.19), the angle of attack in structural coordinates is then,

$$\alpha_{\frac{1}{4}} = \alpha_o + \alpha_S \sin k\tau + \alpha_C \cos k\tau \tag{3.128}$$

where,

$$\alpha_o = \theta_R + \frac{1}{2} \phi_\alpha\, \tilde{q}_{2o} \tag{3.129}$$

$$\alpha_S = \frac{1}{2} \phi_\alpha\, \tilde{q}_{2S} + \phi_h\, k\, \tilde{q}_{1C} + \frac{1}{4} \phi_\alpha\, k \tilde{q}_{2C} \tag{3.130}$$

$$\alpha_C = \frac{1}{2} \phi_\alpha\, \tilde{q}_{2C} - \phi_h\, k\, \tilde{q}_{1S} - \frac{1}{4} \phi_\alpha\, k\, \tilde{q}_{2S} \tag{3.131}$$

The above formulations can then be placed into Eq. (3.68) and its appropriate sub-components to form the transferred C_{Z2}. The full expression will not be listed

here due to its complexity. When solving for the full flutter solutions, C_{Z2} is programmed in the computer code as it appears in Eq. (3.68). The code, however, is specified to place the transferred values of α, θ and h into the appropriate components as required.

3.4c Assembling of Flutter Equations

Once the aerodynamic forces are set up for this analysis, it still remains to assemble the full flutter equations. Employing the harmonic balance method, forcing terms of the full flutter Eqs., (3.103) and (3.104), can be expressed in their harmonic elements. Recall Eqs. (3.99) and (3.100), where lift and moment coefficients in structural coordinates are related to their counter part in aerodynamic coordinates. Inserting those formulations with their appropriate elements, namely Eqs. (3.121), (3.122) and (3.123) and Eqs. (3.68) with transferred values of α, into the forcing terms, then gives,

$$\begin{aligned}\int_0^1 \phi_h \, C_{L\frac{1}{2}} \, dx = &\int_0^1 \phi_h \left[C_{L1o} + C_{L1S1} \sin k\tau + C_{L1C1} \cos k\tau \right] d\tilde{x} \\ &+ \int_0^1 \phi_h \left[C_{L2o} + C_{L2S1} \sin k\tau + C_{L2C1} \cos k\tau \right] d\tilde{x}\end{aligned} \tag{3.132}$$

$$\begin{aligned}\int_0^1 \phi_\alpha \, C_{M\frac{1}{2}} \, d\tilde{x} = &\int_0^1 \phi_\alpha \left[\left(C_{M1o} + \frac{1}{4} C_{L1o} \right) + \left(C_{M1S1} + \frac{1}{4} C_{L1S1} \right) \sin k\tau + \left(C_{M1C1} + \frac{1}{4} C_{L1C1} \right) \cos k\tau \right] d\tilde{x} \\ &+ \int_0^1 \phi_\alpha \left[\left(C_{M2o} + \frac{1}{4} C_{L2o} \right) + \left(C_{M2S1} + \frac{1}{4} C_{L2S1} \right) \sin k\tau + \left(C_{M2C1} + \frac{1}{4} C_{L2C1} \right) \cos k\tau \right] d\tilde{x}\end{aligned} \tag{3.133}$$

Notice that Eqs. (3.132) and (3.133) contains only first harmonic terms. In the present study, it is not the intention to model the fine details of the nonlinear

motion. Therefore, harmonic balance method was employed, which is suitable for describing the gross aspects of the nonlinear problem. This idea is further amplified by the use of a semi-empirical aerodynamic model, which ignores the fine details of the fluid flow. It was therefore decided to use only first harmonic terms for the total flutter analysis, while the aerodynamic analysis by itself, namely, fitting of the aerodynamic model (see Appendix B), can use several harmonics. Furthermore, the angle of attack at 75% span is taken to be the average angle of attack for the entire wing span. This assumption greatly simplifies the formulation and is implemented in the nonlinear portion of the aerodynamic forces by evaluating all mode shapes at the specified span location.

With additional algebra work, Eqs. (3.132) and (3.133) expand to the form,

$$
\begin{aligned}
\int_0^1 \phi_h \, C_{L\frac{1}{2}} \, d\tilde{x} = {} & I_4 \, a_{oL} \, \theta_R + I_2 \frac{a_{oL}}{2} \tilde{q}_{2o} \\
& + \left[I_1 \left(E_{L1} \, \tilde{q}_{1S} + E_{L2} \, \tilde{q}_{1C} \right) + I_2 \left(E_{L3} \, \tilde{q}_{2S} + E_{L4} \, \tilde{q}_{2C} \right) \right] \sin k\tau \\
& + \left[I_1 \left(-E_{L2} \, \tilde{q}_{1S} + E_{L1} \, \tilde{q}_{1C} \right) + I_2 \left(-E_{L4} \, \tilde{q}_{2S} + E_{L3} \, \tilde{q}_{2C} \right) \right] \cos k\tau \\
& + I_4 \, B_{Lo} + \left[I_4 \left(B_{LS1} \frac{\alpha_S}{\alpha_V} - B_{LC1} \frac{\alpha_C}{\alpha_V} \right) \right] \sin k\tau \\
& + \left[I_4 \left(B_{LS1} \frac{\alpha_C}{\alpha_V} + B_{LC1} \frac{\alpha_S}{\alpha_V} \right) \right] \cos k\tau
\end{aligned}
\tag{3.134}
$$

$$\int_0^1 \phi_\alpha \, C_{M\frac{1}{2}} \, d\tilde{x} = I_5 \, a_{oT} \, \theta_R + I_3 \frac{a_{oT}}{2} \tilde{q}_{2o}$$
$$+ \left[I_2 \left(E_{T1} \, \tilde{q}_{1S} + E_{T2} \, \tilde{q}_{1C} \right) + I_3 \left(E_{T3} \, \tilde{q}_{2S} + E_{T4} \, \tilde{q}_{2C} \right) \right] \sin k\tau$$
$$+ \left[I_2 \left(-E_{T2} \, \tilde{q}_{1S} + E_{T1} \, \tilde{q}_{1C} \right) + I_3 \left(-E_{T4} \, \tilde{q}_{2S} + E_{T3} \, \tilde{q}_{2C} \right) \right] \cos k\tau$$
$$+ I_5 \, B_{To} + \left[I_5 \left(B_{TS1} \frac{\alpha_S}{\alpha_V} - B_{TC1} \frac{\alpha_C}{\alpha_V} \right) \right] \sin k\tau$$
$$+ \left[I_5 \left(B_{TS1} \frac{\alpha_C}{\alpha_V} + B_{TC1} \frac{\alpha_S}{\alpha_V} \right) \right] \cos k\tau \tag{3.135}$$

where variables with a subscript L denote components associated with lift coefficient and I's are the aerodynamic integrals. Components with a subscript T represent terms associated with transferred values of moment coefficients. They are written as,

$$a_{oT} = a_{oM} + \frac{a_{oL}}{4} \tag{3.136}$$

$$E_{T1} = E_{M1} + \frac{E_{L1}}{4} \tag{3.137}$$

$$E_{T2} = E_{M2} + \frac{E_{L2}}{4} \tag{3.138}$$

$$E_{T3} = E_{M3} + \frac{E_{L3}}{4} \tag{3.139}$$

$$E_{T4} = E_{M4} + \frac{E_{L4}}{4} \tag{3.140}$$

$$B_{To} = B_{Mo} + \frac{B_{Lo}}{4} \tag{3.141}$$

$$B_{TS1} = B_{MS1} + \frac{B_{LS1}}{4} \tag{3.142}$$

$$B_{TC1} = B_{MC1} + \frac{B_{LC1}}{4} \tag{3.143}$$

Finally assembling the full flutter equations by introducing Eq. (3.112) into left hand sides of Eqs. (3.103) and (3.104), the differential form of the equation of motion. Similarly, substituting Eqs. (3.134) and (3.135) into the right hand sides of the equations of motion. Matching terms of both sides would give a system of six coupled, nonlinear equations. They are of the form,

$$\mu \pi I_1 \Omega^2 k_\alpha^2 \tilde{q}_{1o} = I_4 a_{oL} \theta_R + I_2 \frac{a_{oL}}{2} \tilde{q}_{2o} + I_4 B_{Lo} \tag{3.144}$$

$$\mu \frac{\pi}{4} r_\alpha^2 I_3 k_\alpha^2 \tilde{q}_{2o} = I_5 a_{oT} \theta_R + I_3 \frac{a_{oT}}{2} \tilde{q}_{2o} + I_5 B_{To} \tag{3.145}$$

$$\mu \pi I_1 \left(\Omega^2 k_\alpha^2 - k^2\right) \tilde{q}_{1S} = I_1 \left(E_{L1} \tilde{q}_{1S} + E_{L2} \tilde{q}_{1C}\right) + I_2 \left(E_{L3} \tilde{q}_{2S} + E_{L4} \tilde{q}_{2C}\right) + I_4 \left(B_{LS1} \frac{\alpha_S}{\alpha_V} - B_{LC1} \frac{\alpha_C}{\alpha_V} \right) \tag{3.146}$$

$$\mu \pi I_1 \left(\Omega^2 k_\alpha^2 - k^2\right) \tilde{q}_{1C} = I_1 \left(-E_{L2} \tilde{q}_{1S} + E_{L1} \tilde{q}_{1C}\right) + I_2 \left(-E_{L4} \tilde{q}_{2S} + E_{L3} \tilde{q}_{2C}\right) + I_4 \left(B_{LC1} \frac{\alpha_S}{\alpha_V} + B_{LS1} \frac{\alpha_C}{\alpha_V} \right) \tag{3.147}$$

$$\mu \frac{\pi}{4} r_\alpha^2 I_3 \left(k_\alpha^2 - k^2\right) \tilde{q}_{2S} = I_2 \left(E_{T1} \tilde{q}_{1S} + E_{T2} \tilde{q}_{1C}\right) + I_3 \left(E_{T3} \tilde{q}_{2S} + E_{T4} \tilde{q}_{2C}\right) + I_5 \left(B_{TS1} \frac{\alpha_S}{\alpha_V} - B_{TC1} \frac{\alpha_C}{\alpha_V} \right) \tag{3.148}$$

$$\mu \frac{\pi}{4} r_\alpha^2 I_3 \left(k_\alpha^2 - k^2\right) \tilde{q}_{2C} = I_2 \left(-E_{T2}\, \tilde{q}_{1S} + E_{T1}\, \tilde{q}_{1C}\right)$$
$$+ I_3 \left(-E_{T4}\, \tilde{q}_{2S} + E_{T3}\, \tilde{q}_{2C}\right) + I_5 \left(B_{TC1} \frac{\alpha_S}{\alpha_V} + B_{TS1} \frac{\alpha_C}{\alpha_V} \right)$$

(3.149)

Equations (3.144) through (3.149) are the full flutter equations which this study is based on. Notice, again, the symmetries that exist between Eqs. (3.146) and (3.147) . In both the linear and nonlinear portion of the aerodynamic force terms, the coefficient appearing with the sine terms in Eq.(3.146) are same as the cosine term coefficients in Eq. (3.147). The cosine term coefficients are the negative of the coefficients appearing with sine terms in Eq. (3.147). Similar symmetries also exist between Eqs. (3.148) and (3.149). These symmetries reflect the fact that, if complex sinusoidal motion is assumed for the generalized coordinates, these six equations could be combined and form a system of three complex equations. This system of nonlinear Rayleigh-Ritz aeroelastic equations can then be solved by using Newton-Raphson iteration method (see Appendix E).

The theory described in all previous sections was implemented using FORTRAN code with Microsoft FORTRAN™ compiler Ver. 5.10 on a IBM compatible 386, 25 MHz personal computer. The source code of all programs written are listed in Appendix F. The Newton-Raphson solver employs a finite difference scheme for all numerical differentiation. The library routines of LUDCMP and LUBKSB [Ref. 40], were also employed to perform matrix inversion.

CHAPTER 4

RESULTS

A summary of linear flutter analysis results are shown in Table 1. The results are also shown in graphics form in Figs. 7 through 9. All linear analysis results were generated using the physical properties listed in Appendix A, Table 4. The analytic results for linear flutter thoery using the Padé Approximation with unsteady, incompressible aerodynamic forces, incorporating one bending mode and one torsion mode, are shown in Fig 7. The tend towards coalescence of the bending and torsion mode can be seen clearly in the graph. As expected, the torsional mode was the critical flutter mode, which crosses the imaginary axis at 21.44 m/s. The analytic results for linear flutter theory using the typical section U-g method with complex sinusoidal aerodynamic force formulation is shown in Fig. 8. Figure 9 shows the results of the U-g method with the modifications for varying spanwise deflection, as described in Section 2.4. Again, the torsional mode was the critical flutter mode and the divergence velocity was slightly lower than the flutter velocity.

The same linear results can also be obtained by using the harmonic balance method to solve the complete flutter equations formulated in Chapter 3. This was accomplished by inserting the root angle of attack, θ_R, as zero, and eliminating all nonlinearity in the formulation. Comparison of results from the various analytic methods shown in Table 1 are seen to be essentially identical.

As shown in Table 1, the linear flutter velocity, V_F, from all four analysis methods are higher than the linear divergence velocity, V_D, because the given properties characterize a composite wing without bending-torsion structural coupling, and both the elastic axis and the C.G. are at the mid-chord. The trend towards coalescence of the bending and torsion frequencies can also be seen clearly in Fig. 8 and Fig. 9 – dropping of the torsional frequency from about 24.2 Hz to 12.98 Hz and eventually to 8 Hz, while the bending frequency drops from around 4.2 Hz to 0 Hz as it approaches the divergence velocity.

The results for nonlinear, large amplitude flutter theory using the harmonic balance method are shown in Figs. 10 to 12. The figures are paired in groups of two. Fig. 10 shows the graphs of static position assuming no flutter, and the average wing angle from static to full stall flutter, versus velocity. Both the static position and the average wing angle represent the sum of root angle of attack and the twist at the 75% span location due to aerodynamic force. Fig. 11 shows the limit cycle oscillation amplitude versus velocity and frequency with constant root angle of attack (θ_R = 1°, 5°, 10°, 15°) . Fig. 12 shows flutter velocity and frequency versus increasing root angle of attack.

In Fig. 10, for each curve of constant root angle of attack, both the steady, static analysis (solid lines), and full, unsteady flutter analysis (dashed lines) are presented, so as to show where the flutter starts. The trend shows that the average wing angle exhibits a sharp decrease when the velocity is increased past the flutter boundary for low root angle of attack, θ_R= 1° , while for larger root angle of attack, θ_R=5°, 10°, and 15°, the drop is more gradual. The reason for the sudden drop at low root angle of attack is because, when the root angle of attack is below static stall angle the behavior is still essentially governed by the linear aerodynamics, so the oscillation growth is still essentially exponential up until

deep stall is reached. therefore, a small change in velocity, would result in large increase in total angle. The characteristics of static position for large root angle of attack are essentially the same as for the low root angles of attack, except that the change from light stall to deep stall is more gradual, since the wings are already in deep stall from the initial angle of attack input.

In Fig. 11, the trend shows decreasing flutter velocity with increasing root angle of attack. Notice, for the θ_R=1° case, the velocity began to decrease at around an oscillation amplitude of 12°. This is due to the oscillation penetrating the negative side of the lift deviation curve. The same trend can be observed from the θ_R=5° curve. Also notice, for root angle of attack of 10° and 15° at low oscillation amplitude, the velocity is constant up to a point. This is because the root angle of attack here is in the stall range initially, and while the oscillation amplitude is small, the oscillation range stays only in the stall range. When the oscillation become large again, the oscillating range exits and enters the stall range, and the trend of increasing velocity with increasing amplitude returns.

Fig. 11 also shows the limit cycle oscillation frequency. Here, the frequency increases with increasing root angle of attack. As the oscillation amplitude is increased, the frequency drops slightly until the amplitude penetrates the negative deviation curve, and then the frequency increases.

The analytic flutter boundaries are presented in Fig. 12. These were defined as oscillations for amplitudes less than 1°. Figure 12 shows that the flutter velocity starts at the linear flutter velocity, however, due to the close proximity of linear flutter speed and linear divergence velocity, it immediately begins to exhibit nonlinear behavior. An increase in the root angle of attack causes the flutter velocity to drop and the flutter motion to become more purely torsional. This can

also be seen in Fig. 12, where the flutter frequency migrates closer to the natural torsion frequency.

The results and trends obtained here seem to correlate generally with the experimental results obtained by Dunn [Ref. 14]. Further closer correlation would probably require improved aerodynamic fitting of the appropriate Reynold's number aerodynamics, and inclusion of an additional structural nonlinearity.

Methods	k	V_F (m/sec)	ω_F (Hz)	V_D(m/sec)
Padé Approx.*	0.278	21.44	13.56	20.83
U-g method*	0.278	21.43	13.55	20.82
U-g method**	0.263	21.69	12.98	20.82
HBM**	0.263	21.70	12.95	20.86

* Typical Section
** Varying spanwise deflection

Table 1. Linear flutter characteristics

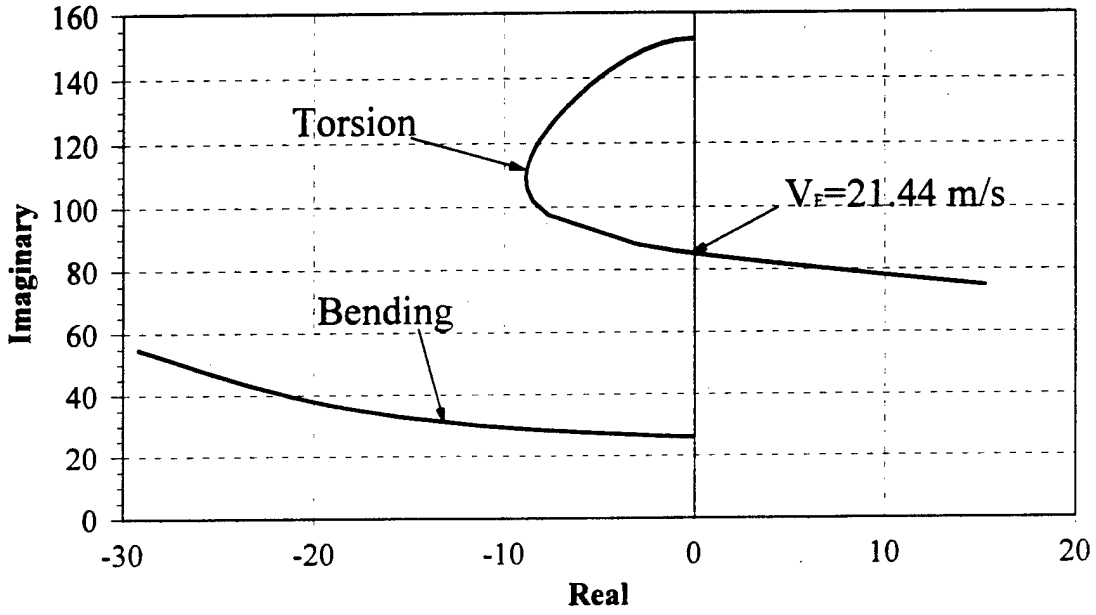

Figure 7. Padé Approximation

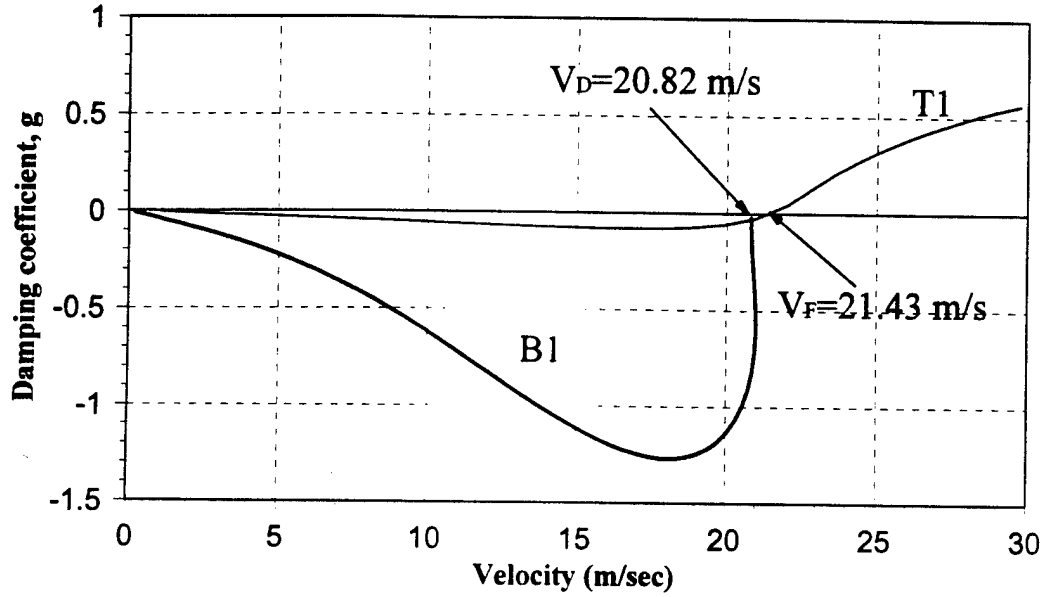

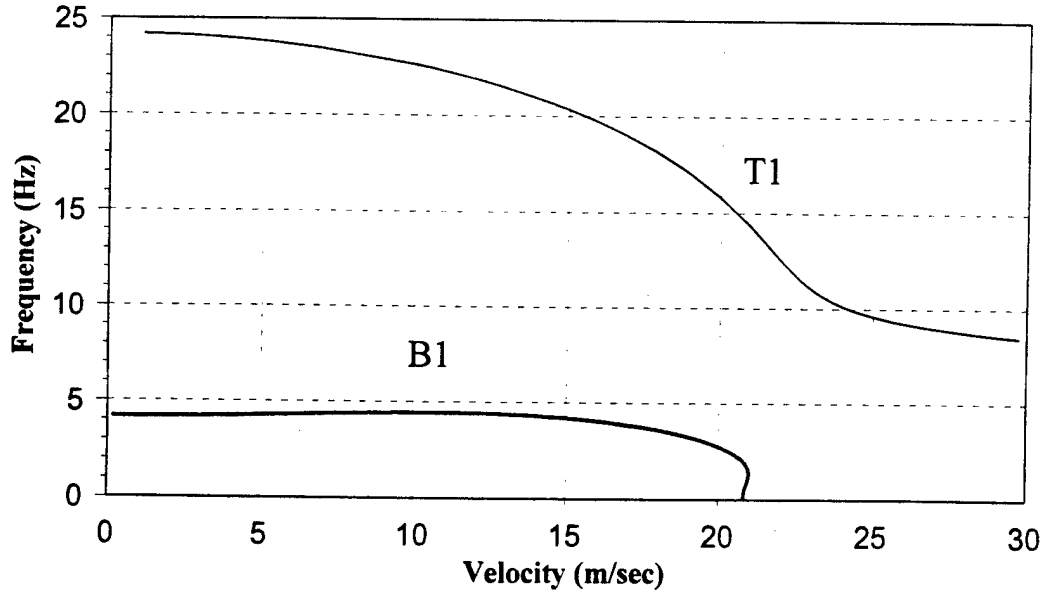

Figure 8. U-g flutter analysis (Typical section)

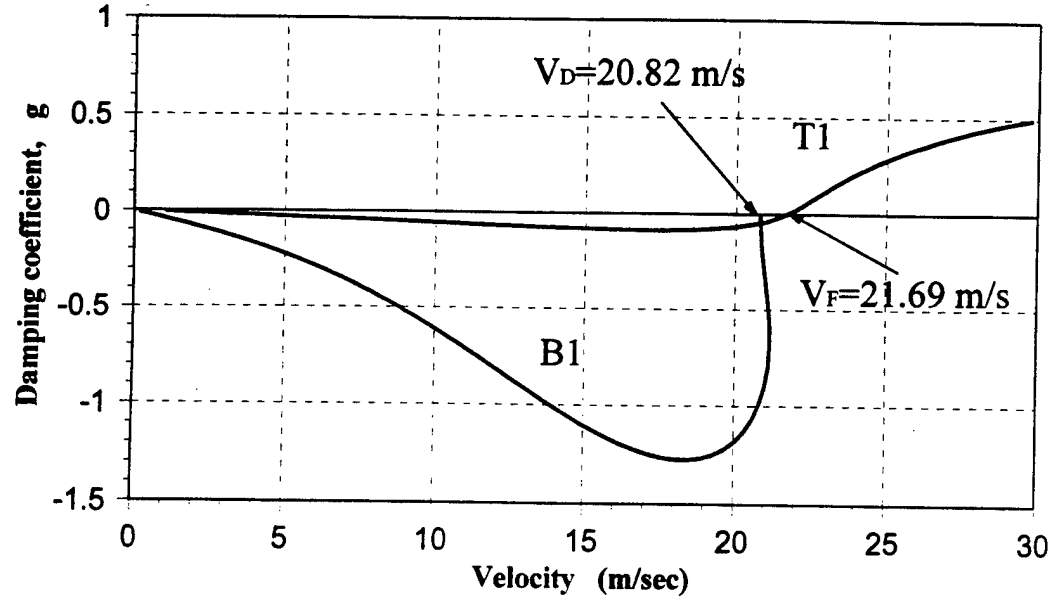

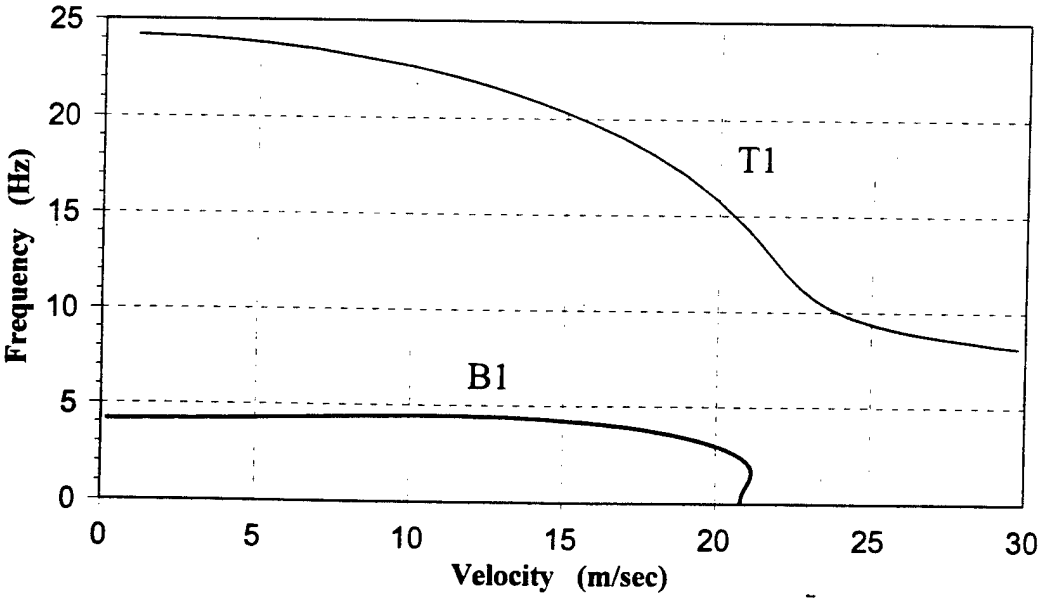

Figure 9. U-g flutter analysis (Varying spanwise deflection)

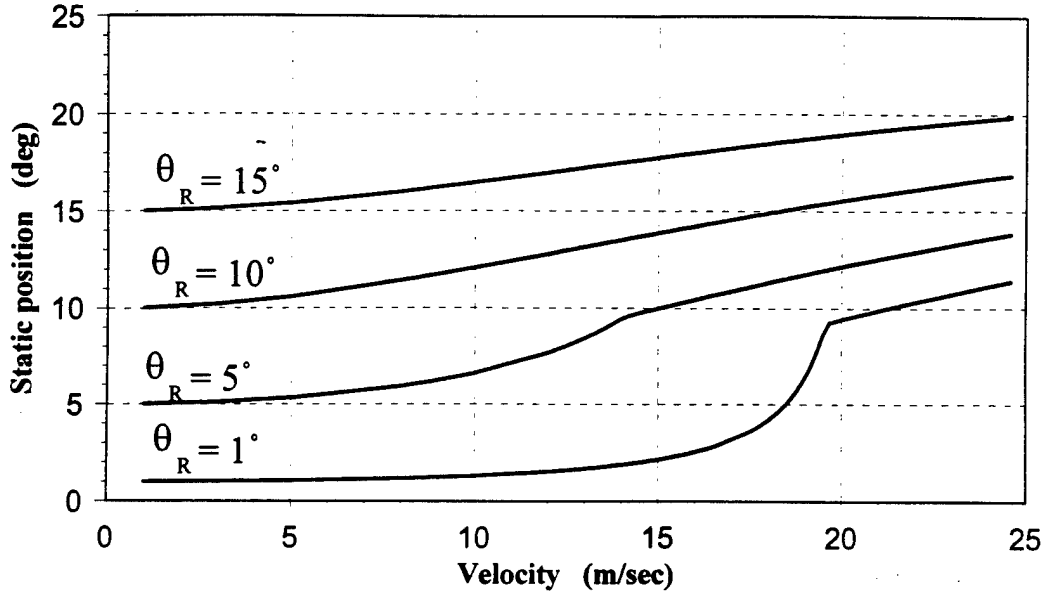

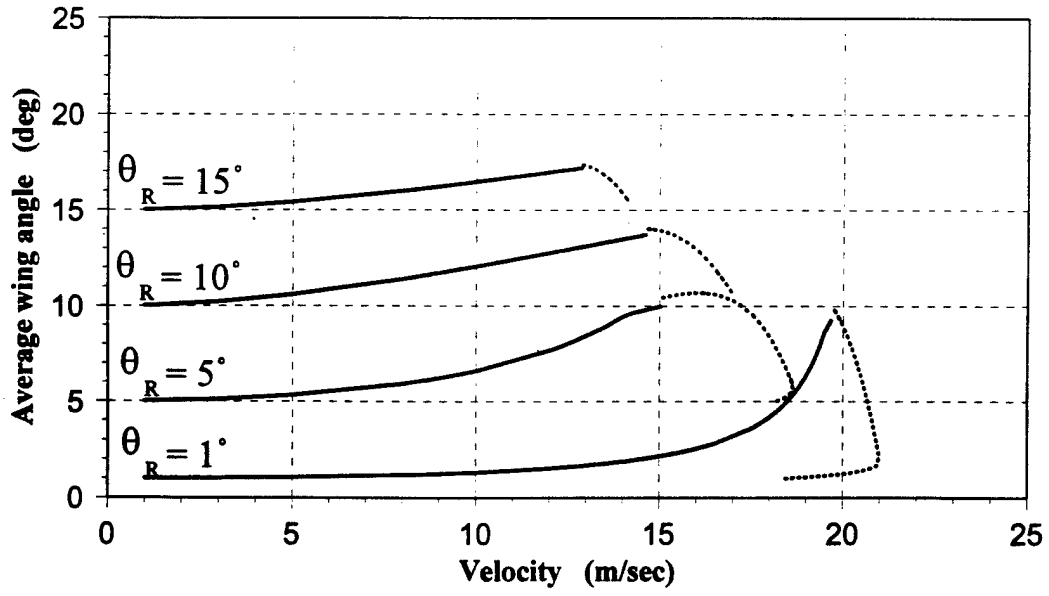

Figure 10. Static position and average angle

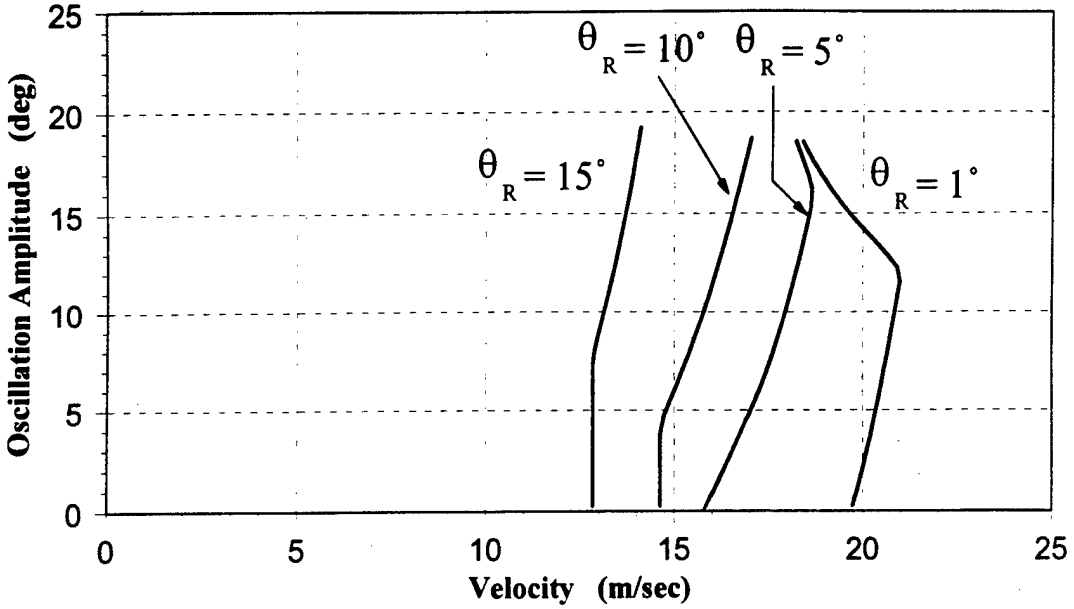

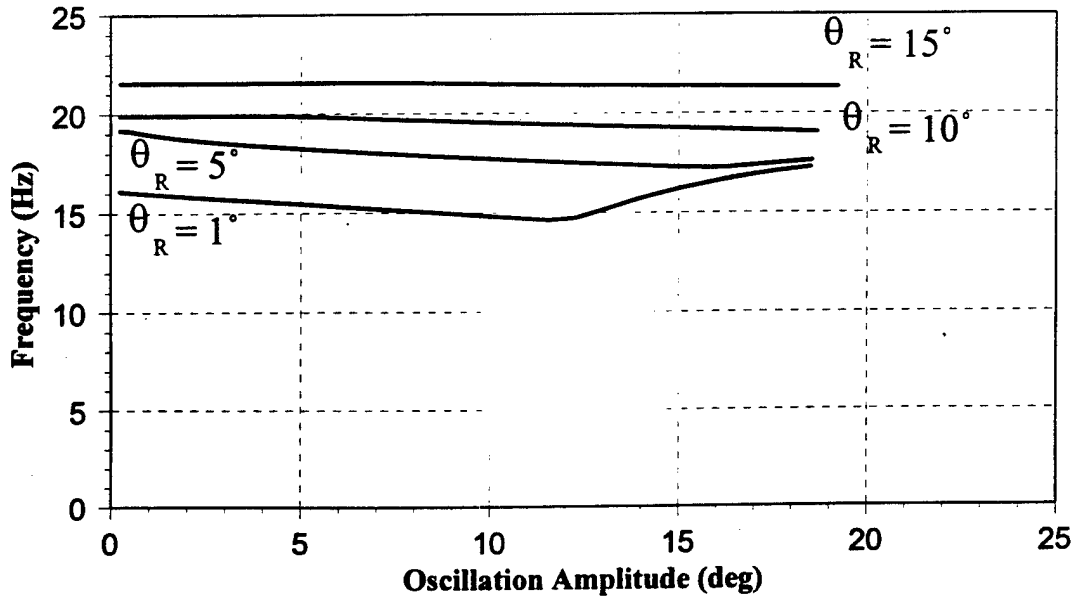

Figure 11. Limit Cycle oscillation amplitude versus velocity and frequency

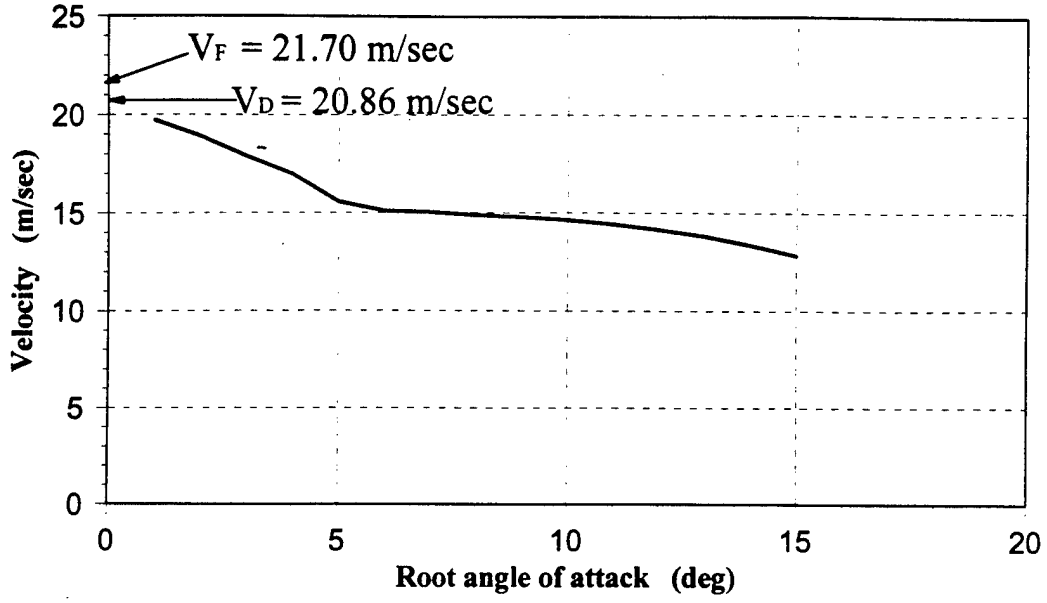

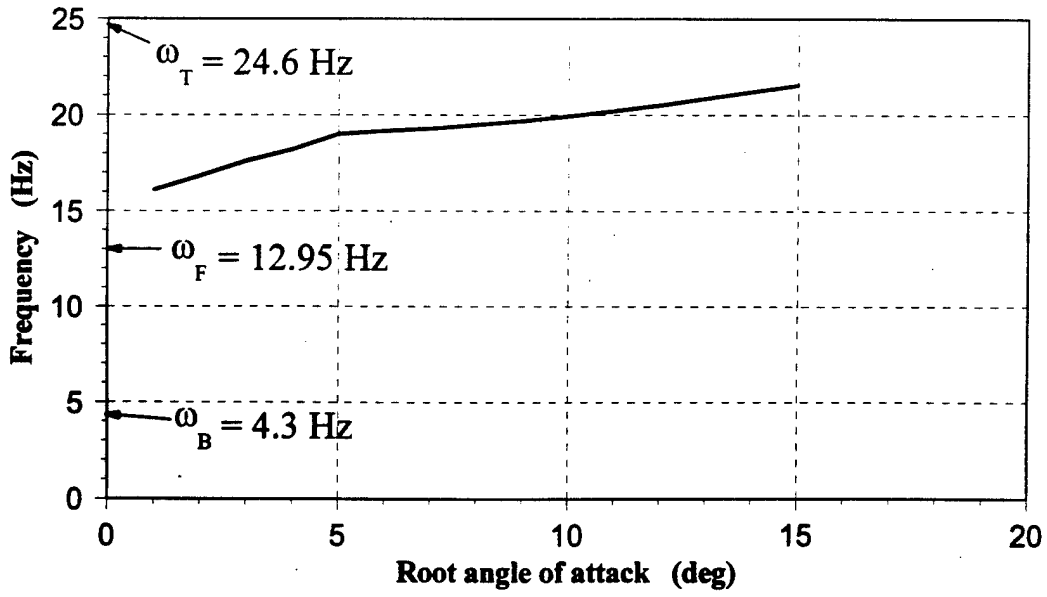

Figure 12. Flutter boundary and frequency variation

CHAPTER 5

CONCLUSIONS

The present investigation has developed a simple aeroelastic flutter analysis using the ONERA aerodynamic model to predict stall flutter behavior of a 3-dimensional wing. The formulation included nonlinearities in aerodynamic effects, and uses the harmonic balance method together with a Newton-Raphson numerical solution technique.

In keeping with the objective, some simplifications were made for convenience, but the model still retained the essential nonlinear characteristics of the aerodynamics. For example, a single break point approximation of aerodynamic force curves was used, only first bending and first torsion mode shapes were considered, the angle of attack at 75% span was taken as the average angle of attack for the entire wing, and only first harmonic terms in the harmonic balance method were used. These modifications can be extended to more complex formulations as need arises.

As shown in Chapter 4, the results of the analytical method exhibit almost all trends from experimental data and observation, as found for example by Dunn in [Refs. 14 and 15]. The trends show the flutter speed decreases as the root angle of attack increases. The results also show the flutter frequency increases toward the torsional natural frequency as the root angle of attack increases. The analysis

produced nonlinear limit cycle oscillations, specifically, it showed the "hardening" trend as the amplitude of limit cycle oscillation increases.

The present study also investigated the fitting of the ONERA aerodynamic model to measured experimental aerodynamic stall flutter characteristics. The results described in Appendix B show approximate representation of the 2-dimensional nonlinear aerodynamic force up to certain reduced frequencies, k, and oscillation amplitude α_v.

The current investigation concentrated specifically on the nonlinearity of aerodynamic forces. A structural nonlinearity can also be readily incorporated into the formulation in a similar manner, by this harmonic balance procedure, as discussed briefly in Appendix F. This would further improve correlation between analysis and experiment.

It should be mentioned before closing that for simplicity, the analyses in this report were all done in the frequency domain using the harmonic balance method. As such, they are capable of capturing the steady nonlinear limit cycles that often appear at larger amplitudes of oscillation. An alternative approach to nonlinear flutter behavior can be done in the time domain, using the same ONERA aerodynamic equations and integrating the equations in time. See Tang and Dowell [Ref. 31, 32]. These time domain solutions, when integrated for long enough times, often do settle down to the steady nonlinear limit cycle solutions investigated in this report. However, some nonlinear regimes may also lead to unbounded solutions, while other regimes may lead to bounded, but nonperiodic, chaotic-type solutions. These chaotic solutions can occur for example, when oscillations get trapped at the end points of a free-play structural nonlinearity, and are very sensitive to the initial starting conditions. See, for example, Tang and Dowell [Refs. 31, 32], Hauenstein, Zara, Eversman, and Qumei [Ref. 33] and Yang and Zhao [Ref. 34] for more details on these nonlinear solutions.

BIBLIOGRAPHY

1. Bisplinghoff, R. L., Ashley, H., and Halfman, R. L., *Aeroelasticity, Addison-Wesly*, Cambridge, MA, 1955.

2. Dowell, E. H., Curtiss, H. C. Jr., Scanlan, R. H., Sisto, F., *A Modern Course in Aeroelasticity*, 2nd Ed., Kluner Academic Publisher, Dordrecht, The Netherlands, 1989.

3. Fung, Y. C., *An Introduction to the Theory of aeroelasticity*, New York, NY, Dover Publications, 1969.

4. Ham, N.D., "Aerodynamic Loading on a 2-Dimensional Airfoil During Dynamic Stall," *AIAA Journal*, Vol. 6, No. 10, October 1968, pp. 1927-1934.

5. Ham, N. D., and Garelick, M. S., "Dynamic Stall Considerations in Helicopter Rotors," Journal of the American Helicopter Society, Vol. 13, No. 2, April 1968, pp. 49-55.

6. Giesing, J. P., "Nonlienar 2-Dimensional Potential Flow with Lift," Journal of Aircraft, Vol. 5, No. 2, March/April 1968, pp. 135-143.

7. Crimi, P., and Reeves, B. L., "A Method for Analyzing Dynamic Stall of Helicopter Rotor Blades," NASA CR-2009, May 1972.

8. Rao, B. M., Maskew, B., and Dvorak, F. A., "Theoretical Prediction of Dynamic Stall on Oscillating Airfoils," American Helicopter Society Paper 78-62, 1978.

9. Chi, R. M., "Separated Flow Unsteady Aerodynamic Theory," *Journal of Aircraft*, Vol. 22, No. 11, November 1985, pp. 956-964.

10. Tran, C.T. and Petot, D., "Semi-Empirical Model for the Dynamic Stall of Airfoils in View of Application to the Calculation of Responses of a Helicopter in Forward Flight," *Vertica*, Vol. 5, No. 1, 1981, pp. 35-53.

11. Dat, D., and Tran, C.T., "Investigation of the Stall Flutter of an Airfoil with a Semi-Empirical Model of 2-D Flow," *Vertica*, Vol. 7, No. 2, 1983, pp. 73-86.

12. Peters, D. A., "Toward a Unified Lift Model for Use in Rotor Blade Stability Analyses," *Journal of the American Helicopter Society*, Vol. 30, No. 3, July 1985, pp. 32-43.

13. Dunn, P. E., "Stall Flutter of Graphite/Epoxy Wings with Bending-Torsion Coupling," M.S. Thesis, Department of Aeronautics and Astronautics, M.I.T., May 1989. Also Technology Laboratory for Advanced Composites (TELAC) Report 89-5, M.I.T., May 1989.

14. Dunn, P. E., "Nonlinear Stall Flutter of Wings with Bending-Torsion Coupling," Ph.D. Thesis, Department of Aeronautics and Astronautics, M.I.T., December 1991. Also Technology Laboratory for Advanced Composites (TELAC) Report 91-16A, M.I.T., December 1991.

15. Dunn, P. E., and Dugundji, J., "Nonlinear Stall Flutter and Divergence Analysis of Cantilevered Graphite/Epoxy Wings." *AIAA Journal*, Vol. 30, No. 1, Januarry 1992, pp. 153-162.

16. Petot, D., and Loiseau, H., "Successive Smoothing Algorithm for Constructing the Semi-Empirical Model Developed at ONERA to Predict Unsteady Aerodynamic forces," NASA TM-76681, March 1982.

17. Petot, D., and Dat, R., "Unsteady Aerodynamic Loads on an Oscillating Airfoil with Unsteady Stall," 2nd Workshop on Dynamics and Aeroelasticity Stability Modeling of Rotorcraft Systems, Florida Atlantic University, Boca Raton, Florida, November 1987.

18. Petot, D., "Dynamic Stall Modeling of the NACA 0012 Profile," Short Note, *Recherché Aerospatiales*, 1984-6, pp. 55-58.

19. Rainey, A. G., "Preliminary Study of Some Factors which Affect the Stall-Flutter Characteristics of Thin Wings," NACA TN-3622, March 1956.

20. Rainey, A. G., "Measurement of Aerodynamic Forces for Various Mean Angles of Attack on an Airfoil Oscillating in Pitch and on Two Finite-Span Wings Oscillating in Bending with Emphasis on Damping in the Stall," NACA TR-1305, November 1957.

21. Fukushima, T., and Dadone, L. U., "Comparison of Dynamic Stall Phenomena for Pitching and Vertical Translation Motions," NASA CR-2693, 1977.

22. McAlister, K.W., Carr, L. W., and McCroskey, W. J., "Dynamic Stall Experiments on the NACA 0012 Airfoil," NASA TP-1100, January 1978.

23. McAlister, K. W., Pucci, S. L., McCroskey, W. J., and Carr, L. W., "An Experimental Study of Dynamic Stall on Advanced Airfoil Sections Volume 1: Summary of the Experiment," NASA TM-84245, July 1982.

24. McAlister, K. W., Pucci, S. L., McCroskey, W. J., and Carr, L. W., "An Experimental Study of Dynamic Stall on Advanced Airfoil Sections Volume 2: Pressure and Force Data," NASA TM-84245, September 1982.

25. Landsberger, B., and Dugundji, J., "Experimental Aeroelastic Behavior of Unswept and Forward Swept Graphite/Epoxy Wings," *Journal of Aircraft*, Vol. 22, No. 8, August 1985, pp. 679-686.

26. Dugundji, J., "Simple Expressions for Higher Vibration Modes of Uniform Euler Beams," *AIAA Journal Technical notes*, Vol. 26, No. 8, August 1988, pp. 1013-1014.

27. Crawley, E. F., and Dugundji, J., "Frequency Determination and Non-Dimensionalization for Composite Cantilever Plates," *Journal of Sound and Vibration,* Vol. 72, No. 1, 1980, pp. 1-10.

28. Press, W. H., Teukolsky, S. A., et. al, *Numerical Recipes in FORTRAN*, 2nd Edition, Cambridge, UK, Cambridge University Press, 1992.

29. Kuo, C. C., Morino, L., and Dugundji, J., "Perturbation and Harmonic Balance Methods for Nonlinear Panel Flutter," AIAA Journal, Vol. 10, No. 11, November 1972, pp. 1479-1484.

30. Dugundji, J., "Nonlinear Problems of Aeroelasticity," *Computational Nonlinear Mechanics in Aerospace Engineering*, Editor, Satya Atluri, *Progress in Astronautics and Aeronautics*, Vol. 146, 1992, pp. 127-155.

31. Tang, D.M. and Dowell, E.H., "Flutter and Stall Response of a Helicopter Blade with Structural Nonlinearity," *Journal of Aircraft*, Vol. 29, No. 5, Sept-Oct. 1992, pp. 953-959.

32. Tang, D.M., and Dowell, E.H., "Experimental and Theoretical Study for Nonlinear Aeroelastic Behavior of a Flexible Rotor Blade," *33rd AIAA/ASME/ASCE/AHS/ASC Structures, Structural Dynamics and Materials Conference, Dallas, TX, April 13-15, 1992*, AIAA-92-2253-CP.

33. Hauenstein, A.J., Zara, J.A., Eversman, W., Qumei, I.K., "Chaotic and Nonlinear Dynamic Response of Aerosurfaces with Structural Nonlinearities," *33rd AIAA/ASME/ASCE/AHS/ASC Structures, Structural Dynamics and Materials Conference, Dallas, TX April 13-15, 1992*, AIAA-92-2547-CP.

34. Yang, Z.C. and Zhao, L.C., "Analysis of Limit Cycle Flutter of an Airfoil in Incompressible Flow," *J. of Sound and Vibration*, Vol. (123), No. 1, 1988, pp. 1-12.

APPENDIX A
COEFFICIENTS OF AERODYNAMIC FORCES

This section lists the coefficients of the aerodynamic force models used in present study. Some of the coefficients were derived from aerodynamic theory, others were obtained from previous works [Ref. 14].

The linear portion of ONERA , 2-dimensional aerodynamic formulation, are described by equations (3.2) and (3.3). The linear coefficients (s_{Z1}, s_{Z2}, s_{Z3}, λ_1, λ_2, and a_{oZ}) were derived from 2-dimensional incompressible flow theory. In the complete aerodynamic, incompressible flow theory, lift can be formulated as,

$$L = \pi \rho b^2 \left[-\ddot{h} + U\dot{\theta} - b a \ddot{\theta} \right] + 2\pi \rho U b C(k) \left[-\dot{h} + U\theta + b\left(\frac{1}{2} - a\right)\dot{\theta} \right] \tag{A.1}$$

where a is a nondimensional parameter defining the distance from the mid-chord to the elastic axis divided by half-chord length (aft direction is defined as positive). For the present study, $a = -1/2$ and the h and θ above are consequently defined at the quarter-chord. Again, define the non-dimensional time variable τ, where the non-dimensional time derivative is denoted by " * ". Equation (A.1) then becomes,

$$L = -\pi\rho U^2 \ddot{h} + \pi\rho U^2 b\,\dot{\theta} - \pi\rho b a U^2 \ddot{\theta} + 2\pi\rho U b C(k)\left[-\frac{U}{b}\dot{h} + U\theta + b\left(\frac{1}{2} - a\right)\frac{U}{b}\dot{\theta}\right] \tag{A.2}$$

with some algebraic manipulation equation (A.2) becomes,

$$L = \frac{1}{2}\rho U^2 c\left(C_{L1} - C_{L\gamma}\right) + \frac{1}{2}\rho U^2 c\, C_{L\gamma} \tag{A.3}$$

where C_{L1} - $C_{L\gamma}$ and $C_{Z\gamma}$ are,

$$C_{L1} - C_{L\gamma} = -\pi\frac{\ddot{h}}{b} + \pi\dot{\theta} - \pi a\ddot{\theta} \tag{A.4}$$

$$C_{L\gamma} = C(k)\left[-2\pi\frac{\dot{h}}{b} + 2\pi\theta + 2\pi\left(\frac{1}{2} - a\right)\dot{\theta}\right] \tag{A.5}$$

Substituting value of a and equation (2.5) into equation (A.4) gives,

$$C_{L1} = \pi\dot{\alpha} + \frac{\pi}{2}\ddot{\theta} + C_{L\gamma} \tag{A.6}$$

where the angle of attack $\alpha = \theta - \dot{h}/b$. Place the single lag pole approximation of the Theodorsen function, defined in Eqs. (3.25) and (3.26), into equation (A.5). Similarly, substitute equation (2.5) into equation (A.5). This results in the following equation from which the coefficients can then be found,

$$\dot{C}_{L\gamma} + .15C_{L\gamma} = .15(2\pi)\left(\alpha + \dot{\theta}\right) + .55(2\pi)\left(\dot{\alpha} + \ddot{\theta}\right) \tag{A.7}$$

The coefficients of linear moment formulations were found in a similar way. The linear coefficients are summarized in Table 2.

The values of aerodynamic integrals appeared in equations (3.134), (3.135) and (3.144) to (3.148) are shown in Table 3. The integrands are the mode shapes, or combinations of mode shapes for a cantilevered beam.[Ref. 26 and 27]. Note that for simplicity, only first bending and torsion modes were used.

$$I_1 = \int_0^1 \phi_h^2 \, d\tilde{x} \tag{A.8}$$

$$I_2 = \int_0^1 \phi_h \, \phi_\alpha \, d\tilde{x} \tag{A.9}$$

$$I_3 = \int_0^1 \phi_\alpha^2 \, d\tilde{x} \tag{A.10}$$

$$I_4 = \int_0^1 \phi_h \, d\tilde{x} \tag{A.11}$$

$$I_5 = \int_0^1 \phi_\alpha \, d\tilde{x} \tag{A.12}$$

Additionally, as mentioned in Chapter 3, for the nonlinear portion of the aerodynamic force, stalling was only evaluated at the 75% span point. It was decided that the behavior at 75% span is typical of the entire wing. This idea relates back to the 2-dimensional typical section analysis described in Section 2.1.

The material properties and characteristics were obtained from previous study. These properties describes the characteristics of the $[0_3/90]_s$ graphite/epoxy test specimen (see table 4).

Coefficients	Lift	Moment
s_{Z1}	3.142	-0.786
s_{Z2}	1.571	-0.589
s_{Z3}	0.0	-0.786
λ_1	0.15	0.15
λ_2	0.55	0.55
a_{oZ}	6.28	0.0

Table 2. Linear aerodynamic coefficients ($a = -1/2$)

I_1	I_2	I_3	I_4	I_5
1.0000	0.6779	0.5000	0.7830	0.6366

Table 3. Aerodynamic integrals

M = 0.283 kg/m	ρ = 1.23 kg/m^3
S_α = 0.0 kg	**c** = 0.140 m
I_α = 0.343 e -3 kg-m	**l** = 0.559 m
K_h = 206.4 N/m^2	**b** = 0.070 m
K_α = 8.209 N/rad	ω_h = 27.02 rad/sec
S = 0.783 m^2	ω_α = 154.6 rad/sec

Table 4. Specimen properties from previous study

APPENDIX B
FITTING OF ONERA AERODYNAMIC MODEL

Fitting of the 2-dimensional ONERA aerodynamic coefficients to the experimental lift and moment data of the oscillating, stalled NACA 0012 airfoil given in Ref. 24 is explained in this section. This is done, first, to determine the coefficients which correctly model the aerodynamic forces. Second, the fitting of the aerodynamics allows for closer examination of the effects of each of the harmonics on the aerodynamic hysteresis cycle.

The aerodynamic force coefficients can be written in harmonic form by assuming harmonic motion, as described in Section 3.3. The nonlinear coefficients in equation (3.4), r_1, r_2 and r_3, were determined by Petot and Loiseau [Ref. 16] for an OA 209 airfoil. These coefficients were later modified by Dunn and Dugundji [Ref. 15]. All of the previous formulation of these coefficients were extremely complex. In this study, adhering to the objective of simplifying nonlinear analytical methods, these coefficients were simplified. They are of the form,

$$r_1 = r_{10} + r_{12}\left(\Delta C_{Zo}\right)^2 \tag{B.1}$$

$$r_2 = \left[r_{20} + r_{22}\left(\Delta C_{Zo}\right)^2\right]^2 \tag{B.2}$$

$$r_3 = r_{30} + r_{32}\left(\Delta C_{Zo}\right)^2 \tag{B.3}$$

The major simplification comes in terms of using only the constant term of the nonlinear deviation factor, ΔC_Z, where previous works had used the full terms. The coefficients, r_{10}, r_{12}, r_{20}, r_{22}, r_{30}, and r_{32}, are then determined by fitting to the experimental data by McAlister, Pucci, McCroskey and Carr [Ref. 24]. The coefficients along with the stall angle, α_1, and the slope of nonlinear deviation, b_1, are summarized in Table 5. Table 6 shows the reduced frequency, k, the vibratory angle, α_v, and the angle of attack, α_o, for each of the experimental cases to be fitted. Note, when transferring aerodynamic forces (Section 3.4b) from quarter chord to mid chord, the effect of moment is small compared to that of the lift. Therefore, only the lift is fitted to the experimental results. In the present analysis, the coefficients, r_i, used for the moment is the same as those used for the lift.

Fourier analysis was performed to extract the first and second harmonics of the experimental data in preparation for fitting comparison (see Table 7). The resulting aerodynamic hysteresis loop from the fitting process are plotted against the experimental data in Fig. 13. In addition, the static approximation of lift and moment curve used in the fitting process is shown in Fig. 14.

Each individual harmonic component affects the appearance of the hysteresis cycle distinctly. The gross characteristics of each harmonic are shown in Fig. 15. Fig. 15a shows the effect of the first sine harmonic to the hysteresis. It generally follows along the linear force curve. The first cosine harmonic influences the hysteresis cycle on the amount of deviation from the linear curve due to static stalling, as shown by Fig. 15b. If the second harmonic sine term is large enough, a crossing of the hysteresis loop appears as shown by Fig. 15c. Finally, the

second cosine term determines the degree of curvature of the resultant hysteresis loop (see Fig. 15d). Collectively, each of these harmonic terms influence the cycle. However, these are just broad generalities. In reality, other physical aspects also influence the nature of fluid flow. Nevertheless, this exercise gives insight into the basic building blocks of the appearance of the hysteresis loops.

$r_{10} = 0.700$	$r_{12} = 0.150$	$\alpha_1 = 10°$
$r_{20} = 0.246$	$r_{22} = 0.005$	b_1 -- **lift** = 8.30
$r_{30} = -0.024$	$r_{32} = 0.116$	b_1 -- **moment** = 0.40

Table 5. Aerodynamic fitting parameters

Case	α_0	α_v	k
1	9.8°	9.9°	0.104
2	9.8°	9.9°	0.151
3	9.8°	9.9°	0.253
4	14.9°	9.9°	0.104
5	14.9°	9.9°	0.153
6	14.7°	14.0°	0.104

Table 6. Aerodynamic fitting specifications

Experimental Values -- C_L

Case	C_0	S_1	C_1	S_2	C_2
1	0.818	0.747	0.420	0.159	-0.123
2	0.883	0.748	0.347	0.072	0.022
3	0.983	0.801	0.389	0.113	-0.073
4	0.897	0.497	0.574	0.013	-0.027
5	0.868	0.662	0.519	-0.014	0.063
6	0.826	0.661	0.506	0.056	0.016

Analytical Results -- C_L

Case	C_0	S_1	C_1	S_2	C_2
1	0.632	0.688	0.316	0.121	0.012
2	0.632	0.751	0.312	0.083	-0.012
3	0.632	0.766	0.338	0.039	-0.021
4	0.764	0.503	0.504	0.071	0.024
5	0.764	0.620	0.468	0.051	0.009
6	0.588	0.771	0.581	0.122	0.055

Table 7. Harmonic components of aerodynamic fitting results

Experimental Values -- C_M

Case	C_0	S_1	C_1	S_2	C_2
1	-0.090	-0.097	-0.017	0.016	0.080
2	-0.125	-0.103	-0.002	0.038	0.063
3	-0.128	-0.074	0.015	0.080	0.013
4	-0.058	-0.130	-0.036	-0.025	0.063
5	-0.037	-0.142	-0.017	0.003	0.051
6	-0.086	-0.131	-0.042	-0.02	0.065

Table 7 continued, Harmonic components
of aerodynamic fitting results

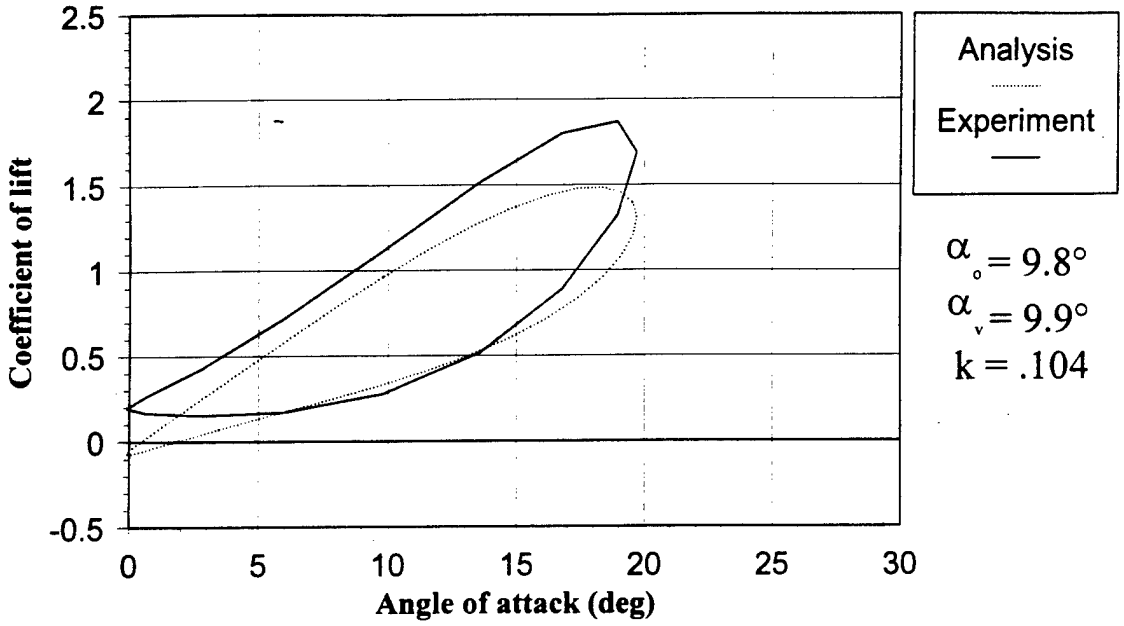

a. Case 1

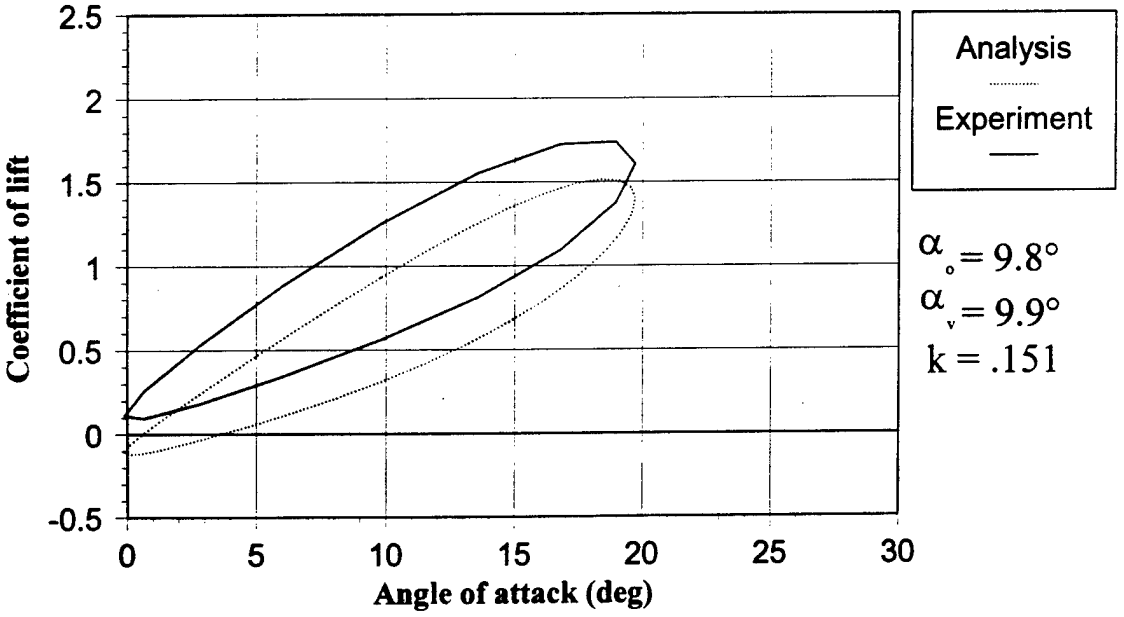

b. Case 2

Figure 13. Aerodynamic fitting

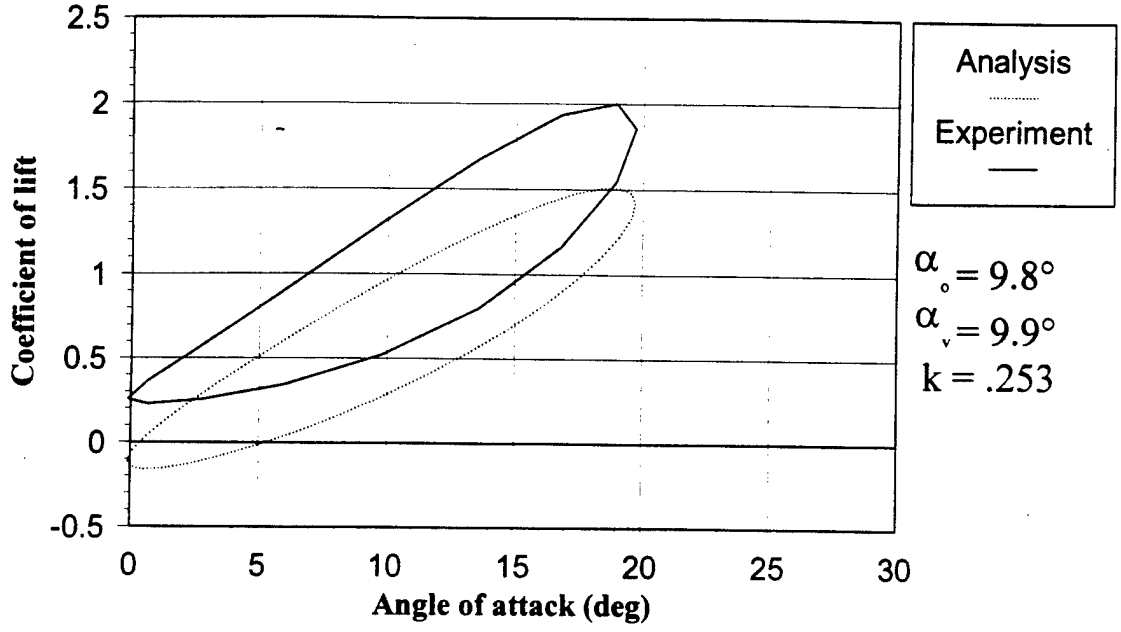

c. Case 3

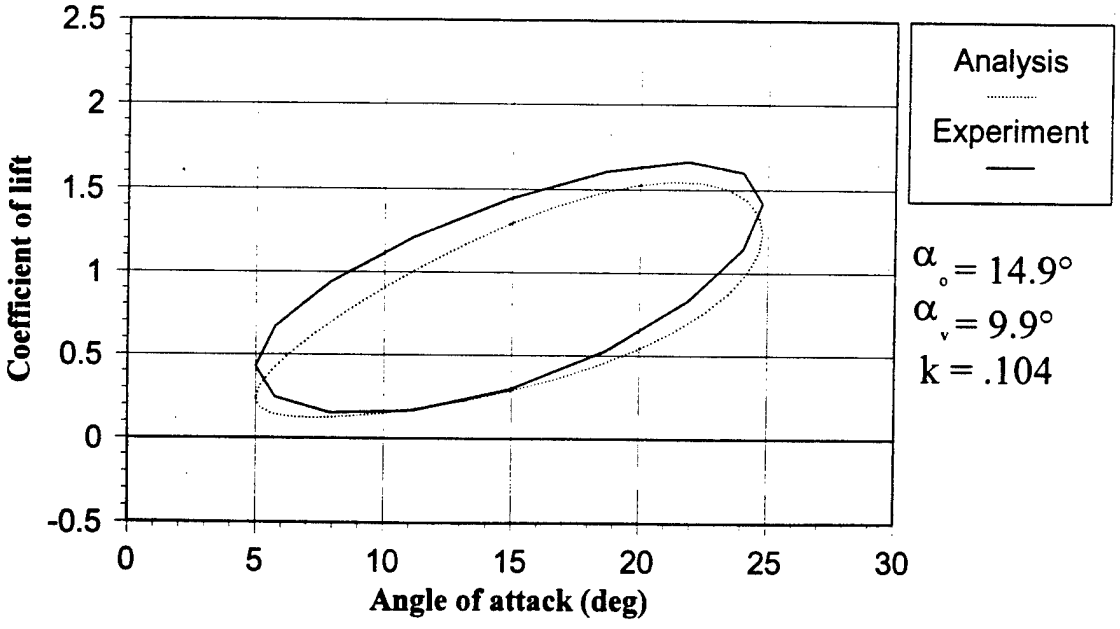

d. Case 4

Figure 13. continued, Aerodynamic fitting

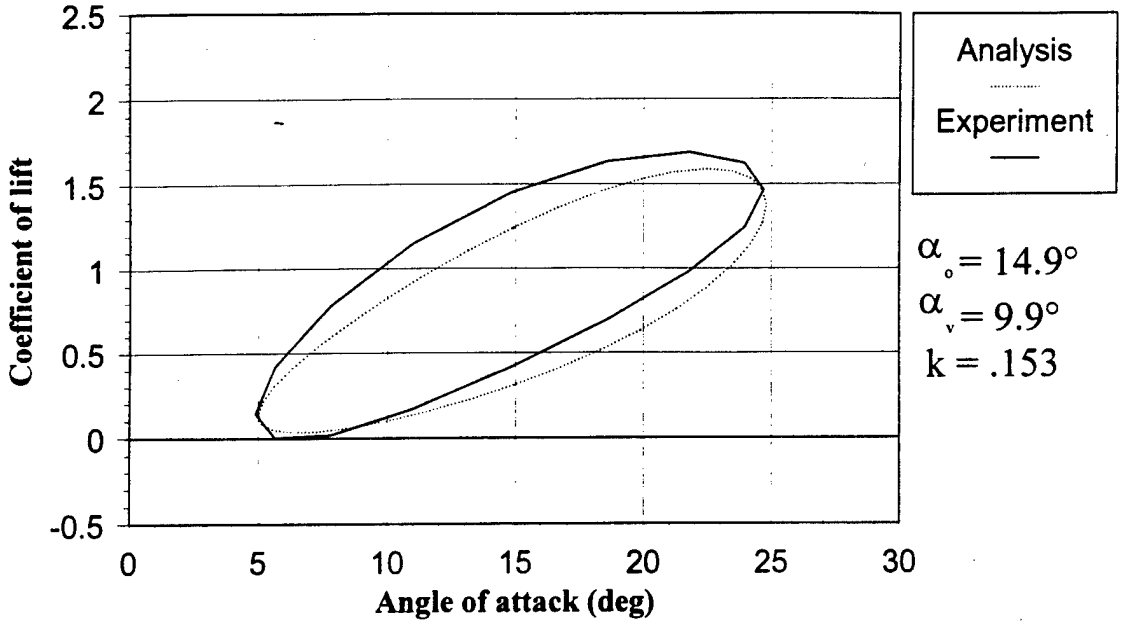

e. Case 5

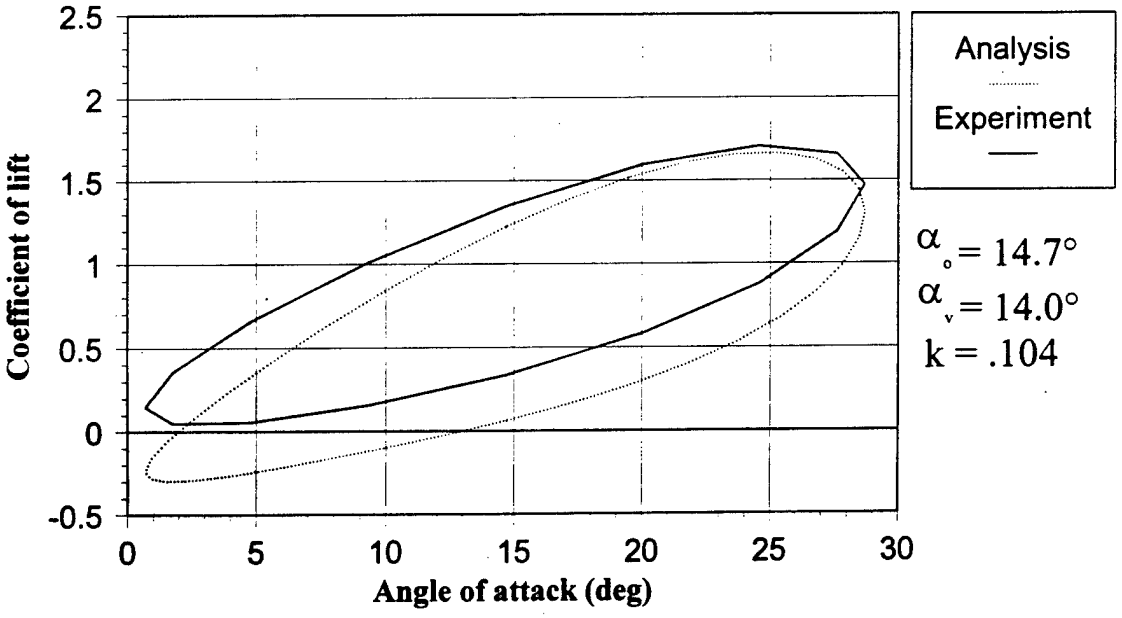

f. Case 6

Figure 13. continued, Aerodynamic fitting

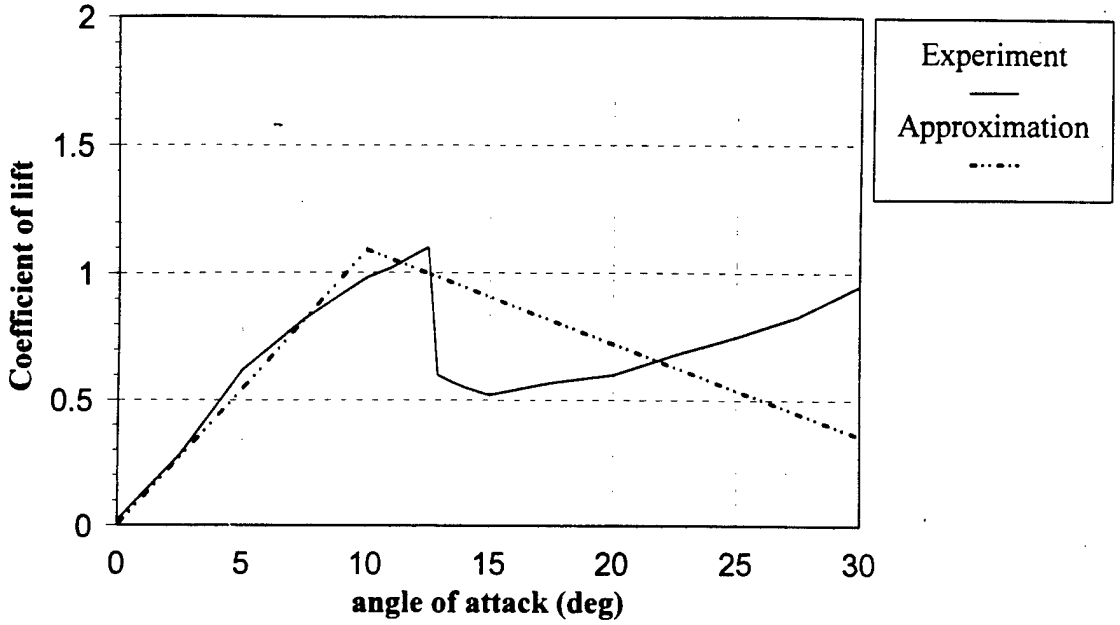

a. Static lift curve approximation

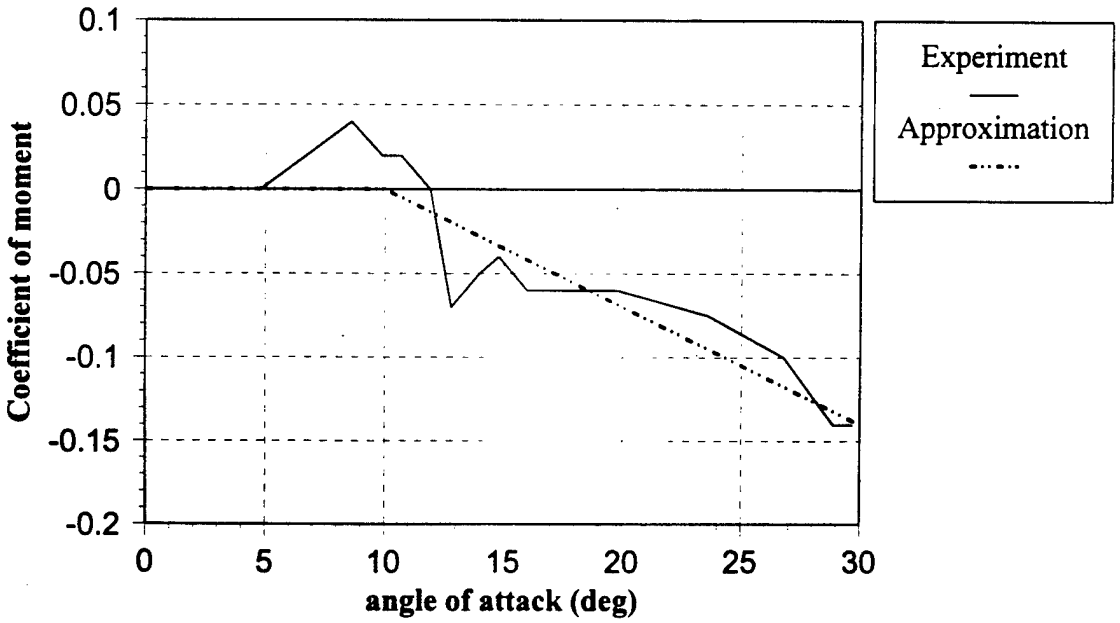

b. Static moment curve approximation

Figure 14. Static aerodynamic force curves

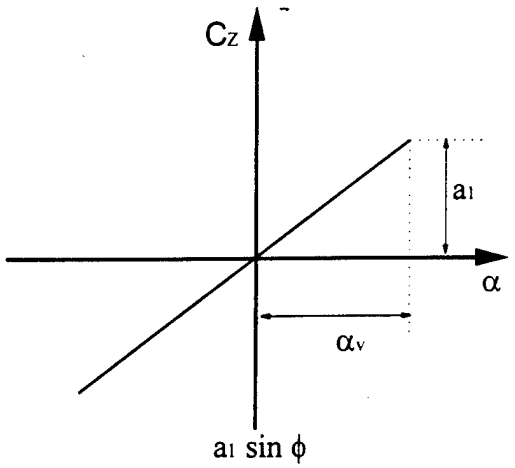

a1 sin ϕ

a. First harmonic sine term

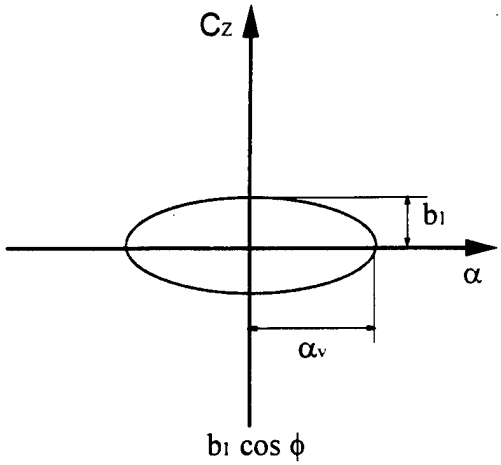

b1 cos ϕ

b. First harmonic cosine term

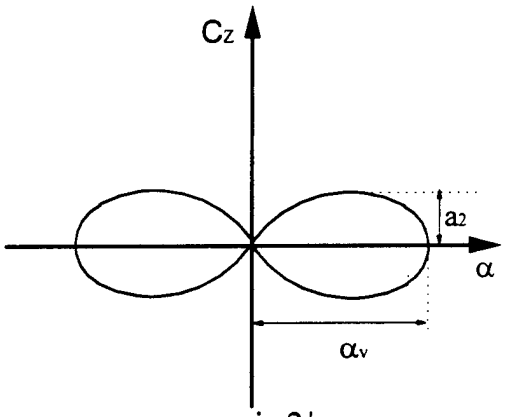

a2 sin 2ϕ

c. Second harmonic sine term

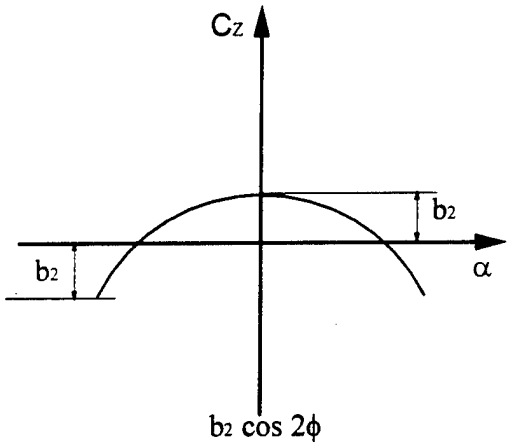

b2 cos 2ϕ

d. Second harmonic cosine term

Figure 15. Effects of harmonics

APPENDIX C
EXPERIMENTAL DATA FOR FITTING

As a reference for the fitting study described in the previous section, the original experimental data from McAlister, Pucci, McCroskey, and Carr [Ref. 24] is included here.

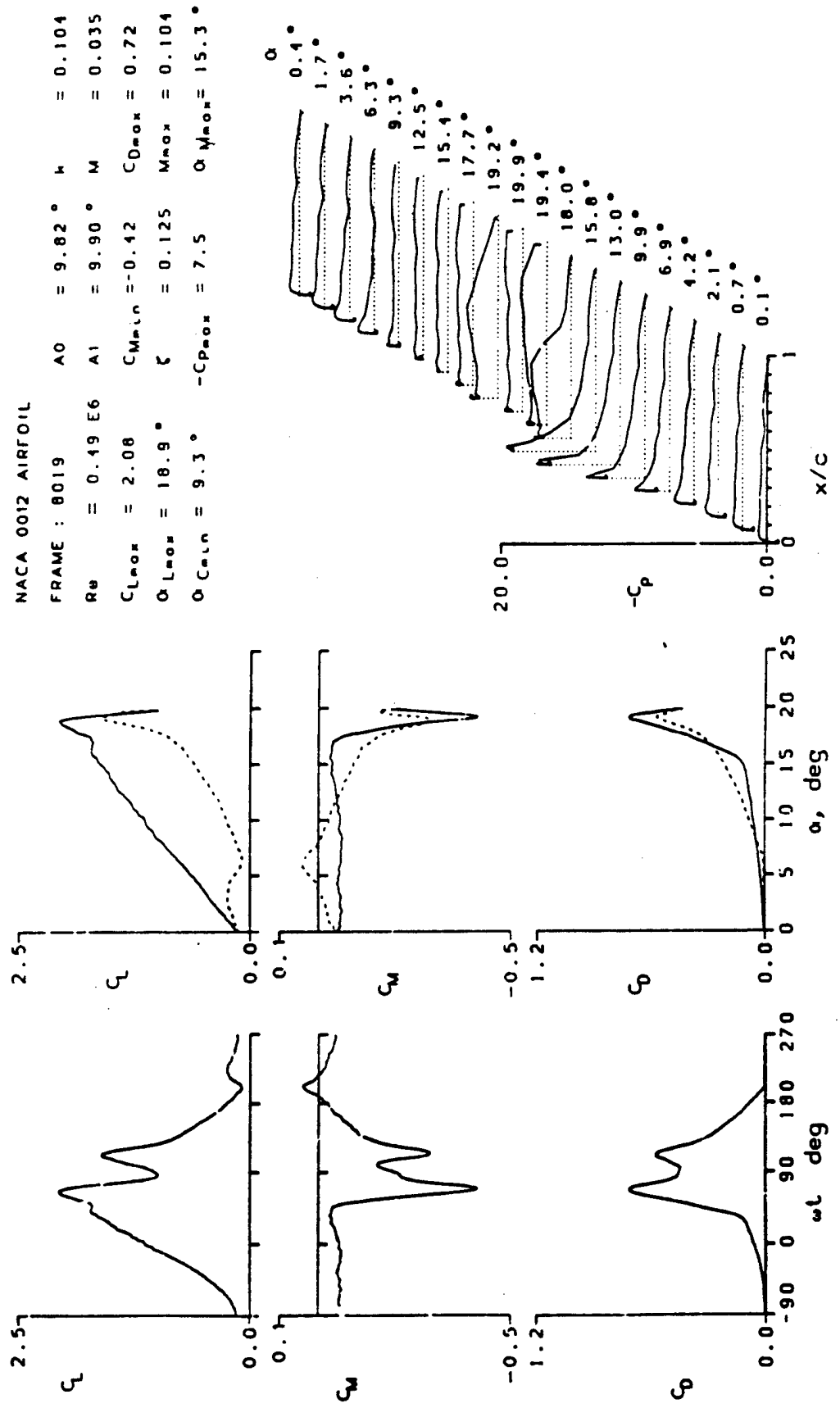

Figure 12.- Continued.

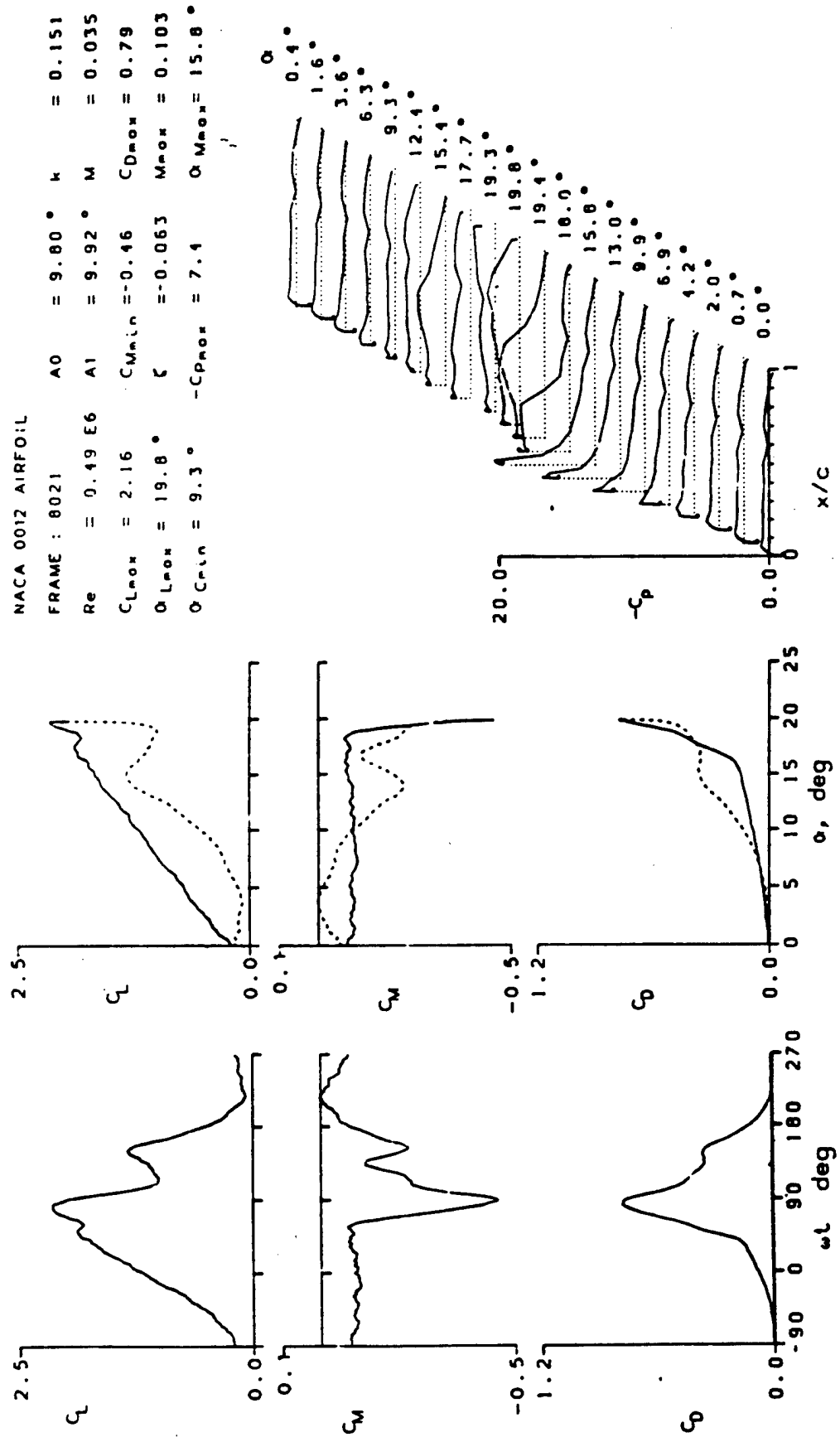

Figure 12.- Continued.

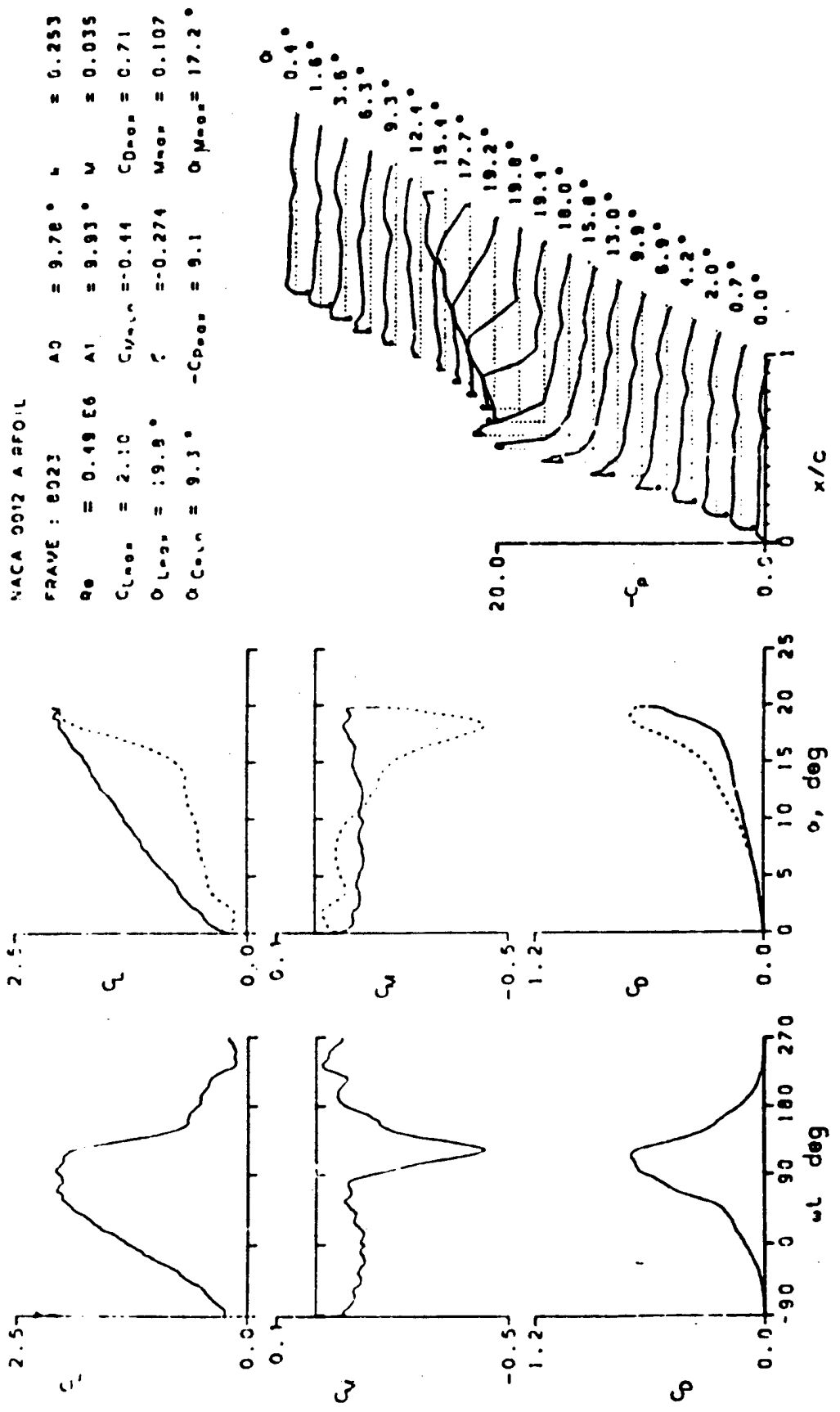

Figure 12.- Continued.

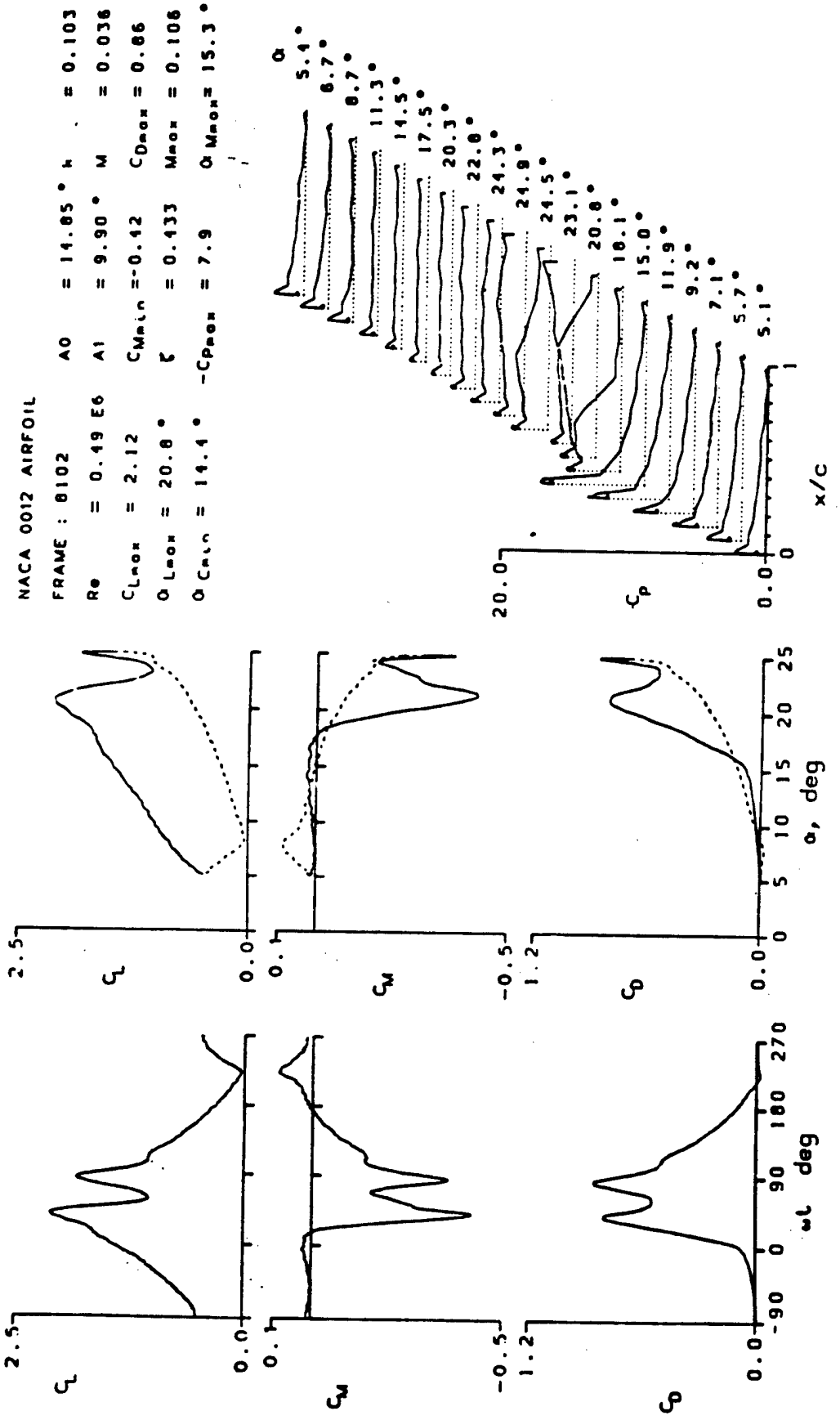

Figure 12.- Continued.

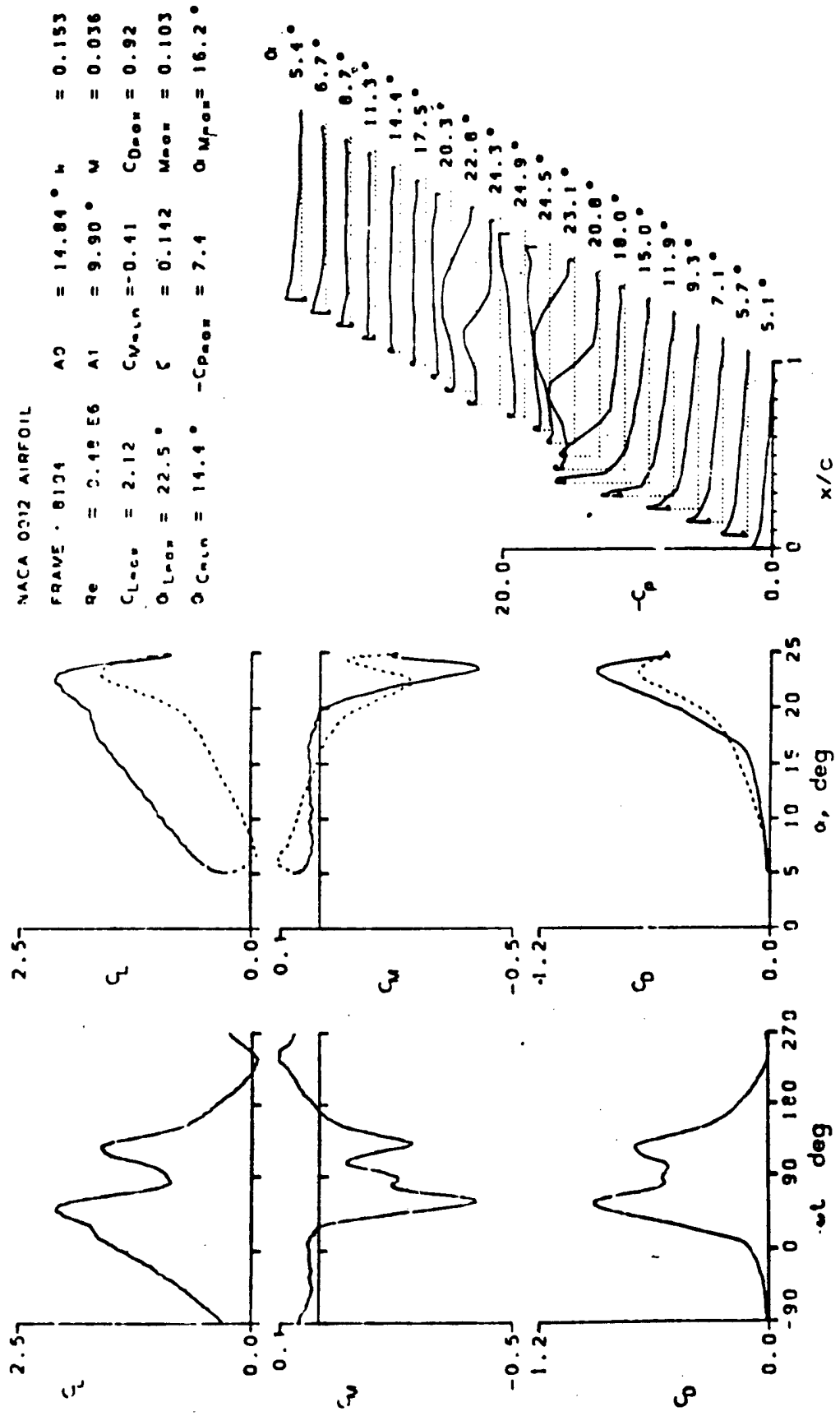

Figure 12.- Continued.

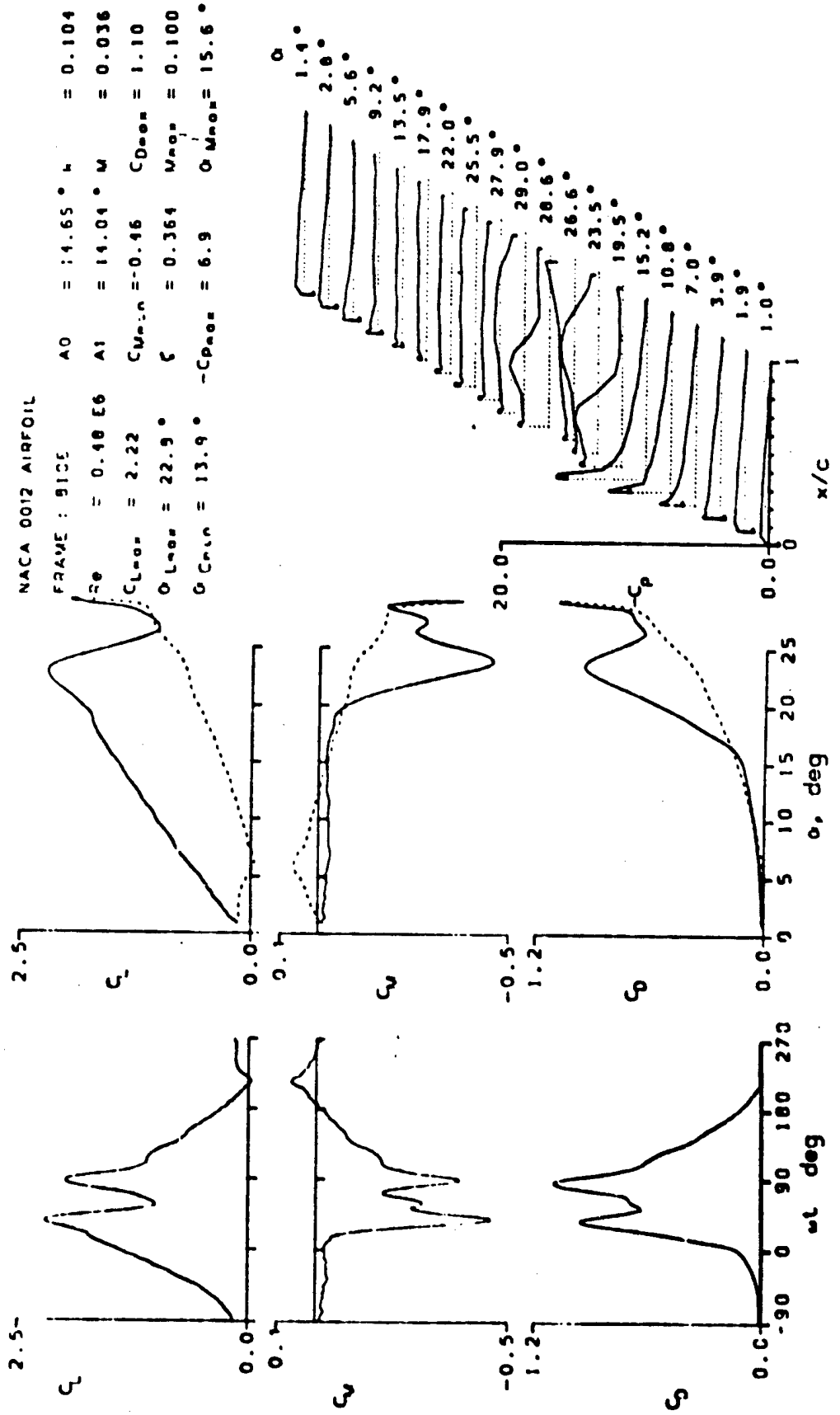

Figure 12.- Continued.

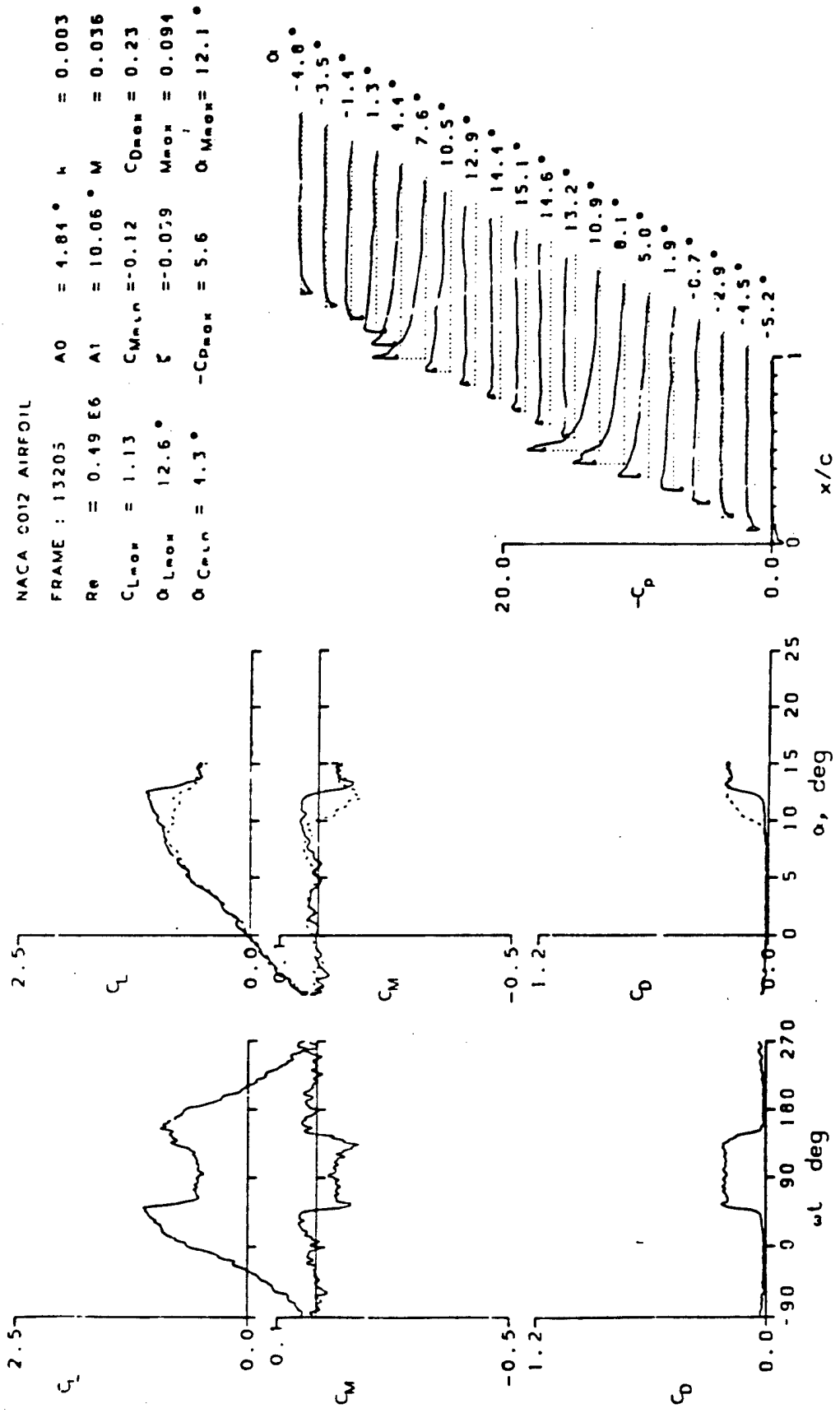

Figure 12.- Continued.

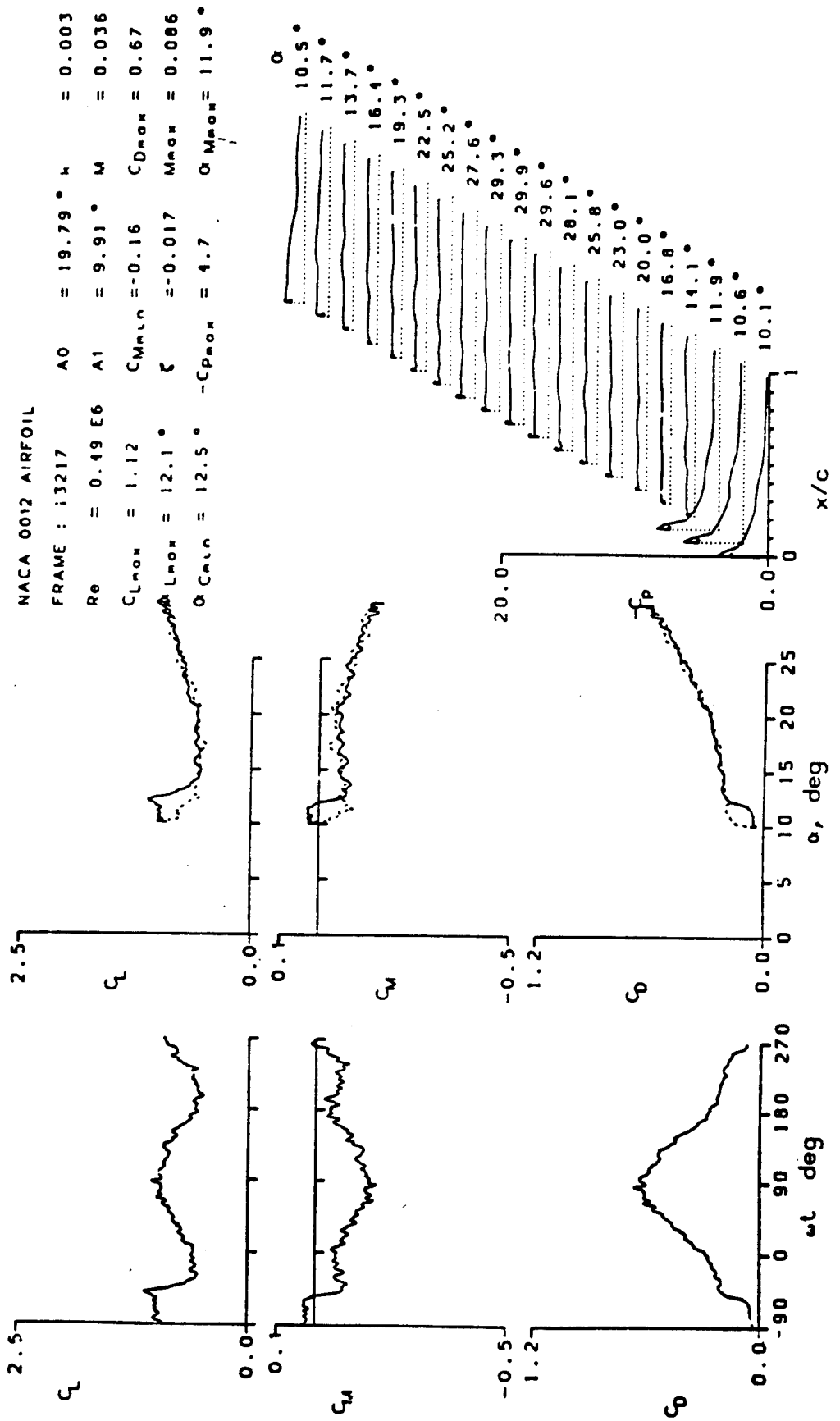

Figure 12.- Continued.

APPENDIX D
AERODYNAMIC FORCE CURVES

Equations (3.41) to (3.43) gives the nonlinear aerodynamic force deviation curve, where,

$$\Delta C_{Zo} = \frac{b_1 \alpha_V}{\pi}\left[\left(\frac{\alpha_1 - \alpha_o}{\alpha_V}\right)\left(\phi_1 - \frac{\pi}{2}\right) + \cos\phi_1\right] \tag{D.1}$$

$$\Delta C_{ZS1} = \frac{b_1 \alpha_V}{\pi}\left[-\left(\phi_1 - \frac{\pi}{2}\right) - \frac{1}{2}\sin(2\phi_1)\right] \tag{D.2}$$

$$\Delta C_{ZC2} = \frac{b_1 \alpha_V}{\pi}\left[-\frac{1}{2}\cos\phi_1 - \frac{1}{6}\sin 3\phi_1\right] \tag{D.3}$$

The non-dimensional time parameter, ϕ_1, associated with the above formulation are still applicable, as stated in Eqs. (3.44) and (3.45),

$$\phi_1 = \begin{cases} \sin^{-1}\delta & \text{if} \quad -1 < \delta < 1 \\ +\dfrac{\pi}{2} & \text{if} \quad \delta > 1 \\ -\dfrac{\pi}{2} & \text{if} \quad \delta < -1 \end{cases} \tag{D.4}$$

where,

$$\delta = \frac{\alpha_1 - \alpha_o}{\alpha_v} \tag{D.5}$$

This single break point, simplified model of the lift curve is shown in Figure 3. In the present study, with the combination of root angle of attack and oscillation amplitude, the range of oscillation amplitude may reach the negative portion of the force curve. As a result, symmetric aerodynamic force curves were used. The negative portion of the force curves were accounted for by including a second stall angle $\tilde{\alpha}_1$, where $\tilde{\alpha}_1 = -\alpha_1$. The negative portion of the aerodynamic force was then combined with the single sided formulation to yield the expanded version of Eqs. (D.1), (D.2) and (D.3),

$$\begin{aligned}\Delta C_{Zo} = &\frac{b_1 \alpha_V}{\pi}\left[\left(\frac{\alpha_1 - \alpha_o}{\alpha_V}\right)\left(\phi_1 - \frac{\pi}{2}\right) + \cos\phi_1\right] \\ &- \frac{b_1 \alpha_V}{\pi}\left[\left(\frac{\tilde{\alpha}_1 - \alpha_o}{\alpha_V}\right)\left(\tilde{\phi}_1 + \frac{\pi}{2}\right) + \cos\tilde{\phi}_1\right]\end{aligned} \tag{D.6}$$

$$\begin{aligned}\Delta C_{ZS1} = &\frac{b_1 \alpha_V}{\pi}\left[-\left(\phi_1 - \frac{\pi}{2}\right) - \frac{1}{2}\sin 2\tilde{\phi}_1\right] \\ &- \frac{b_1 \alpha_V}{\pi}\left[-\left(\tilde{\phi}_1 + \frac{\pi}{2}\right) - \frac{1}{2}\sin 2\tilde{\phi}_1\right]\end{aligned} \tag{D.7}$$

$$\begin{aligned}\Delta C_{ZC2} = &\frac{b_1 \alpha_V}{\pi}\left[-\frac{1}{2}\cos\phi_1 - \frac{1}{6}\sin 3\phi_1\right] \\ &- \frac{b_1 \alpha_V}{\pi}\left[-\frac{1}{2}\cos\tilde{\phi}_1 - \frac{1}{6}\cos 3\tilde{\phi}_1\right]\end{aligned} \tag{D.8}$$

where the addendum to Eqs. (3.34) and (3.35) are,

$$\tilde{\phi}_1 = \begin{cases} \sin^{-1}\tilde{\delta} & \text{if} \quad -1 < \tilde{\delta} < 1 \\ +\dfrac{\pi}{2} & \text{if} \quad \tilde{\delta} > 1 \\ -\dfrac{\pi}{2} & \text{if} \quad \tilde{\delta} < -1 \end{cases} \tag{D.9}$$

and,

$$\tilde{\delta} = \frac{\tilde{\alpha}_1 - \alpha_o}{\alpha_{1'}} \tag{D.10}$$

Fig. 16 shows the resulting symmetric aerodynamic force curve.

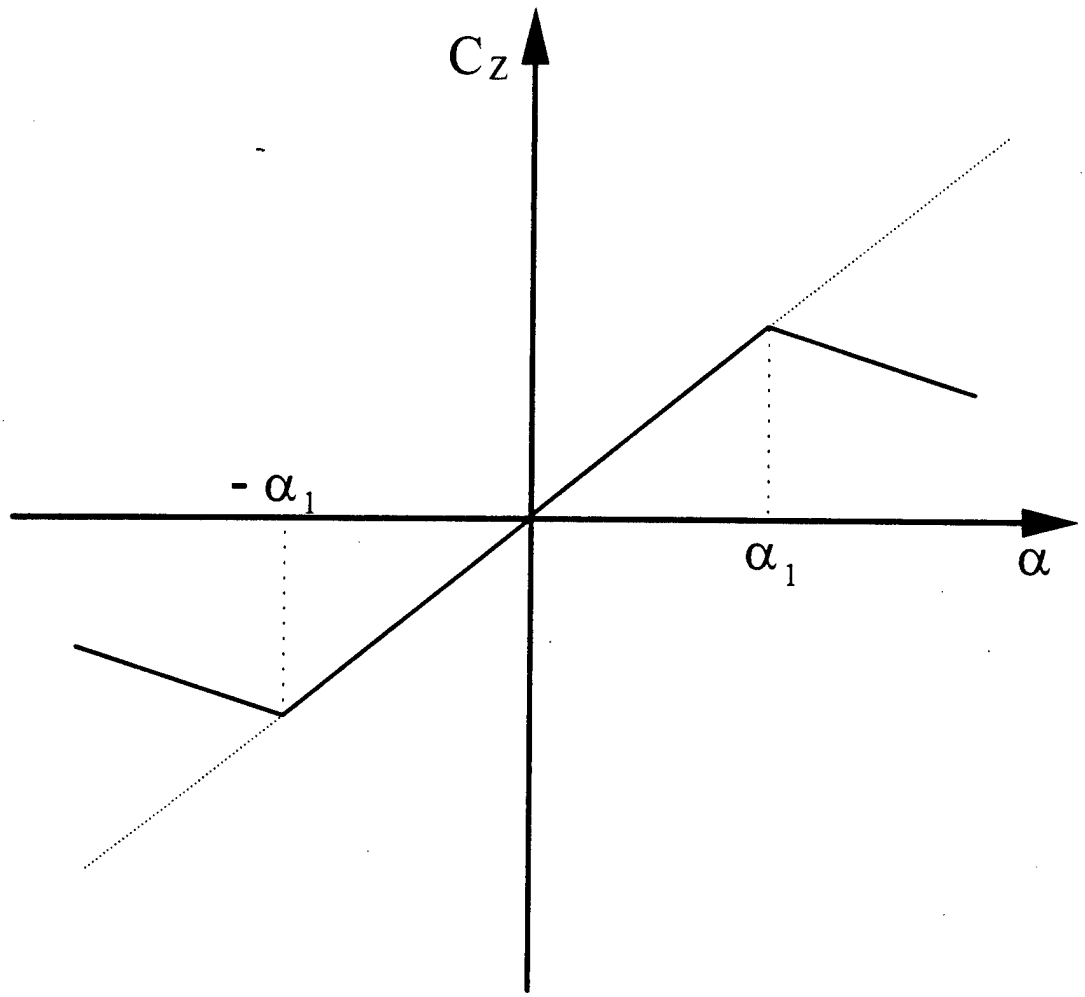

Figure 16. Symmetric aerodynamic force curve

APPENDIX E
NEWTON-RAPHSON METHOD

The Newton-Raphson method is a powerful iterative algorithm for solving nonlinear equations. This method gives one a very efficient means of converging to a solution, provided that a sufficiently good initial guess has been established.

A typical problem, deals with N functional equations to be zeroed, involving variables x_i, where i=1,2,..., N,

$$F_i(x_1, x_2, \ldots, x_N) = 0 \tag{E.1}$$

where x denotes the state vector and F denotes the entire vector of residual functions. The functions F can be expanded in Taylor series

$$F_i(x + \delta x) = F_i(x) + \sum_{j=1}^{N} \frac{\partial F_i}{\partial x_j} \delta x_j + O(\delta x^2) \tag{E.2}$$

The matrix of partial derivatives in above equation is the Jacobian matrix J. By neglecting terms of order δx^2 and higher and setting $F(x + \delta x) = 0$, the resulting equations become a set of linear equations which define the correction factor δx that move each function closer to zero simultaneously,

$$\delta x_{(n)} = -J^{-1} F(x_{(n)}) \tag{E.3}$$

The corrections are then added to the solution vector,

$$x_{(n+1)} = x_{(n)} + \delta x_{(n)} \tag{E.4}$$

and the process is iterated to convergence.

The Newton-Raphson iteration method is applied to the present analysis by rearranging equation (3.89) as

$$[M]\{\ddot{q}\} + [K]\{q\} - \{Q\} = 0 \tag{E.5}$$

Equation (E.5) is the matrix form of a system of six nonlinear equations with six unknowns. The unknowns, or the state vector x is comprised of the harmonic components of the modal amplitudes, q_{io}, q_{is}, and q_{ic}. Some adjustment of the state vector is made to ensure convergence to the non-trivial solution. The adjustment involves setting the sine component of one mode, q_{2S} to a small constant, which defines the amplitude level of the oscillation, while its cosine component, q_{2C}, is set to zero, since the flutter limit cycle oscillations can start at any arbitrary phase. The mode chosen was the torsional mode, since the torsional mode dominates the oscillation behavior. These two components were replaced by k_α and k, the reduced torsional frequency and reduced flutter frequency respectively. The resulting state vector x is then,

$$x = \begin{Bmatrix} q_{1o} \\ q_{2o} \\ q_{1S} \\ q_{1C} \\ k_\alpha \\ k \end{Bmatrix} \tag{E.6}$$

The Jacobian matrix was solved numerically. This was done by increasing the state vector x a small amount, finding the incremental change in the residual vector F, and then evaluating the partial derivative $\partial F_i / \partial x_j$; as $\Delta F_i / \Delta x_j$.

The Newton-Raphson procedure for solving flutter problems by introducing k and k_α into the state vector x described here, is similar to that used by Kuo, Morino, and Dugundji [Ref. 29] for nonlinear panel flutter.

APPENDIX F
INCLUDING STRUCTURAL NONLINEARITIES

The inclusion of structural nonlinearities is relatively straightforward with the Harmonic Balance Method. An example of a simple cubic torsional nonlinearity was included in the analysis of Dunn & Dugundji [Ref. 15]. The present appendix shows a simple cubic torsional structural nonlinearity included in the previous analyses of this report. Other types of structural nonlinearities can also be simply incorporated.

Turning to the nonlinear flutter analysis of Section 3.4, one modifies the basic equations of motion Eqs. (3.89) to read,

$$M_{11}\,\ddot{q}_1 + K_{11}\,q_1 = Q_1 \tag{F.1}$$

$$M_{22}\,\ddot{q}_2 + K_{22}\left(1 + C_N\,\theta_{ST}^2\right) q_2 = Q_2 \tag{F.2}$$

where the structural twist angle at the tip, θ_{ST}, is related to the twist coordinate q_2, through the relation,

$$\theta_{ST} = \frac{1}{c}\,\phi_\alpha(\ell)\,q_2 = \frac{1}{c}\,q_2 \tag{F.3}$$

See Eqs. (3.78), (3.80), and (3.85). The nonlinear stiffness constant, C_N, is of the order of 20 for the experimental parameters given in Table 4. After nondimensionalization, Eqs (F.1) and (F.2) lead to the nonlinear structural counterparts of Eqs. (3.103) and (3.104), namely,

$$\mu\pi I_1\left(\ddot{\tilde{q}}_1 + \Omega^2 k_\alpha^2 \tilde{q}_1\right) = \int_0^1 \phi_h C_{L1/2}\, d\tilde{x} \tag{F.4}$$

$$\mu \frac{\pi}{4} r_\alpha^2 I_3\left(\ddot{\tilde{q}}_2 + k_\alpha^2 \tilde{q}_2\right) = \int_0^1 \phi_\alpha C_{M1/2}\, d\tilde{x} - \mu \frac{\pi}{4} r_\alpha^2 I_3 k_\alpha^2 C_N \frac{i}{4} \tilde{q}_2^3 \tag{F.5}$$

Introducing Harmonic Balance,

$$\tilde{q}_i = \tilde{q}_{io} + \tilde{q}_{iS} \sin k\tau + \tilde{q}_{iC} \cos k\tau \tag{F.6}$$

leads to the additional nonlinear terms on the right hand sides of Eqs. (3.145), (3.148) and (3.149) respectively, namely,

$$-\mu \frac{\pi}{16} r_\alpha^2 I_3 k_\alpha^2 C_N\left(\tilde{q}_{2o}^2 + \frac{3}{2}\left[\tilde{q}_{2S}^2 + \tilde{q}_{2C}^2\right]\right)\tilde{q}_{2o} \tag{F.7}$$

$$-\mu \frac{\pi}{16} r_\alpha^2 I_3 k_\alpha^2 C_N\left(3\,\tilde{q}_{2o}^2 + \frac{3}{4}\left[\tilde{q}_{2S}^2 + \tilde{q}_{2C}^2\right]\right)\tilde{q}_{2S} \tag{F.8}$$

$$-\mu \frac{\pi}{16} r_\alpha^2 I_3 k_\alpha^2 C_N\left(3\,\tilde{q}_{2o}^2 + \frac{3}{4}\left[\tilde{q}_{2S}^2 + \tilde{q}_{2C}^2\right]\right)\tilde{q}_{2C} \tag{F.9}$$

The new modified nonlinear Eqs. (3.144) to (3.149) can then be solved using the Newton-Raphson iteration method, as described previously.

For a more general structural nonlinearity, $F_N = F_N(\alpha, \dot{\alpha})$, one can characterize the nonlinearity as in the previous aerodynamic case, by assuming the motion α to be described as

$$\alpha = \alpha_o + \alpha_v \sin\phi \tag{F.10}$$

See previous Eq. (3.33). Then by placing this motion back into F_N, one can represent the corresponding nonlinear force as,

$$F_N = B_{No} + B_{NS1} \sin\phi + B_{NC1} \cos\phi \tag{F.11}$$

where the Fourier coeffecients are given as,

$$B_{No} = \frac{1}{2\pi} \int_0^{2\pi} F_N(\alpha,\dot{\alpha})\, d\phi \tag{F.12}$$

$$B_{NS1} = \frac{1}{\pi} \int_0^{2\pi} F_N(\alpha,\dot{\alpha}) \sin\phi\, d\phi \tag{F.13}$$

$$B_{NC1} = \frac{1}{\pi} \int_0^{2\pi} F_N(\alpha,\dot{\alpha}) \cos\phi\, d\phi \tag{F.14}$$

This is analogous to Eqs. (3.37) to (3.40). Finally, upon noting that $\phi = k\tau + \xi$, one can revert back to the basic forms,

$$\alpha = \alpha_o + \alpha_S \sin k\tau + \alpha_C \cos k\tau \tag{F.15}$$

$$F_N = F_{No} + F_{NS1} \sin k\tau + F_{NC1} \cos k\tau \tag{F.16}$$

as in the previous Eqs. (3.67) to (3.71). These nonlinear forces Eq. (F.16) are then easily incorporated into the Harmonic Balance analysis.

APPENDIX G
ANALYSIS CODES

In the process to complete this study, many programs were written. A small portion of them were written as a learning tool for the author, others are building blocks for the final full flutter analysis. Furthermore, in order to save precious time, some codes were compiled several times with only minute differences. Thus, only those codes which are essential to aiding the completeness of this thesis are listed here.

All codes were in FORTRAN and compiled with Microsoft FORTRAN™ compiler Ver. 5.10 on an IBM compatible 386, 25 MHz personal computer. Some subroutines were taken from Numerical Recipe book [Ref. 28]. They are also available on Athena computing system.

```
cccccccccc
c AEROL1.FOR  Aerodynamic forces. Harmonic Balance
c              method used.
c           - Linear Lift, CL1
c  Warren Chen, 2-19-93
cccccccccc
      parameter (nn=2)
      double precision cl1
      real phi,k,phid,theta
      k=0.2
      open(5,file='aero1.in',status='old')
      open(9,file='aerol1.out',status='unknown')
      write(9,*)' AERODYNAMIC FORCES'
      write(9,*)' LIFT-LINEAR PORTION'
      write(9,1000)'K= ',k
      write(9,*)' '
      write(9,*)' '
      write(9,*)'THETA(deg)          Cl1'
      write(9,*)'----------------------'
10    continue
      read(5,*)phid
      if (phid.ge.999.9) then
      goto 500
      endif
      phi=(phid*3.1416)/180.0
      call funcv(k,phi,cl1,theta)
      thetad=theta*180.0/3.14159
      write(9,2000)thetad,'             ',cl1
      goto 10
 500  continue
      write(9,*)'End of Data'
      stop
C================================================
c  formats
C================================================
 1000 format(' ',a,f7.4)
 2000 format(' ',f5.1,a,f6.4)
 3000 format(' ',a,f8.6)
      end

C=====================================================
c   Subroutine to calculate lift
```

```
C=====================================================
      subroutine funcv(k,phi,p,theta)
C=====================================================
      real sl1,sl2,sl3,aol,lam1,lam2,tho,ths,thc,
     $ phi,k,hc,hs,b,theta
      real*8 p,ls,lc,f,g,clgo,clgs,clgc
C_____________________________________________________
C     Variable initialization
C_____________________________________________________
      b=.07
      sl1=2.142
      sl2=1.571
      sl3=0.0
      aol=5.9
      lam1=0.15
      lam2=0.55
      tho=0.0
      ths=0.175
      thc=0.0
      hc=0.0
      hs=0.0
C
      ls=aol*(ths-k*hc/b-k*thc)
      lc=aol*(thc+k*hs/b+k*ths)
      f=(k**2*lam2+lam1**2)/(lam1**2+k**2)
      g=k*lam1*(lam2-1)/(lam1**2+k**2)
      clgo=aol*tho
      clgs=f*ls-g*lc
      clgc=g*ls+f*lc
      theta=tho+ths*sin(phi)+thc*cos(phi)
      p=(sl1*(-k*thc-(hs/b)*k**2)-sl2*ths*k**2
     $ -sl3*k*thc+clgs)*sin(phi)
     $ +(sl1*(ths*k-(hc/b)*k**2)
     $ -sl2*thc*k**2+sl3*k*ths+clgc)*cos(phi)
     $ +clgo
C
      return
      end
```

```
cccccccccc
c AEROL4.FOR  Aerodynamic forces. Harmonic Balance
c              method used.
c       -     Total Lift,  Cl1+cl2
c New Basic Case.  Taken from McAlister's NASA
c        experimental work.
c New parameters(stall angles, lift curve slopes,
c        more accurate r1,r2,r3's
c        by taking into account variability of Dcz's
c        Trying to get a better fitting by vary
c        r1,r2,r3.
c
c Warren Chen, 3-7-93
cccccccccc
c
      real*8 phi,k,phid,theta,cz2c2,cz2s2,f,g
     $ ,cz2c1,cz2s1,cz20,clgo,cls,clc,cl1,cl2
     $ ,alpha0d,alphavd,alpha0,avib,r1,r2,r3
      write(*,*)'ccccccccccccccccccccccccccccccccccc'
      write(*,*)'cThis program calculates the first c'
      write(*,*)'cand second harmonic components of c'
      write(*,*)'cthe 2-d liftloop.                  c'
      write(*,*)'c The program inputs are:           c'
      write(*,*)'c    reduced frequency, k,          c'
      write(*,*)'c    average wing angle,in degrees c'
      write(*,*)'c    vibration angle,in degrees     c'
      write(*,*)'c The output is saved in file       c'
      write(*,*)'c    AEROL4.OUT                     c'
      write(*,*)'ccccccccccccccccccccccccccccccccccc'
      write(*,*)' '
      write(*,*)'Enter k:'
      read(*,*)k
      write(*,*)'Enter alpha0 in deg:'
      read(*,*)alpha0d
      write(*,*)'Enter alphav in deg:'
      read(*,*)alphavd
      alpha0=alpha0d*3.1415926/180.0
      avib=alphavd*3.1415926/180.0
      open(9,file='aerol4.out',status='unknown')
      write(9,*)' AERODYNAMIC FORCES---TOTAL LIFT
     $ AEROL4.out'
      write(9,1000)'INPUT:      K= ',k,'alpha0= '
```

```
     $ ,alpha0d,'            alphav= ',alphavd
      write(9,*)' '
      call funcvl(alpha0,avib,k,phi,theta,clgo,cls
     $ ,clc,f,g,cl1)
      call funcvn(alpha0,avib,r1,r2,r3,k,phi
     $ ,cz2c2,cz2s2,cz2c1,cz2s1,cz20,cl2)
      write(9,5000)'F= ',f,' G= ',g
      write(9,6000)'r1= ',r1,'   r2= ',r2,'    r3=
     $ ',r3
      write(9,*)' '
      write(9,*)'Linear portion, Cl1'
      write(9,4000)'cl10= ',clgo,'   cl1s= ',cls,'
     $ cl1c= ',clc
      write(9,*)' '
      write(9,*)'NonLinear portion, Cl2'
      write(9,4000)'cl20= ',cz20,'   cl2s1= ',cz2s1,'
     $ cl2c1= ',cz2c1
      write(9,5000)'cl2s2= ',cz2s2,'   cl2c2= ',cz2c2
      write(9,*)' '
      write(9,*)'Complete Cl'
      write(9,4000)'c0= ',clgo+cz20,'  s1= ',cls+cz2s1
     $ ,'  c1= ',clc+cz2c1
      write(9,5000)'s2= ',cz2s2,'  c2= ',cz2c2
      write(9,*)' '
      write(9,*)'PHI    THETA         CL1       CL2
     $ CL'
      write(9,*)'(deg)   (deg)'
      write(9,*)'-------------------------------------'
c
c
      phid=0.0
10    continue
      if (phid.ge.361.0) then
      goto 500
      endif
      phi=(phid*3.1415826)/180.0
      call funcvl(alpha0,avib,k,phi,theta,clgo,cls
     $ ,clc,f,g,cl1)
      call funcvn(alpha0,avib,r1,r2,r3,k,phi,cz2c2,
     $ cz2s2,cz2c1,cz2s1,cz20,cl2)
      thetad=theta*180.0/3.1415926
      write(9,2000)phid,thetad,cl1,cl2,cl1+cl2
```

```
      phid =phid + 15.0
      goto 10
 500  continue
      write(9,*)' '
      write(9,*)'End of Data'
      stop
c
c  formats
c
 1000 format(' ',a,f6.3)
 2000 format(' ',f6.1,f8.3,f9.3,f9.3,f8.3)
 3000 format(' ',a,f8.6)
 4000 format(' ',a,f8.4,a,f8.4,a,f6.4)
 5000 format(' ',a,f6.4,a,f6.4)
 6000 format(' ',a,f5.3,a,f5.3,a,f6.3)
      end
c
cccc
c Subroutine to calculate the linear portion
cccc
c
      subroutine funcvl(alpha0,avib,k,phi,theta,clgo
     $ ,p1s,p1c,f,g,p)
      real*8 sl1,sl2,sl3,aol,lam1,lam2,alpha0
     $ ,avib,thc,p,phi,k,hc,hs,b,theta,p1s,p1c
     $ ,ls,lc,f,g,clgo,clgs,clgc
c
      b=.07
      sl1=3.142
      sl2=1.571
      sl3=0.0
      aol=6.28
      lam1=0.15
      lam2=0.55
      thc=0.0
      hc=0.0
      hs=0.0
c
      ls=aol*(avib-k*hc/b-k*thc)
      lc=aol*(thc+k*hs/b+k*avib)
      f=(k**2*lam2+lam1**2)/(lam1**2+k**2)
      g=k*lam1*(lam2-1)/(lam1**2+k**2)
```

```
      clgo=aol*alpha0
      clgs=f*ls-g*lc
      clgc=g*ls+f*lc
      theta=alpha0+avib*sin(phi)+thc*cos(phi)
      p1s=(sl1*(-k*thc-(hs/b)*k**2)-sl2*avib*k**2-
     $ sl3*k*thc+clgs)
      p1c=(sl1*(avib*k-(hc/b)*k**2)-
     $ sl2*thc*k**2+sl3*k*avib+clgc)
      p=p1s*sin(phi)+p1c*cos(phi)+clgo
      return
      end
c
cccc
c Subroutine to calculate the Nonlinear portion
cccc
c
      subroutine funcvn(alpha0,avib,r1,r2,r3,k,phi
     $ ,cz2c2,cz2s2,cz2c1,cz2s1,cz20,p2)
      double precision dcz0,dczs1,dczc2,r0,rs1,rc1,rs2
     $ ,k1,k2,k3,k4,cz2c2,cz2s2,cz2c1,cz2s1,cz20
     $ ,alpha1,b1,alpha0,avib,r1,r2,r3,phi1,k,p2,phi
     $ ,pent2,phi1t,alpha1t
c
      alpha1=0.1745
      alpha1t=-0.1745
      b1=8.3
c
      pent=(alpha1-alpha0)/avib
      if (pent .gt. 1.0) then
      phi1=1.571
      else if (pent .lt. -1.0) then
      phi1=-1.571
      else
      phi1=asin(pent)
      endif
c
      pent2=(alpha1t-alpha0)/avib
      if (pent2 .gt. 1.0) then
      phi1t=1.571
      else if (pent2 .lt. -1.0) then
      phi1t=-1.571
      else
```

```
      phi1t=asin(pent2)
      endif
c
      dcz0=(b1*avib/3.14159)*(-pent*(1.571-phi1)
     $ +cos(phi1))-(b1*avib/3.14159)*(pent2*
     $ (phi1t+1.571)+cos(phi1t))
      dczs1=(b1*avib/3.14159)*((1.571-phi1)-
     $ 0.5*sin(2.0*phi1))-(b1*avib/3.14159)*
     $ (-(phi1t+1.571)-0.5*sin(2.0*phi1t))
      dczc2=(b1*avib/3.14159)*(-0.5*cos(phi1)-
     $ 0.166667*cos(3.0*phi1))
     $ -(b1*avib/3.14159)*(-0.5*cos(phi1t)-
     $ 0.166667*cos(3.0*phi1t))
      r1=0.7+0.15*dcz0**2
      r2=(0.2465+0.005*dcz0**2)**2
      r3=(-0.4+1.91*dcz0**2)*(0.2465**2)
      k1=r2-k*k
      k2=r1*k
      k3=r2-4*k*k
      k4=2*r1*k
      r0=-r2*dcz0
      rs1=-r2*dczs1
      rc1=-r3*k*dczs1
      rs2=2*r3*k*dczc2
      rc2=-r2*dczc2
      cz20=r0/r2
      cz2s1=(k1*rs1+k2*rc1)/(k1**2+k2**2)
      cz2c1=(k1*rc1-k2*rs1)/(k1**2+k2**2)
      cz2s2=(k3*rs2+k4*rc2)/(k3**2+k4**2)
      cz2c2=(k3*rc2-k4*rs2)/(k3**2+k4**2)
      p2=cz20+cz2s1*sin(phi)+cz2c1*cos(phi)
     $ +cz2s2*sin(2.0*phi)+cz2c2*cos(2.0*phi)
      return
      end
```

```
ccccc
c  FOURI.FOR - Program to calculate Fourier Coefficients
c             Output:1st and 2nd harmonics of aero
c                          hysteresis curve values
c  Warren Chen 3-16-93
ccccc

      parameter(n=16,m=8)
      integer i
      real*8 f(1:n),c0,c1,s1,c2,s2
      open(5,file='fouri.in',status='old')
      open(9,file='fouri.out',status='unknown')
      do i=1,n
       read(5,*)f(i)
      enddo
      c0=0.0
      c1=0.0
      c2=0.0
      s1=0.0
      s2=0.0
      do i=1,n
       c0=c0+f(i)
       s1=s1+f(i)*dsin(6.2832*(i-1)/n)
       c1=c1+f(i)*dcos(6.2832*(i-1)/n)
       s2=s2+f(i)*dsin(6.2832*(i-1)/m)
       c2=c2+f(i)*dcos(6.2832*(i-1)/m)
      enddo
      c0=c0/n
      s1=s1/m
      c1=c1/m
      s2=s2/m
      c2=c2/m
      write(9,*)'Fourier Coefficients'
      write(9,*)'Aerodynamic Moments'
      write(9,*)'    c0     s1      c1      s2      c2'
      write(9,1000)c0,s1,c1,s2,c2
1000  format(' ',f7.3,f7.3,f7.3,f7.3,f7.3)
      end
```

```
cccccccccc
c  HARM7d1.FOR  Complete 3-D flutter program,
c          x(1)=q10, x(2)=q20, x(3)=q1s, x(4)=q1c,
c              x(5)=k2, x(6)=k.
c          Complete Aerodynamics (symmetric
c               aeroforce curves)
c  Warren Chen, 4-29-93
cccccccccc
      integer n,np,indx,i,t,j
      parameter (nn=6)
      real*8 x(1:nn),fvec(1:nn),fjac(1:nn,1:nn),delta(nn)
     $ ,fs,fq,avib,avibd,alpha0,alpha0d,phi1t,phi1
      real y(nn,nn),d,theta0,theta0d,q2s
      write(*,*)'Enter Root Angle (in degrees)'
      read(*,*)theta0d
      theta0=theta0d*3.14159/180.0
      write(*,*) Enter q2s:'
      read(*,*)q2s
      write(*,*)'Enter Initial value of q10:'
      read(*,*)x(1)
      write(*,*)'Enter Initial value of q20:'
      read(*,*)x(2)
      write(*,*)'Enter Initial value of q1s:'
      read(*,*)x(3)
      write(*,*)'Enter Initial value of q1c:'
      read(*,*)x(4)
      write(*,*)'Enter Initial value of k2:'
      read(*,*)x(5)
      write(*,*)'Enter Initial value of k:'
      read(*,*)x(6)
      n=6
      np=6
      do i=1,n
      delta(i)=5.0
      enddo
      t=0
      open(5,file='harm7d1.in',status='old')
      open(9,file='harm7d1.out',status='unknown')
      write(9,*)' '
      write(9,*)'Harm7d1.out'
      write(9,*)'Complete aerodynamics'
```

```
      write(9,*)' '
      write(9,*)'INPUT'
      write(9,3000)'Root angle: ',theta0d,' deg'
      write(9,*)' '
      write(9,5500)'q2s','q10','q20','q1s','q1c','k2'
     $ ,'k','Fs(m/s)'
     $ ,'w(Hz)','a0','av'
      write(9,*)'---------------------------------------'
   10 continue
      if (dabs(delta(6)).le.1.0d-4 .and.
     $ dabs(delta(5)).le.1.0d-4 .and.
     $ dabs(delta(4)).le.1.0d-4 .and.
     $ dabs(delta(3)).le.1.0d-4 .and.
     $ dabs(delta(2)).le.1.0d-4 .and.
     $ dabs(delta(1)).le.1.0d-4)then
           goto 500
      endif
      t=t+1
      call funcv(theta0,q2s,alpha0,avib,phi1,phi1t
     $ ,n,x,fvec)
      call fdjac(q2s,theta0,n,x,fvec,np,fjac)
      do i=1,n
       do j=1,n
        y(i,j)=0.
       enddo
       y(i,i)=1.
      enddo
      call ludcmp(fjac,n,np,indx,d)
      do j=1,n
      call lubksb(fjac,n,np,indx,y(1,j))
      enddo
      do j=1,n
       delta(j)=0.
      do i=1,n
         delta(j)=delta(j)+y(j,i)*fvec(i)
      enddo
      enddo
c
      do i=1,n
       x(i)=x(i)-delta(i)
      enddo
      if (t.ge.25)then
```

```
          goto 500
        endif
        goto 10
  500   continue
        if (t .ge. 25)then
        write(*,*)'Not converged'
        goto 600
        endif
        fs=10.882/x(5)
        fq=(fs*x(6)/0.07)/6.28
        avibd=avib*180.0/3.14159
        alpha0d=alpha0*180.0/3.14159
        write(9,5000)q2s,x(1),x(2),x(3),x(4),x(5)
       $ ,x(6),fs,fq,alpha0d,avibd
        do i=1,n
         x(i)=x(i)+0.0001
        enddo
        do i=1,n
         delta(i)=5.0
        enddo
        t=0
        read(5,*)q2s
        if (q2s .ge. 999.0) then
        goto 600
        endif
        goto 10
   600  continue
        write(9,*)' '
        write(9,*)'End of data'
        stop
c
c=======================================================
c     formats
c=======================================================
 1000 format(' ',i2,1x,i2,a,f17.9)
 2000 format(' ',f17.9)
 3000 format(' ',a,f8.3,a)
 4000 format(' ',a,f6.4)
 4200 format(' ',a8,a8,a8,a8,a8,a8)
 4400 format(' ',f9.4,f9.4,f9.4,f9.4,f8.4,f7.4)
 5000 format(' ',f4.3,f7.4,f7.4,f7.4,f7.4,f7.4,f7.4,f8.3
     $ ,f8.3,f7.3,f7.3)
```

```
 5100 format(' ',i3,f8.4,f8.4,f8.4,f8.4)
 5500 format(' ',a3,a6,a6,a7,a7,a7,a7,a8,a8,a7,a7)
 5600 format(' ',a,a7,a7,a7,a7)
      end

c=======================================================
c    Subroutine to find the Jacobian matrix
c=======================================================
      subroutine fdjac(q2s,theta0,n,x,fvec,np,df)
      integer n,np,nmax
      real*8 df(np,np),fvec(n),x(n),eps,f(40),alpha0,avib
     $ ,phi1,phi1t
      parameter (nmax=40,eps=1.e-4)
      integer i,j
      real h,temp,theta0
      do j=1,n
       temp=x(j)
       h=eps*abs(temp)
       if(h.eq.0.)h=eps
       x(j)=temp+h
       h=x(j)-temp
       call funcv(theta0,q2s,alpha0,avib,phi1,phi1t,n,x,f)
       x(j)=temp
       do i=1,n
         df(i,j)=(f(i)-fvec(i))/h
       enddo
      enddo
c
       return
       end
c=======================================================
c subroutine to find flutter velocity, frequency
c=======================================================
      subroutine funcv(theta0,q2s,alpha0,avib,phi1
     $ ,phi1t,n,x,P)
      integer n
      real M,Ia,Pi,rho,c,l,b,wh,wa,q2c,q2s,I1,I2,I3,I4,I5
     $ ,theta0,alpha1,alpha1t,sl1,sl2,sl3,aol
     $ ,lam1,lam2,sm1,sm2,sm3
     $ ,aom,b1,b2,phia,phih
      real*8 x(n),P(n),om,ra,CL20,CM20,alpha0
     $ ,alphas,alphac,avib,mu,f,G,BoL,B1L
```

```
      $ ,B2L,B3L,B4L,BoM,B1M,B2M,B3M,B4M,pent,pent2
      $ ,phi1,phi1t,dcL0,dcLs1,r1L,r2L,r3L
      $ ,k1L,k2L,rs1L,rc1L,ALs1
      $ ,BLc1,dcM0,dcMs1,r1M,r2M,r3M,k1M
      $ ,k2M,rs1M,rc1M,AMs1,BMc1
c_____________________________________________________
c     Variable initialization
c_____________________________________________________

       I1=1.0
       I2=0.6779
       I3=0.5
       I4=0.783
       I5=0.6366
       q2c=0.0
       M=0.158
       Ia=192.0 e -6
       Pi=3.14159
       rho=1.23
       c=0.14
       l=0.559
       b=c/2.0
       wh=27.02
       wa=154.6
       phia=0.844605
       phih=1.31538
       alpha1=0.2094
       alpha1t=-0.2094
       alpha0=theta0+0.5*phia*x(2)
       alphas=phia*(0.5*q2s+0.25*x(6)*q2c)
      $ +phih*(x(6)*x(4))
       alphac=phia*(0.5*q2c-0.25*x(6)*q2s)-
      $ phih*(x(6)*x(3))
       avib=dsqrt(alphas**2+alphac**2)
       om=wh/wa
       mu=(M/l)/(Pi*rho*b**2)
       ra=(dsqrt(Ia/M))/b
c
c=====================================================
c  Linear Lift
c=====================================================
       sl1=3.142
```

```
      sl2=1.571
      sl3=0.0
      aol=5.73
      lam1=0.15
      lam2=0.55
      F=(x(6)**2*lam2+lam1**2)/(lam1**2+x(6)**2)
      G=(x(6)*lam1*(lam2-1))/(lam1**2+x(6)**2)
      BoL=x(2)*aol*0.5
      B1L=x(6)*(0.25*x(6)*sl1-0.5*x(6)*sl2
     $ -0.25*G*aol)+0.5*F*aol
      B2L=x(6)*(0.5*sl1+0.5*sl3+0.25*F*aol)+0.5*G*aol
      B3L=x(6)*(sl1*x(6)+G*aol)
      B4L=F*aol*x(6)
c================================================
c  Linear Moment
c================================================
      sm1=-0.786
      sm2=-0.589
      sm3=-0.786
      aom=0.0
      BoM=x(2)*aom*0.5
      B1M=x(6)*(0.25*x(6)*sM1-0.5*x(6)*sM2-0.25*G*aoM)
     $ +0.5*F*aoM
      B2M=x(6)*(0.5*sM1+0.5*sM3+0.25*F*aoM)+0.5*G*aoM
      B3M=x(6)*(sM1*x(6)+G*aoM)
      B4M=F*aoM*x(6)
c
c================================================
c  Nonlinear Lift
c================================================
      b1=8.6
      pent=(alpha1-alpha0)/avib
      if (pent .gt. 1.0) then
      phi1=1.571
      else if (pent .lt. -1.0) then
      phi1=-1.571
      else
      phi1=dasin(pent)
      endif
c
      pent2=(alpha1t-alpha0)/avib
      if (pent2 .gt. 1.0) then
```

```
      phi1t=1.571
      else if (pent2 .lt. -1.0) then
      phi1t=-1.571
      else
      phi1t=dasin(pent2)
      endif
c
      dcL0=(b1*avib/3.14159)*(-pent*(1.571-
     $ phi1)+dcos(phi1))-(b1*avib/3.14159)*
     $ (pent2*(phi1t+1.571)+dcos(phi1t))
      dcLs1=(b1*avib/3.14159)*((1.571-phi1)-
     $ 0.5*dsin(2.0*phi1))
     $ -(b1*avib/3.14159)*(-(phi1t+1.571)-
     $ 0.5*dsin(2.0*phi1t))
      CL20=-dcL0
      r1L=0.6+0.1*dcL0**2
      r2L=(0.2465+0.005*dcL0**2)**2
      r3L=(-3.7399+7.0*dcL0**2)*r2L
      k1L=r2L-x(6)*x(6)
      k2L=r1L*x(6)
      rs1L=-r2L*dcLs1
      rc1L=-r3L*x(6)*dcLs1
c
      ALs1=(k1L*rs1L+k2L*rc1L)/(k1L**2+k2L**2)
      BLc1=(k1L*rc1L-k2L*rs1L)/(k1L**2+k2L**2)
c
c
c================================================
c  Nonlinear Moment
c================================================
      b2=0.48
      dcM0=(b2*avib/3.14159)*(-pent*(1.571-
     $ phi1)+dcos(phi1))
     $ -(b2*avib/3.14159)
     $ *(pent2*(phi1t+1.571)+dcos(phi1t))
      dcMs1=(b2*avib/3.14159)*((1.571-phi1)
     $ -0.5*dsin(2.0*phi1))
     $ -(b2*avib/3.14159)*(-(phi1t+1.571)-
     $ 0.5*dsin(2.0*phi1t))
      CM20=-dcM0
      r1M=0.25+0.1*dcM0**2
      r2M=(2.0+0.1*dcM0**2)**2
```

```
      r3M=(5.0-0.6*dcM0**2)*r2M
      k1M=r2M-x(6)*x(6)
      k2M=r1M*x(6)
      rs1M=-r2M*dcMs1
      rc1M=-r3M*x(6)*dcMs1
c
      AMs1=(k1M*rs1M+k2M*rc1M)/(k1M**2+k2M**2)
      BMc1=(k1M*rc1M-k2M*rs1M)/(k1M**2+k2M**2)
c================================================
c Equations
c================================================
      p(1)=mu*Pi*I1*om**2*x(5)**2*x(1)-I4*aol*theta0
     $ -I2*BoL-I4*CL20
c
      p(2)=mu*(Pi/4.0)*ra**2*I3*x(5)**2*x(2)-0.25*I5*aol*
     $ theta0-0.25*I3*BoL-0.25*I5*CL20-I5*CM20
c
      p(3)=mu*Pi*I1*(-x(6)**2*x(3)+om**2*x(5)**2*x(3))
     $ -I2*(q2s*B1L-q2c*B2L)-I1*(x(3)*B3L+x(4)*B4L)
     $ -I4*ALs1*alphas/avib+I4*BLc1*alphac/avib
c
      p(4)=mu*Pi*I1*(-x(6)**2*x(4)+om**2*x(5)**2*x(4))
     $ -I2*(q2s*B2L+q2c*B1L)-I1*(-x(3)*B4L+x(4)*B3L)
     $ -I4*ALs1*alphac/avib-I4*BLc1*alphas/avib
c
      p(5)=mu*(Pi/4.0)*ra**2*I3*(-x(6)**2*q2s
     $ +x(5)**2*q2s)
     $ -0.25*I3*(q2s*B1L-q2c*B2L)-0.25*I2*(x(3)*B3L
     $ +x(4)*B4L)
     $ -I3*(q2s*B1M-q2c*B2M)-I2*(x(3)*B3M+x(4)*B4M)
     $ -I5*AMs1*alphas/avib+I5*BMc1*alphac/avib
     $ -0.25*I5*ALs1*alphas/avib+0.25*I5*BLc1*alphac/avib
c
      p(6)=mu*(Pi/4.0)*ra**2*I3*(-x(6)**2*q2c
     $ +x(5)**2*q2c)
     $ -0.25*I3*(q2s*B2L+q2c*B1L)-0.25*I2*(-x(3)*B4L
     $ +x(4)*B3L)
     $ -I3*(q2s*B2M+q2c*B1M)-I2*(-x(3)*B4M+x(4)*B3M)
     $ -I5*AMs1*alphac/avib-I5*BMc1*alphas/avib
     $ -0.25*I5*ALs1*alphac/avib-0.25*I5*BLc1*alphas/avib
c
      return
```

```
      end
c
c
c
c================================================
c L-U decomposition
c================================================
      subroutine ludcmp(a,n,np,indx,d)
      parameter (nmax=100,tiny=1.0e-20)
      double precision a(np,np),vv(nmax)
      dimension indx(n)
      d=1.
      do 12 i=1,n
       aamax=0.
       do 11 j=1,n
          if (dabs(a(i,j)).gt.aamax) aamax=dabs(a(i,j))
11      continun
      if (aamax.eq.0.) pause 'singular matrix.'
      vv(i)=1./aamax
12    continue
      do 19 j=1,n
       do 14 i=1,j-1
       sum=a(i,j)
         do 13 k=1,i-1
           sum=sum-a(i,k)*a(k,j)
13       continue
       a(i,j)=sum
14      continue
      aamax=0.
      do 16 i=j,n
       sum=a(i,j)
       do 15 k=1,j-1
         sum=sum-a(i,k)*a(k,j)
15        continue
      a(i,j)=sum
       dum=vv(i)*abs(sum)
        if (dum.ge.aamax) then
        imax=I
         aamax=dum
       endif
16      continue
      if (j.ne.imax)then
```

```
        do 17 k=1,n
          dum=a(imax,k)
          a(imax,k)=a(j,k)
          a(j,k)=dum
17         continue
         d=-d
         vv(imax)=vv(j)
       endif
       indx(j)=imax
       if(a(j,j).eq.0.)a(j,j)=tiny
       if(j.ne.n)then
        dum=1./a(j,j)
        do 18 i=j+1,n
         a(i,j)=a(i,j)*dum
18         continue
       endif
19     continue
       return
       end
c
c
c=================================================
c    Back substitution
c=================================================
       subroutine lubksb(a,n,np,indx,b)
       dimension  indx(n),b(n)
       double precision a(np,np)
       ii=0
       do 12 i=1,n
        ll=indx(i)
        sum=b(ll)
        b(ll)=b(i)
        if (ii.ne.0)then
        do 11 j=ii,i-1
          sum=sum-a(i,j)*b(j)
11        continue
       else if (sum.ne.0.) then
        ii=I
       endif
       b(i)=sum
12     continue
       do 14 i=n,1,-1
```

```
      sum=b(i)
      do 13 j=i+1,n
       sum=sum-a(i,j)*b(j)
13      continue
      b(i)=sum/a(i,i)
14    continue
      return
      end
```

```
ccccccccccc
c   statics1.FOR  Statics divergence program,
c         x(1)=q10, x(2)=q20
c         Complete Aerodynamics
c         A built-in loop to read k2's from statics1.in,
c          perform Newton Raphson Method and takes the
c          resultant q10 and q20 as the initial guess for
c          the next velocity to insure convergence
c          to the correct roots.
c   Warren Chen, 4-29-93
ccccccccccc
      integer n,np,indx,i,t,j
      parameter (nn=2)
      real*8 x(1:nn),fvec(1:nn),fjac(1:nn,1:nn),delta(nn)
     $ ,alpha1,aoad,aoa,v
      real y(nn,nn),d,theta0,theta0d,kat
      write(*,*)'Enter Root Angle of attack'
      read(*,*)theta0
      write(*,*)'Enter the initial guess for q10:'
      read(*,*)x(1)
      write(*,*)'Enter the initial guess for q20:'
      read(*,*)x(2)
      alpha1=0.2094
      theta0d=theta0*180.0/3.14159
      n=2
      np=2
      do i=1,n
      delta(i)=5.0
      enddo
      t=0
      open(5,file='statics1.in',status='old')
      open(9,file='statics1.out',status='unknown'
     $ ,access='sequential')
      read(5,*)kat
      write(9,*)' '
      write(9,*)'statics1.out'
      write(9,*)'Complete aerodynamics'
      write(9,*)' '
      write(9,5600)'Theta-R','k2','q10','q20'
     $ ,'AOA(deg)','V(m/s)'
```

```
      write(9,*)'-----------------------------------'
   10 continue
      if (dabs(delta(2)).le.1.0d-3 .and.
     $ dabs(delta(1)).le.1.0d-3)then
        goto 500
      endif
      t=t+1
      call funcv(kat,theta0,n,x,fvec)
      call fdjac(kat,theta0,n,x,fvec,np,fjac)
      do i=1,n
       do j=1,n
         y(i,j)=0.
       enddo
       y(i,i)=1.
      enddo
      call ludcmp(fjac,n,np,indx,d)
      do j=1,n
      call lubksb(fjac,n,np,indx,y(1,j))
      enddo
      do j=1,n
       delta(j)=0.
      do i=1,n
         delta(j)=delta(j)+y(j,i)*fvec(i)
      enddo
      enddo
c
      do i=1,n
      x(i)=x(i)-delta(i)
      enddo
      if (t.ge.25)then
        goto 500
      endif
      goto 10
  500 continue
      aoa=theta0+0.5*0.8446*x(2)
      aoad=aoa*180/3.14159
      v=154.6*0.07/kat
      write(9,5100)theta0,kat,x(1),x(2),aoad,v
      x(1)=x(1)+0.0001
      x(2)=x(2)+0.0001
      delta(1)=5.0
      delta(2)=5.0
```

```
      t=0
      read(5,*)kat
      if (kat .ge. 999.0) then
      goto 600
      endif
      goto 10

  600 continue
      write(9,*)' '
      write(9,*)'End of Data'
      stop
c=====================================================
c formats
c=====================================================
 1000 format(' ',i2,1x,i2,a,f17.9)
 2000 format(' ',f17.9)
 3000 format(' ',a,f8.3,a)
 4000 format(' ',a,f6.3)
 4200 format(' ',a8,a8,a8,a8,a8,a8)
 4400 format(' ',f9.4,f9.4,f9.4,f9.4,f8.4,f7.4)
 5000 format(' ',i3,f9.4,f9.4,f9.4,f9.4,f8.4,f7.4)
 5100 format(' ',f7.3,f7.3,f7.4,f7.4,f9.3,f9.3)
 5500 format(' ',a,a8,a8,a8,a8,a8,a8)
 5600 format(' ',a7,a7,a7,a7,a9,a9)
      end


c=====================================================
      subroutine fdjac(kat,theta0,n,x,fvec,np,df)
c=====================================================
      integer n,np,nmax
      real*8 df(np,np),fvec(n),x(n),eps,f(40)
      parameter (nmax=40,eps=1.e-4)
      integer i,j
      real h,temp,kat,theta0
      do j=1,n
       temp=x(j)
       h=eps*abs(temp)
       if(h.eq.0.)h=eps
       x(j)=temp+h
       h=x(j)-temp
       call funcv(kat,theta0,n,x,f)
```

```
          x(j)=temp
         do i=1,n
          df(i,j)=(f(i)-fvec(i))/h
         enddo
        enddo
        return
        end

C=================================================
      subroutine funcv(kat,theta0,n,x,P)
C=================================================
      integer n
      real M,Ia,Pi,rho,l,wh,wa,I1,I3,I4,I5,kat
     $ ,b1,b2,phia,phih,
     $  alpha0,alpha1,alphav,theta0,b,c,I2,mu
      real*8 x(n),P(n),om,ra,CL20,CM20,aol,pent,BoL
      aol=5.73
      alpha1=0.2094
      alphav=0.002
      I1=1.0
      I2=0.6779
      I3=0.5
      I4=0.783
      I5=0.6366
      M=0.158
      Ia=192.0 e -6
      Pi=3.14159
      rho=1.23
      c=0.14
      l=0.559
      b=c/2.0
      wh=27.02
      wa=154.6
      om=wh/wa
      mu=(M/l)/(Pi*rho*b**2)
      ra=(dsqrt(Ia/M))/b
      BoL=x(2)*aol*0.5
C=================================================
c  nonlinear lift
C=================================================
      b1=8.6
      phia=0.8446
```

```
      phih=1.3154
      alpha0=theta0+0.5*phia*x(2)
      pent=(alpha1-alpha0)/alphav
      if (pent .gt. 1.0) then
      phi1=1.571
      else if (pent .lt. -1.0) then
      phi1=-1.571
      else
      phi1=dasin(pent)
      endif
      CL20=-(b1*alphav/3.14159)*(-pent*(1.571-
     $ phi1)+dcos(phi1))
c=====================================================
c  nonlinear moment
c=====================================================
      b2=0.48
      CM20=-(b2*alphav/3.14159)*(-pent*(1.571-
     $ phi1)+dcos(phi1))
c=====================================================
c  equations
c=====================================================
      p(1)=mu*Pi*I1*om**2*kat**2*x(1)-I4*aol*theta0
     $ -I2*BoL-I4*CL20
c
      p(2)=mu*(Pi/4.0)*ra**2*I3*kat**2*x(2)-
     $ 0.25*I5*aol*theta0
     $ -0.25*I3*BoL-0.25*I5*CL20-I5*CM20
c
      return
      end

c=================================================
c L-U decomposition
c=================================================
      subroutine ludcmp(a,n,np,indx,d)
      parameter (nmax=100,tiny=1.0e-20)
      double precision a(np,np),vv(nmax)
      dimension indx(n)
      d=1.
      do 12 i=1,n
       aamax=0.
       do 11 j=1,n
```

```
          if (dabs(a(i,j)).gt.aamax) aamax=dabs(a(i,j))
11       continun
        if (aamax.eq.0.) pause 'singular matrix.'
        vv(i)=1./aamax
12      continue
        do 19 j=1,n
         do 14 i=1,j-1
         sum=a(i,j)
           do 13 k=1,i-1
             sum=sum-a(i,k)*a(k,j)
13         continue
         a(i,j)=sum
14        continue
        aamax=0.
        do 16 i=j,n
         sum=a(i,j)
         do 15 k=1,j-1
           sum=sum-a(i,k)*a(k,j)
15          continue
        a(i,j)=sum
         dum=vv(i)*abs(sum)
          if (dum.ge.aamax) then
          imax=I
           aamax=dum
         endif
16        continue
        if (j.ne.imax)then
         do 17 k=1,n
           dum=a(imax,k)
           a(imax,k)=a(j,k)
           a(j,k)=dum
17          continue
          d=-d
         vv(imax)=vv(j)
        endif
        indx(j)=imax
        if(a(j,j).eq.0.)a(j,j)=tiny
        if(j.ne.n)then
         dum=1./a(j,j)
         do 18 i=j+1,n
          a(i,j)=a(i,j)*dum
18          continue
```

```
      endif
19    continue
      return
      end

C=================================================
C     Back substitution
C=================================================
      subroutine lubksb(a,n,np,indx,b)
      dimension  indx(n),b(n)
      double precision a(np,np)
      ii=0
      do 12 i=1,n
       ll=indx(i)
       sum=b(ll)
       b(ll)=b(i)
       if (ii.ne.0)then
       do 11 j=ii,i-1
         sum=sum-a(i,j)*b(j)
11        continue
      else if (sum.ne.0.) then
       ii=I
      endif
      b(i)=sum
12    continue
      do 14 i=n,1,-1
      sum=b(i)
      do 13 j=i+1,n
       sum=sum-a(i,j)*b(j)
13      continue
      b(i)=sum/a(i,i)
14    continue
      return
      end
```